Smart implants for mucoperiosteal tissue expansion in cleft palate defects

Inaugural dissertation

to

be awarded the degree of Dr. sc. med. presented at

the Faculty of Medicine

of the University of Basel

by

Kasturi Koteswara Prasad Nalabothu

From Chennai, India

Basel, 2021

Approved by the Faculty of Medicine

On application of

First supervisor	Prof. Dr. med. dent. Carlalberta Verna
Second supervisor	Prof. Dr. med. Dr. med. dent. Hans- Florian Zeilhofer
External expert	Prof. Dr. Shinji Kobayashi
Further advisors	Prof. PhD. Michel Dalstra
	PD Dr. med. Dr. med. dent. Andreas Müller

Basel, 12.02.2021
(Date of acceptance of the Faculty)

……..
Dean
Prof. Primo Leo Schär

Contents **Page numbers**

Acknowledgements

First and foremost, I would like to express my profound and genuine gratitude to my main supervisor Professor Carlalberta Verna for giving me the opportunity to join the Orthodontic Research group and work in a multidisciplinary project. I am sincerely grateful to her constant guidance, sharing knowledge and being an exceptional source of inspiration throughout my course. I shall remain indebted to her forever for making me a better individual both professionally and personally.

I would like to sincerely thank my co-supervisor Professor Hans- Florian Zeilhofer for his constant support, supervision and suggestions. He has been a driving force with strong motivation for innovation and offering invaluable advice through the entire process.

It is with great respect and candour that I express my thanks to Dr. Andreas Müller for his relentless encouragement, support and magnificent guidance in helping me better myself and scaffolding my ideas with this constant encouragement, support and timely help throughout the process. Without his innovative ideas, surgical expertise, motivation and encouragement, this study would not have been possible. It was an enriching experience to have spent four years of my life under his guidance. I am very excited about our future research together!

With deep sense of gratitude, I would like to sincerely thank my co- supervisor Michel Dalstra for sharing his knowledge and ideas about 3-D imaging and guiding me through the hidden world of finite element modelling. I am forever indebted for his constant support and dedication and always having time for discussion at any hour of the day. I am also extremely grateful to Mr. Markus Steineck for his help with the magnetic experiments and technical know-how.

I would like to express my sincere thanks and gratitude to Dr. Ravikant Singh for providing the access to use his patients which made my research possible. I extend my sincere thanks to Dr. Benito Benitez for his constant encouragement, support and motivation towards completion of my PhD

I express a note of special thanks to my friends and colleagues who went through hard times along with me, cheered me on and celebrated my accomplishments. I want to take a moment to thank them Dario Arnold, Kim Mueller, Vesna Vidovic, Oliver Stadler, Simone Horn, Olivia Engeler, Gianluca Cassina and Kevin Sieber. I extend my special thanks to Ignacio Filippon, Remi Ammann and Tobias Horn for their moral support and taking good care of me.

I am deeply indebted to Jasna and Hans Nussberger for taking me into their family and taking good care of me like their own son from the time I arrived to Switzerland till now. I would also like to thank them for introducing me to the incredible swiss culture, cuisine and lovely friends.

I would like to thank my parents Rama Rao and Vimala for the sacrifices they have made to see me succeed for which I am deeply indebted.

Last but not least I wish to thank my wife Michelle who has stood by me throughout this entire process and has made countless sacrifices to help me get to this point. I am forever indebted to her for her endless love, encouragement and support to me and my children Devansh and Aaria Faye during my studies here.

Abstract

Cleft lip and palate are the most common craniofacial malformations, affecting one in every 500 to 700 live births, thus accounting for about 220,000 new cases each year worldwide with tremendous variations across geographic areas, ethnic groups and socioeconomic status. Affected children have a range of both functional and aesthetic problems comprising of feeding difficulties due to incomplete oral seal, swallowing, nasal regurgitation, respiratory problems, hearing difficulties due to abnormalities in the palatal musculature, and speech impairments due to air escape and articulations problems. The surgery can solve the problems, but the two major factors which determine a good surgical outcome and its assessment are the interpretation of the actual size of the cleft and generation of periosteal tissue to close the defect. The surgeons faced a challenge to measure the cleft size due to wide diversity in methodologies employed which resulted in improper estimation of the deficient palatal tissue and thus resulted contradictory results in measuring outcomes such as occlusion or midface skeletal development. We have introduced the vomer edge for establishing a validated 3D measuring method for the width, area and height of the true cleft with reproducible landmarks for easy and accurate measurement of the outcomes in unilateral cleft lip and palate patients. The passive plate therapy provided to UCLP patients gave favourable anatomical conditions for subsequent surgical palatal repair in patients by alleviating the problems of tissue deficiency to some extent. We therefore adopted periosteal tissue distraction osteogenesis as potential treatment strategy to target the tissue deficiency while using the magnetic forces to exert necessary strain. In our study, we have assessed whether the dental magnets have the potential to act as a device to generate mucoperiosteal tissue in UCLP. We have used in-silica approach in the form of 3D FE-model and found that strain levels in the palatal segments of the cleft for the load cases do reach

1500 μstrain limit, a requirement for bone formation, according to the mild overload window of the Mechanostat theory proposed by Harold Frost. We further examined the forces, which reach threshold for regeneration of the hard and soft tissue volumes along the cleft edges in both UCLP and BCLP by means of periosteal distraction. We found that a 5N attraction force could initiate generation of soft and hard tissues along the cleft edges in in-silico model within the optimal biological limits.

List of abbreviations

BCLP	Bilateral cleft lip and palate
CFA	Craniofacial anomalies
CL	Cleft lip
CL/P	Cleft lip- with or without cleft palate
CP	Cleft palate
CLP	Cleft lip and palate
OFC	Orofacial clefts
RCT	Randomized controlled trial
UCLP	Unilateral cleft of the lip and palate
BCLP	Bilateral cleft of the lip and palate
VPI	Velo-pharyngeal incompetence
WHO	World Health Organization
GWAS	Genome wide association studies
ICD	International classification of diseases
DO	Distraction osteogenesis
PDO	Periosteal distraction osteogenesis
MTE	Mucoperiosteal tissue expansion
FE	Finite Element
3D	Three-dimensional

4. Introduction

Orofacial clefting represents the most occurring congenital deformity after heart deformities, spina bifida and limb deformities [1]. Cleft lip and palate (CLP) can affect maxilla, palate, vomer, and soft tissue structures such as the lips and nose resulting on orofacial and craniofacial deformity. Affected children acquire a spectrum of functional as well as aesthetic complications. These comprise feeding complications at birth due to challenges associated with oral seal, swallowing, nasal regurgitation, respiratory problems, hearing difficulties due to deformities in the palatal musculature and speech disorders due to nasal escape and articulation disturbances [1] . Therefore, early and complete surgical repair of lip and palate is encouraged to normalize food intake, speech development and aesthetics [2][3][4].

4.1 Incidence of orofacial cleft lip and or palate

Cleft lip and palate affects about 1.7 per 1000 live births worldwide with large variations across geographic areas, ethnic groups and socioeconomic status [4][5]. The highest birth prevalence is seen in Asian or Amerindian populations with 1/500 live births, intermediate range was noted in European-derived populations at about 1/1000 and the lowest was noted in African derived populations at 1/2500 [1][4][5][6]. In South America, the incidence of CL/P is 1/1150 [7] and the recurrence rate among siblings is about 4% similar to sibling's risk in other populations [8].

In Switzerland, the birth prevalence of cleft lip with or without cleft palate (CL/P) is between 0.83 and 0.96 and for isolated cleft palate from 0.59 to 0.69 per 1000 live births [4][9].

4.1.1 Distribution of cleft

Most often the predominance of CL/P is seen in males and predominance of CP is seen in females [10][11]. Unilateral clefts form 76% of all CLP with higher predominance on left side

(52%) compared to the right side (24%) [11]. Bilateral clefts form around 24% of all the CLP cases in Europe and world-wide [11].

4.2 Embryology of CLP

The development of the face begins during the 4th week of intrauterine life when neural crest cells migrate and combine with mesoderm to form the facial primordia [12]. The central segment of the face comprises the forehead, supraorbital ridges, nose, philtrum and primary palate are derived from the frontonasal process. The fusion of the frontonasal process, right and left nasomedial process of the maxilla results in formation of the upper lip and premaxilla [4]. The upper lip formation completes during the 5th or 6th week of embryonic development and failure of fusion results in cleft lip. Prior to the 6th week of development, the primary palate includes that portion of the upper airway that will develop into the lip, alveolar ridge and the hard palate segment extending back to the incisive foramen. The separation between nasal and oral cavities occurs during the 6th week and contains the premaxilla and four maxillary incisor teeth. The fusion of the palatal shelves begins at the incisive foramen and advances towards the posterior palate and the fusion is completed at the end of the 12 weeks of intrauterine life. Failure of the fusion process results in a cleft palate [4].

4.3 Aetiology of CLP

The aetiology of orofacial clefts is complex and heterogeneous. It can be characterized as part of syndrome where it is termed syndromic and non-syndromic or isolated when it occurs beyond other malformations or syndromes. The majority of orofacial clefts are categorized as non-syndromic clefts that is 70% of all CL/P cases [13] and are as aforementioned to be multifactorial in origin. The causes for CLP are linked to genetics with involvement of wide variety of genes, environmental and gene-environment interaction.

4.3.1 Genetic aetiology

The understanding of genetic factors involved in clefting is crucial to improve the clinical care of individuals with cleft lip and palate malformations. Fogh-Andersen [14] was among the early ones who proposed that genetic factors contribute to the non-syndromic CL/P after observing elevated prevalence of clefting in relatives of a patient with cleft. The evidence has shown that in siblings of children affected with cleft lip with or without cleft palate the frequency of occurrence is 4%, whereas the frequency increases to 16.7% if one of the parents has been affected [15]. The risk of having a cleft palate in siblings of a family with unaffected relatives is 1.7%, when there is a history of clefting in family members other than the parents the occurrence risk increases to 7.2% [15]. When one of the parents of a patient with a cleft palate has clefting the frequency of a sibling having the same malformation increases to 15.4% [15].

Various approaches like linkage analysis and associations studies of candidate genes have been conducted to seek for genetic non-syndromic CL/P. The first gene associated with non-syndromic CL/P transforming growth factor alpha (TGF- alpha) locus has been identified and has shown variation in different population groups [16]. Genome-wide association studies (GWAS) have led to the detection of at least 43 genes/loci associated with non-syndromic CL/P [17][18][19]. The genetic variants in the region of the interferon regulatory factor 6 (IRF6) gene have shown the strongest association with non-syndromic CL/P among different populations[17][18][20]. The mutations in the gene for IRF6 gene causes Van der Woude's syndrome [21], which account for 2% of all the CL/P cases with a prevalence of 1/34000 live births worldwide [22]. MSX1 gene was also identified having a major role in the development of cleft palate (CP) and tooth agenesis and any alterations in MSX1 led to CP more frequently than alterations in other genes [23].

4.3.2 Environmental risk factors

Several environmental factors have been found to increase the risk of CL/P and are classified into four extensive groups: womb environment, external environment, nutrition and drugs. There

are several known teratogens that increase the risk for CL/P and these include antiepileptic drugs (phenytoin, valproic acid) thalidomide, dioxin (pesticide), retinoic acid [24], and maternal alcohol use and maternal cigarette smoking [25]. It was found that embryonic exposure to tobacco during the first trimester resulted in increased risk for CL/P [25]. Twenty or more cigarettes per day result in a twofold increase whereas less than 20 cigarettes per day resulted in a 1.5-fold increase and this was due to recurrent deficiency in the amount of oxygen reaching the tissues induced by nicotine affects facial development [25].

Nutrition during pregnancy has been suggested as another contributing factor for CL/P. Daily intake of folic acid during the first three months of pregnancy seem to partially prevent the occurrence of orofacial clefts and is widely used in different national health protocols [26].

4.3.3 Associated anomalies

There are over 487 syndromes identified to be associated with CL/P in the 2001 version of the London Dysmorphology Database [27]. The overall incidence of cleft associated anomalies was around 29.2% and the most common ones affected are the musculoskeletal, cardiac and central nervous system were the predominant ones according to the EUROCAT workgroup in the European Union [28]. The most frequent chromosomal anomaly was trisomy with higher prevalence in CL/P than CL only [28]. The musculoskeletal anomalies, polydactyly and limb reductions were also reported along with malformation in the cardiovascular system. In 28.9% malformations of the cardiovascular system, the ventricular and atrial septal defect were the most common followed by tetralogy of Fallot [28].

Middle ear (otitis media) is a very common condition in children with CL/P and CP and with a prevalence rate of a least 90% [29]. Feeding, speech and language difficulties, hearing impairment and low self-esteem are other problems associated with CL/P patients [30].

4.4 Cleft anatomy

The extent of involvement of hard and soft tissue can vary considerably among the patients. It might range from a small notch of the vermillion border of the lip to a complete defect affecting the alveolus up to the floor of the nose unilaterally or bilaterally.

4.4.1 Anatomy of UCLP

The anterior part of the primary palate segment on the cleft side often tilts superiorly and medially into the cleft area in complete UCLP. The deficiency of mucosa and the underlying bone are characteristic features of clefts of the secondary hard palate. The amount of distance between the palatal shelves varies depending on the severity of the cleft. Shortening of the velar musculature and its abnormal insertion contribute to the deficiency of the palatal mucosa [31].

4.4.2 Anatomy of BCLP

The alveolar ridge is divided into three segments in patients with BCLP. The premaxillary segment is often protruded and might be deviated to one side while the lateral segments are generally collapsed. The anatomy in BCLP patients may vary considerably and can be summarized based on the extent and severity of the cleft. Usually the columella is remarkably short and the nasal tip is broad. The nasal alae are flat adopting an S-shaped curvature due to latero-inferior and posterior displacement. The deformation of the lateral cartilages with short extensively separated medial crura causes the nostril to be horizontally conformed. The nasal floor is missing and there is a displacement of the septum and the anterior nasal spine [32].

4.4.3 Anatomy of CP

In cleft palate (CP) patients where the secondary palate is affected, both the hard and soft tissues may be involved. Palatal clefts might extend from a bifid uvula to a V-shaped cleft reaching the incisive foramen. The degree of separation of the palatal shelves varies substantially [31].

4.5 Cleft classification

Different systems have been described to classify orofacial clefts based on the anatomical, embryological and epidemiological conditions [14][33][34][35]. Tessier described the most extensive and comprehensive classification of craniofacial clefting using 14 meridians [36]. The pictographic Y-stripe representation of cleft phenotype developed by Kernahan and Stark was blamed for being too complicated and burdensome to use [34]. The LAHSHAL classification describe by Kriens [37] represents the cleft involvement for lip, A for alveolus for hard palate and S for soft palate. LASH points out a right sided cleft while SHAL left sided cleft involvement. LAHSHAL represents a bilateral cleft. Lower case refers to submucosal clefts and bifid uvula. The classification of Van Der Meulen delineates orofacial clefts based on where the development arrest occurs in the embryogenesis [38]. The international classification of diseases (ICD) [39] has simplified the classification of clefts and is globally used for epidemiological, health management and diagnostic purposes. ICD-10 includes congenital malformations such as different cleft types. Group Q35 includes cleft palate, Q36 refers to cleft lip and Q37 for cleft lip and palate. The code Q30.2 is used to identify cleft associated malformations of the nose [39].

4.6 Cleft size and intrinsic tissue deficiency

The cleft size/width at birth is highly variable and its assessed-on appearance at birth. The two main major factors which influence a good surgical outcome and its assessment are the amount of palatal tissue present and interpretation of cleft size. Cleft severity is interpreted as either an intrinsic amount of palatal and alveolar tissue deficiency.

4.6.1 Evidence of tissue deficiency

A comparison with non-treated cleft lip and palate patients the mid-facial growth is similar when compared with non-cleft patients without apparent restriction of the growth [40]. However, significant correlation between the cleft size and the growth of maxilla in patients with large cleft

had a more retrusive maxilla [41]. This impairment of growth is due to extensive deficient tissue in critical areas rather than damaging the bone itself [42]. Further investigations confirmed that 4.1° reductions of SNA between 8 and 16 years and further reduction of the anteroposterior intermaxillary relationship (ANB) was due to the tissue deficiency and not influenced by mandibular growth. Deficient tissue adjacent to the pterygopalatine tuberosity sutures can inhibit the forward growth of the maxilla leading to reduction in maxillary length [42]. The vertical growth of the maxilla will also be negatively affected by deficient tissue in the palate that anchors the periodontal fibers attached to the teeth [42].This reduction in anteroposterior and vertical growth of the maxilla will result in a malocclusion in patients with cleft in their adolescence. Hence it is important to have enough tissue to mitigate all the associated problems.

4.6.2 Current methods to solve tissue deficiency

Intrinsic palatal tissue deficiency finds its basis in the genetic and anatomical etiological factors. The genetically determined developmental malformations would lead to more severe defects with a larger palatal tissue deficiency [14] which results in being the main determinant for the development of upper jaw [43].

The approaches to mitigate the tissue deficiency in modern day use have their own advocates and numerous methods were employed, but is still not known which the best is for a given individual. The majority of the approaches for tissue deficiency mitigations are primarily based on non-surgical and surgical methods.

4.6.2.1 Surgical methods to mitigate tissue deficiency

Cleft palate closure by surgery depends upon the adequacy of available palatal mucosal tissue. Insufficiency of such soft tissue is a cause for concern in the closure of clefts of the hard palate. Several different surgical techniques evolved over the years to mitigate the problem of tissue deficiency [33][44][45][46][47][48][49][50][51][52][53]. There is no consensus on which is the best protocol until date. In a survey of over 210 European cleft centres it was found that

seventeen different surgical sequences for repairing unilateral complete clefts were identified [54]. In 2005 a scientific basis was put forward for determining the optimal conditions for palatal cleft closure in UCLP and BCLP patients [55]. It was recommended that a surgery of the palate should be performed when the surface area of the cleft space does not exceed 10% of the surrounding palatal surface bounded by alveolar ridges independent of patients age for achieving good facial balance [55]. However, this holds true for palatal clefts which are lesser in size, whereas in larger clefts this recommendation seems to be a challenge as generation of new tissue is an adversity [56].

The designed surgical techniques were based on the three basic surgical principles with minor variations [57] based on the extent of tissue deficit. The first principle is based on single-layer closure as this procedure involves turning over the mucosa from either the oral of the nasal cavity like a page in book while leaving an open wound on the back side of the turned over mucosa [44][45][46][47]. This procedure is also limited to closure only to either the oral or the nasal mucosal side. The second principle involves detaching the oral tissue and shifting it over the cleft area while creating an open wound that heals outside the cleft area from where the tissue has been detached [33][48][49] . The third principle involves tissue from outside the palatal area is used to cover the wound areas that result from the first or second principles [50][51][52][53].The above described principles when applied to close the gap are effective but none were able to generate new mucoperiosteal tissue.

4.6.2.2 Non-surgical methods to mitigate tissue deficiency

The most common non-surgical methods employed to mitigate the tissue deficiency is by applying the principles of presurgical maxillary orthopaedics through palatal appliances [58][59][60]. The principle behind these appliances was gradual approximation of the palatal shelves and thus reduces the alveolar and cleft width prior to surgery. Numerous techniques and appliances existed but they are classified based on the intensity of force levels employed for

infant orthopaedics. The early proponents of this technique were McNeil in 1950 [59] and Hotz and Gnoinski [61] employed medium forces to approximate the segments. The higher forces were applied in the early 1976 by using Latham appliance [62] and later modified by Latham and Millard [63]. The introduction of nasoalveolar molding technique by Grayson with moderate forces to approximate the cleft width and increasing the columella length had bought some respite for cleft surgeons [64]. The vast majority of the proponents of this technique claimed that gradual adaptation of the appliance can stimulate palatal tissue growth [59][60][62][63]. It was later shown that these approaches resulted in retardation of growth of palatal tissue [65]. A randomized controlled trial concluded that using a palatal appliance did not result in any permanent growth change or tissue gain [66].

4.6.2.3 Distraction osteogenesis

The vast majority of the methods placed emphasis on presurgical manipulation of tissue to create dynamics that are more favourable at the time of the definitive repair. However, the surgical and non-surgical methods do not correct the deficiency of the periosteal bone and soft tissue; rather they move the existing tissue into a better location. The introduction of distraction osteogenesis (DO) for the correction of the craniofacial skeleton in the early 1990 [67] has brought some new hope as the process relies on the mechanical induction of new bone formation between bony surfaces that are gradually separated. Transport osteogenesis is a specific type of DO in which a transport disk is created and moved to fill in a defect. First, osteotomies are made and distraction device is applied. A short latency period is allowed to elapse before the distraction phase begins. The bone segments are separated by 0.5 to 1mm/d and osteogenesis is induced between the segments. The tension placed on the bone as the segments are gradually separated also stimulates soft tissue expansion and accommodation of lengthened bone. Not only is new bone created but any related muscles, blood vessels, nerves and mucosa also elongate [67][68][69][70].There is no evidence of application of DO in new born human hard

palate except for its application in treating palatal fistula in adults [70]. The reasons could be because of its surgical procedure, device size and potential damage of dental follicles embedded in the palatal shelf ridge.

Periosteal distraction osteogenesis seems to be a viable option. It is the combination of the guided bone regeneration and tissue expansion. It builds an artificial space between bone surface and periosteum by expanding the periosteum, muscle and skin at the same time. This procedure has the potential to eliminate the need for having osteotomy like in DO [71]. The vast majority of the researches explored the feasibility and superiority through many animal experiments [72][73][74][75][76]. In an experiment in the New Zealand rabbits the periosteal distractor were placed sub-periosteally and on mechanical traction of the periosteum, formation of new bone was observed [73]. Similarly in an another animal experiment in Japanese white rabbits, the area of new bone was formed after 8 weeks of periosteal distraction [75].There is also increasing evidence that magnetic fields can promote bone regeneration directly by attracting growth factors, hormones and polypeptides to the implantation site [77]. The investigations in animal experiments provided evidence suggesting that periosteal distraction osteogenesis (PDO) is an appealing option for utilizing the principles of DO [78][79][80] by evading the challenges posed by DO. PDO results in combined bone and soft tissue generation while avoiding detrimental effects on the bone.

4.6.2.4 Mucoperiosteal tissue expansion (MTE)

The tissue expansion was first reported in the context of palatal fistula repair in 1990 [81]. Following this report, the other authors explored various regiments of MTE for the repair of primary cleft palate [82][83][84]. Mucoperiosteal tissue expansion is a mechanical process of tissue expansion which can be achieved by conventional, prolonged expansion for one to three months and intraoperative tissue expansion called as “intraoperative sustained limited expansion” [85][86]. The general principle employed is that of an “expander” placed under the

mucosa on either ends of the palatal defect in an effort to generate additional tissue that can be used to close the defect. The challenge of this MTE includes expander extrusion or displacement, the possible need for second surgery to remove the expander and repair the palate if the expansion is staged.

4.6.2.5 Smart implants for guiding tissue expansion

Smart implantation of biomaterials began to play a central role in modern strategies in regenerative medicine [87][88][89] and the vast majority of the studies focussed on application of biomaterials for purely bone regeneration [90].The new-born cleft palate comprises of bone and two mucosal layers which makes it difficult target for biomaterial or tissue engineering techniques. Static magnetic fields have been used for bone formation in medical research under a weak magnetic force for a long period [91]. Magnetic forces have also been used in orthodontics to generate tooth movement and to promote tissue reactions [92]. The application of mechanical loading by implantation of magnetic smart implants at the borders of mucoperiosteum of cleft borders seems to provide tissue formation by gradual expansion. The amount of mechanical loading necessary to stimulate tissue formation is not known and use of computational finite element analysis would aid in finding the optimal forces necessary for tissue formation.

4.7 Finite element analysis

The finite element (FE) analysis is a numerical tool used to provide a quantified estimate of the stresses and strains generated in the bone structure under external loading. It brings to light the distribution of the internal loads and deformations. Computational FE analysis has provided crucial basic data for understanding mechanical interactions between the magnets and mucoperiosteal tissue for tissue expansion [93]. The loading distribution depends on the shape, size, architecture of individual anatomical structures and malformations. The exact morphology

of these alterations in turn determines the extent of necessary tissue shift at the time of surgical cleft closure.

4.8 Outcome measurements: cleft palate morphology

A distinctive feature of the cleft palate deformity is the curved vomer. The curved vomer ‘”portion du vomer incurvè” [33] together with true cleft is referred to as “palatal cleft” . Despite the clinical importance of the true cleft region in all cleft palate surgery techniques, to our knowledge this region has not previously been investigated previously in three dimensions. Apart from that there is no consensus on how to measure the cleft size and categorize its severity three dimensionally. This might be because the separation of the maxillary segments [94] is easier to measure while the extent of tissue deficiency is difficult to quantify. Further, defining the landmarks and measuring the cleft palate are commonly performed in two dimensions [94][95][96][97] which represents the simplification of the three dimensional complexity of cleft palate. Hence, there is a need for development of new analysis method based on three dimensional standardized reproducible landmarks using vomer.

5. Aims of the study

The aim of this PhD project was to quantify the tissue deficit in cleft palate using 3D reproducible methods and to find mechanical approaches to minimize the tissue deficit. The aim also involves to understand the principles involved in mitigating tissue deficiency in the cleft palate by quantifying the stresses and strains in the palate of newborns with UCLP and BCLP, simulating the mucoperiosteal loading through magnetic forces and to verify whether loading could reach the necessary threshold for tissue expansion.

To fulfil the aim the following objectives were set in studies (I-III)

I. The aim of this cohort study was to use a new analysis method based on 3D standardized, reproducible landmarks to quantify the morphological changes of the palatal cleft and true cleft areas under passive plate therapy.

II. To quantify the stresses and strains in the palate of newborns with a unilateral cleft lip and palate simulating the periosteal loading through magnetic forces and to verify whether loading could reach the threshold necessary for bone formation.

III. To compare the load transfer of magnetic forces used for periosteal distraction osteogenesis in both UCLP and BCLP *in silico* models and examine whether forces reach the threshold necessary for regeneration of the hard and soft tissue volumes along the cleft edges in both UCLP and BCLP.

6 First study:

Three-Dimensional Morphological Changes of the True Cleft under Passive Presurgical Orthopaedics in Unilateral Cleft Lip and Palate: A Retrospective Cohort Study

Study design: Dr. Prasad Nalabothu, Prof. Michel Dalstra

Financing: FAG (Voluntary Academic Association): CHF 13,406

Project leaders: PD Dr. med. Dr. med. dent. Dr. phil. Andreas A. Mueller

Publication: First authorship, Journal of Clinical Medicine, Impact factor 5.68 (2020), Ranking 15/160 (Q1) in “Medicine, General and Internal”

Article

Three-Dimensional Morphological Changes of the True Cleft under Passive Presurgical Orthopaedics in Unilateral Cleft Lip and Palate: A Retrospective Cohort Study

Prasad Nalabothu [1,2,†], Benito K. Benitez [2,†], Michel Dalstra [1], Carlalberta Verna [1] and Andreas A. Mueller [2,*]

[1] Department of Orthodontics and Pediatric Dentistry, University Center for Dentistry, Basel 4031, Switzerland; prasad.nalabothu@unibas.ch (P.N.); michel.dalstra@dent.au.dk (M.D.); carlalberta.verna@unibas.ch (C.V.)
[2] Department of Oral and Craniomaxillofacial Surgery, University Hospital Basel, Basel 4031, Switzerland; benito.benitez@usb.ch (B.K.B); andreas.mueller@usb.ch (A.A.M.)
[†] They are joint first authors and contributed equally to this work.
[*] Correspondence: andreas.mueller@usb.ch; Tel.: +41-61-328-60-95

Received: 10 March 2020; Accepted: 28 March 2020; Published: date

Abstract: The aim of this cohort study was to quantify the morphological changes in the palatal cleft and true cleft areas with passive plate therapy using a new analysis method based on three-dimensional standardized reproducible landmarks. Forty-five casts of 15 consecutive patients with complete unilateral cleft lip and palate were laser scanned and investigated retrospectively. The landmarks and the coordinate system were defined, and the interrater and intrarater measurement errors were within 1.0 mm. The morphological changes of the cleft palate area after a period of 8 months of passive plate therapy without prior lip surgery are presented graphically. The median decrease in cleft width was 38.0% for the palatal cleft, whereas it was 44.5% for the true cleft. The width of the true and palatal cleft decreased significantly over a period of 8 months. The true cleft area decreased by 34.7% from a median of 185.4 mm^2 (interquartile range, IQR = 151.5–220.1) to 121.1 mm^2 (IQR = 100.2–144.6). The palatal cleft area decreased by 31.5% from a median of 334 mm^2 (IQR = 294.9–349.8) to 228.8 mm^2. The most important clinical considerations are the reproducibility and reliability of the anatomical points, as well as the associated morphological changes. We propose using the vomer edge to establish a validated measuring method for the width, area, and height of the true cleft.

Keywords: cleft lip and palate; cleft palate; three-dimensional; presurgical orthopaedics; true cleft; passive plate; vomer

1. Introduction

The area that surrounds the entrance from the oral into the nasal cavity in cleft lip and palate was described by Victor Veau as "fente vraie" [1], which we translate as "true cleft". Whereas the curved vomer "portion du vomer incurvé" [1] together with the true cleft is referred to as "palatal cleft" and denotes the gap in palatal mucosa. All types of hard palate surgeries aim for tissue to cover the true cleft region in order to produce a functional seal between the oral and nasal cavities. Despite the fundamental clinical importance of the true cleft region in all cleft palate surgery techniques, to our knowledge this region has not previously been investigated in three dimensions.

The anatomical and functional alterations of the cleft lip and palate result in dimensional alterations in the palate. The exact morphology of these alterations in turn determines the extent of the necessary tissue shift at the time of surgical cleft closure and has consequences for healing and growth. The presurgical cleft palate morphology is therefore of great significance for the perioperative and long-term rehabilitation of patients.

However, there is no consensus on how to measure the cleft size and categorize its severity. This might be because the separation of the maxillary segments [2] is easier to measure, while the extent of tissue deficiency is difficult to quantify. Further, defining the landmarks and measuring the cleft palate are commonly performed in

two dimensions [2–5], which represents a simplification of the three-dimensional (3D) complexity of the cleft palate. Moreover, there is a wide diversity of methodologies applied to describe the cleft palate morphology in children with complete unilateral cleft lip and palate. Some researchers measure only the separation between two segments anteriorly [4,5], whereas others measure the cleft width or area between the palatal shelves, which is commonly defined as the cleft area [3,6,7]. The cleft area is quantified as a percentage of the total palatal area rather than as an absolute number. The use of these methods to establish the correlation between the initial cleft size and outcome measurements, such as occlusion or midface skeletal development, has produced contradictory results due to ill-defined landmarks, low-quality dental casts, and lack of general reproducibility [7–9].

The previously used two-dimensional (2D) measurement techniques comprise direct measurements of real plaster casts and measurements of its photographs or photogrammetric models, and measurements of occlusal radiographs [2–7,10–12]. The projection of 3D points onto a 2D plane is affected by the orientation of the cast and the plaster-cast surface area. Most measurements in cleft lip and palate studies, such as of the inclination of the palatal shelves or the surface area of the palatal segments, are 3D in nature and therefore only strictly valid when evaluated in three dimensions [13,14].

The aim of this cohort study was to use a new analysis method based on 3D standardized, reproducible landmarks to quantify the morphological changes of the palatal cleft and true cleft areas under passive plate therapy.

2. Materials and Methods

2.1. Patients and Plaster Casts

This study retrospectively analysed 15 consecutive patients with complete unilateral clefts of the lip, alveolus, and palate who were treated at the last author's (A.A.M.) institute. The subjects comprised 3 females and 12 males, and none of them had Simonart's band. Each infant received passive plate therapy, that lead to 3 plaster casts that had been taken at the following different intervals (total of 45 casts): during the first week after birth (before passive plate therapy) (T0), 3–4 months after birth (ongoing passive plate therapy) (T1), and prior to primary surgery at around 8 months (at the end of passive plate therapy) (T2). Passive plate therapy was applied by the same surgeon (A.A.M.) to all patients. Informed consent was obtained from the children's parents or guardians. The study was performed in accordance with the Declaration of Helsinki, and it was approved by the Ethics Commission of Northwest and Central Switzerland (EKNZ) (project-ID 2018-01561).

2.2. Passive Plate Therapy

After birth, an impression of the palate was taken in the awake infant using an individual impression tray and silicone (Epiform-flex, Dreve-Dentamid, Unna, Germany). The cleft depressions on the plaster cast were blocked out using soft putty (President, Coltène/Whaledent, Altstätten, Switzerland) in order to simulate a normal palatal vault shape and create a free space to the vomer mucosa, to the palatal shelves, and between the alveolar segments. The alternating application of monomer spray (Orthocryl liquid monomer, Dentaurum, Ispringen, Germany) and sprinkling of acrylic powder (Orthocryl polymethylmethacrylate, Dentaurum, Ispringen, Germany) formed a passive plate with a target thickness of 1.5–2.0 mm. A caregiver removed the plate once daily to clean and disinfect it (Octenisept, Schuelke, Norderstedt, Germany). A thin film of tasteless denture adhesive (Kukident Neutral Extra Strong, Kukident, Weinheim, Germany) kept the plate in place. The plate typically became unstable after 3–4 months, when it was renewed. The third impression was taken prior to the lip and palate repair in one cleft surgery at around 8 months.

2.3. Three-Dimensional Analysis

Plaster cast of the infants were scanned and digitized using a high-precision laser scanner (Iscan L2, Imetric Swiss 3D Scanning Systems, Switzerland, precision of <15 μm) and were exported in the STL (stereolithographic) file format. The exported models were then imported into dedicated 3D analysis software (Mimics version 20.0, Materialise, Leuven, Belgium).

The 45 casts were analysed by marking 14 landmarks on each digitized model based on the principles of Stöckli [2] and Mazaheri et al. [10]. The 3D definitions of the measurement landmarks are presented in Tables 1 and 2 and illustrated in Figures 1 and 2.

Table 1. Definition of landmarks for the 3D analysis.

Abbreviation	Name	Definition
Q	Lateral sulcus vertex	Point where the lateral sulcus intersects the crest of the ridge of the greater segment [4]
T/T'	Tuberosity vertex	Points where the tuberosity border intersects the crest of the ridge of the greater (T) and lesser (T') segments [10] The base plane runs through T and T' and is perpendicular to the plane defined by (Q, T, T') The base line connects T–T' within the base plane
g	Greater ridge	Path of the greater segment's palatal shelf ridge, that is at the junction with the vomer [1]
v	Vomer edge	Path along the maximal curvature of the vomer
l	Lesser ridge	Path of the lesser segment's palatal shelf ridge
GA (=VA)	Greater anterior (=Vomer anterior)	Most-anterior point on the ridge of the greater segment where it intersects with the vomer edge
GT	Greater posterior	Point where the ridge of the greater segment intersects the base plane
GM	Greater midpoint	Point halfway between GA and GT following the path on the ridge of the greater segment
LA	Lesser anterior	Most-anterior point on the ridge of the lesser segment ridge
LT	Lesser posterior	Point where the ridge of the lesser segment intersects the base plane
LM	Lesser midpoint	Point halfway between LA and LT following the path on the ridge of the lesser segment
VT	Vomer posterior	Point where the vomer edge intersects the base plane
VM	Vomer midpoint	Point halfway between VA (=GA) and VT following the path on the vomer edge

The coordinate system was established as described by Botticelli et al. [15], by a horizontal plane passing through Q–T/T' and a posterior vertical plane perpendicular to the previous one passing through T/T'. The most-anterior point on the palatal ridge of the greater segment (GA) and the most-anterior point of the vomer edge (VA) were at the same point (Figure 1C, D). This point is referred to anatomically as the innominate sulcus (or "unnamed furrow") [16].

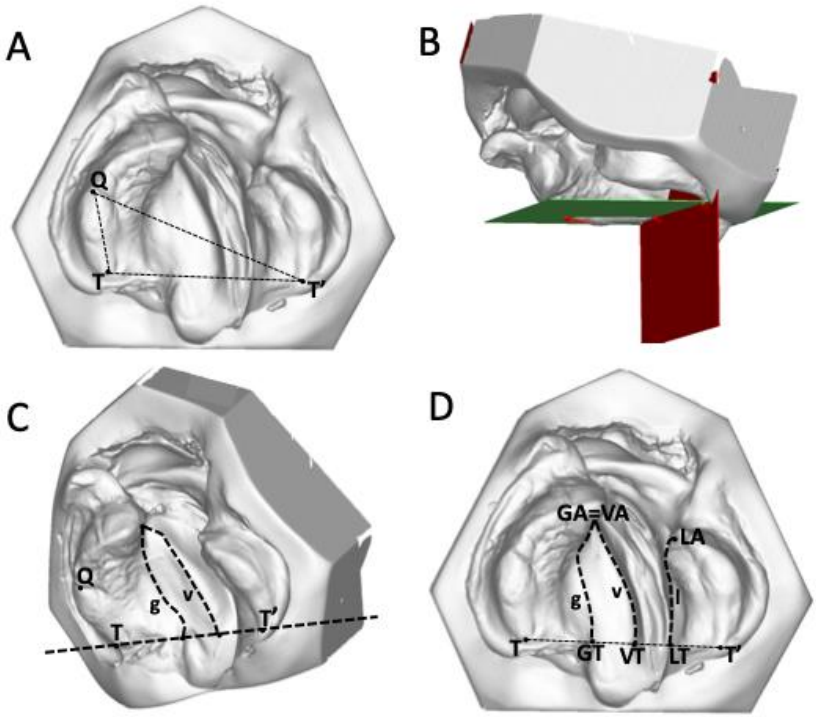

Figure 1. Establishment of a three-dimensional coordinate system. (**A**) and (**B**) A horizontal plane (green) is defined by (Q, T, T'), and a vertical plane (red) is defined by (T, T'). (**C**) and (**D**) The line between VT–VA denotes the vomer edge (v), the line between GT–GA denotes the palatal shelf ridge of the greater segment (g), and the line between LT–LA represents the palatal shelf ridge of the lesser segment (l).

The palatal cleft was delimited by the greater segment's palatal shelf ridge (g) at the junction to the vomer and the lesser segment's shelf ridge (l). The true cleft was delimited by the vomer edge (v) and the lesser segment's palatal shelf ridge (l). The height measurements were performed along the three paths g, l, and v at nine equidistant points each, generated from the ascending order of 0 to 100% (0%, 12.5%, 25%, 37.5%, 50%, 62.5%, 75%, 87.5%, 100%). The height in each point was measured perpendicular to the horizontal plane (Figure 2C, D).

Table 2. Definitions of 3D landmark measurements.

Abbreviation	Description
Cleft area dimensions	
GA/GM/GT–LA/LM/LT	Total palatal cleft area (PCA)
VA/VM/VT–LA/LM/LT	Total true cleft area (TCA)
Transverse dimensions	
GA–LA	Anterior palatal cleft width
GM–LM	Middle palatal cleft width
GT–LT	Posterior palatal cleft width
VA–LA	Anterior true cleft width
VM–LM	Middle true cleft width
VT–LT	Posterior true cleft width
Vertical dimensions[1]	
g-height	Height of the palatal shelf ridge of the greater segment perpendicular to the horizontal plane
l-height	Height of the palatal shelf ridge of the lesser segment perpendicular to the horizontal plane
v-height	Height of the vomer edge perpendicular to the horizontal plane

[1] Vertical dimension measured at nine equidistant points along the paths g, l, and v.

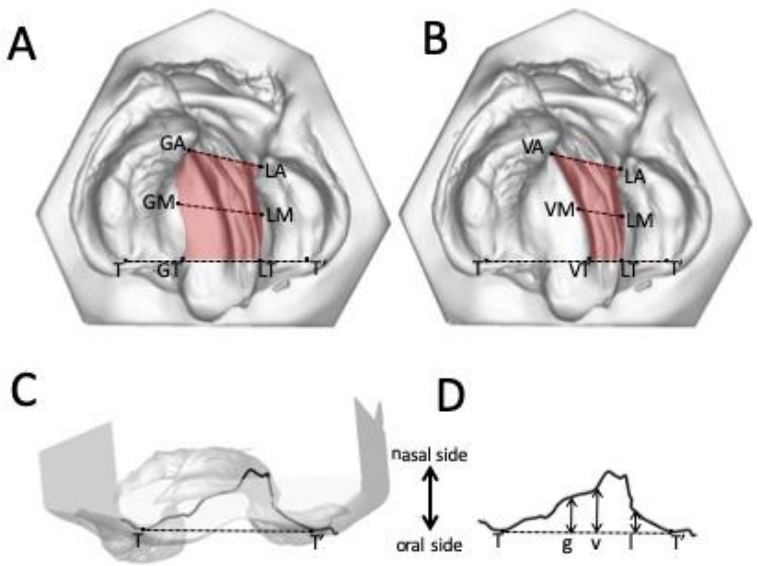

Figure 2. (**A**) Palatal cleft: palatal cleft width (dashed lines) and palatal cleft area (shaded area). (**B**) True cleft: true cleft width (dashed lines) and true cleft area (shaded area). (**C**) and (**D**) The height of the palate to the horizontal plane at the vomer edge (v) and at the greater (g) and lesser (l) palatal shelf ridges.

Connecting corresponding equidistant points from g to l and v to l (0% and 0%, 12.5% and 12.5%, and so forth) led to 8 equidistant quadrangles, which were split into two triangles each, leading to a total of 16 triangles (Figure 3). Surface measurements of defined areas were then approximated as the sum of its comprising triangles.

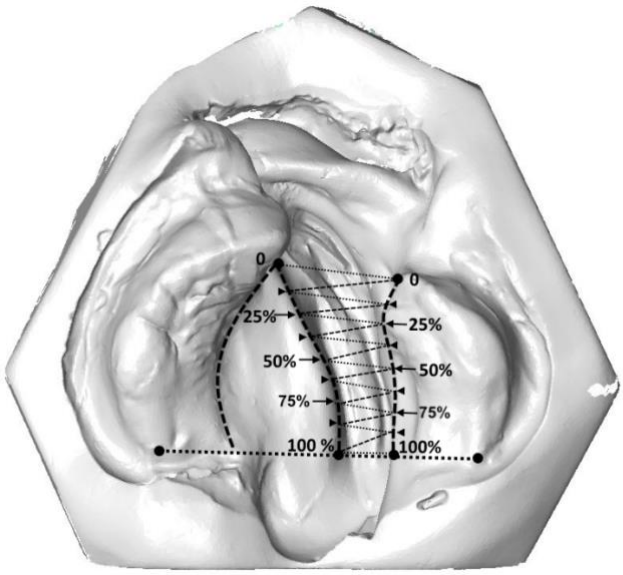

Figure 3. True cleft area measurement connecting equidistant points from the vomer edge to the lesser palatal shelf ridge (0% and 0%, 12.5% and 12.5%, and so forth) led to 8 equidistant quadrangles, which were split into two triangles each, leading to a total of 16 triangles. Surface measurements of defined areas were then approximated as the sum of its comprising triangles.

2.4. Statistical Analysis

The measurements made at time points T0 and T2 were compared using a Wilcoxon signed-ranks test. Statistical significance was assumed at $p < 0.05$. The abovementioned procedures for calculating the cleft width, cleft area, and height of the cleft edges were repeated for 15 of the 45 casts both by the same rater and by a second rater. The differences were investigated to quantify the measurement error of the method according to Dahlberg's formula [17]. The statistical analysis was performed using Stata (version 15.1, StataCorp LLC, Texas, USA).

3. Results

The analysis of landmark positioning in the 3D cast analysis showed that the intrarater measurement errors ranged from 0.7 to 0.9 mm and those for interrater measurements ranged from 0.5 to 1.0 mm.

3.1. Cleft Width

The median palatal cleft width at T0 was 11.4 mm (interquartile range, IQR = 9.8–14.4 mm) in the anterior region (GA–LA), 14.8 mm (IQR = 14.0–15.9 mm) in the midpalatal region (GM–LM), and 13.7 mm (IQR = 12.3–16.7 mm) in the posterior region (GT–LT). The median true cleft width was 13.3 mm (IQR = 10.6–14.4 mm) in the anterior region (VA–LA), 9.9 mm (IQR = 8.1–11.0 mm) in the midpalatal region (VM–LM), and 7.4 mm (IQR = 5.8–10.4 mm) in the posterior region (VT–LT). The narrowing of the palatal and true cleft from T0 to T2 resulted in its width becoming more even from anterior to posterior locations along the cleft (Figure 4). The median palatal cleft width decreased significantly at T2, from 11.4 to 6.5 mm ($z = 3.237$, $p = 0.0012$) in the anterior region (GA–LA), from 14.8 to 9.3 mm ($z = 3.41$, $p = 0.0007$) in the midpalatal region (GM–LM), and from 13.7 to 10.5 mm ($z = 3.18$, $p = 0.0015$) in the posterior region (GT–LT). Similar changes were seen in the true cleft width in the anterior region (VA–LA) (from 13.3 to 6.8 mm, $z = 3.41$, $p = 0.0007$), in the midpalatal region (VM–LM) (from 9.9 to 5.0 mm, $z = 3.41$, $p = 0.0007$), and in the posterior region (VT–LT) (from 7.4 to 4.9 mm, $z = 3.24$, $p = 0.0012$) (Figure 4). The median decrease (from T0 to T2) in cleft width was 38.0% for the palatal cleft, whereas it was 44.5% for the true cleft.

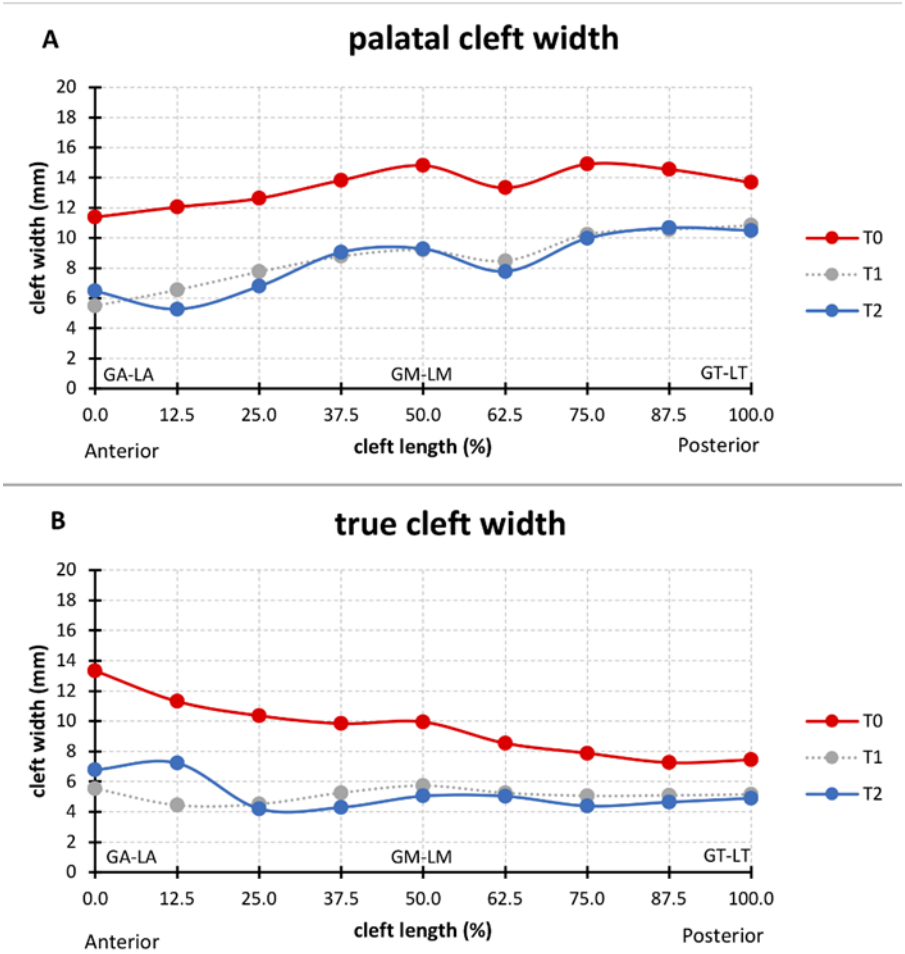

Figure 4. Median (**A**) palatal cleft width (PCW) and (**B**) true cleft width (TCW) before passive plate therapy (T0), after 3–4 month of passive plate therapy (T1), and prior to primary surgery at around 8 months (T2).

3.2. Changes in Palatal and True Cleft Areas

The median total palatal cleft area (PCA) (GA/GM/GT–LA/LM/LT; see Figure 2A) decreased by 31.5% (from T0 to T2), and the median total true cleft area (TCA) (VA/VM/VT–LA/LM/LT; see Figure 2B) decreased by 34.71% (Table 3). In the anterior section, both PCA and TCA were reduced by around one-third (34.4% and 29.2%, respectively). However, in the middle and posterior sections, the reduction in the cleft area was larger for the true cleft than for the palatal cleft. In the middle section, TCA reduced by 29.2% while PCA reduced by 25.5%. The difference was even more pronounced in the posterior section: 41.3% for TCA compared to 18.3% for PCA (Table 3). The median changes from anterior to posterior of each of the eight equidistant quadrangles of the PCA and TCA are displayed in Figure 5.

Table 3. Measured changes in palatal cleft area (PCA) and true cleft area (TCA).

Cleft Area (mm²)	Section		T0 Median (IQR)		T2 Median (IQR)		*p*-Value
PCA	Total	0%–100%	334	(294.9–349.8)	228.8	(205–287.9)	0.0015
	Anterior	0%–25%	75.3	(67.2–93.3)	49.4	(32.0–70.0)	0.0090
	Middle	25%–75%	157.0	(141.5–173.8)	116.9	(99.7–135.0)	0.0076
	Posterior	75%–100%	91.8	(77.5–102.6)	75.0	(61.5–84.2)	0.0090
TCA	Total	0%–100%	185.4	(151.5–220.1)	121.1	(100.2–144.6)	0.0015
	Anterior	0%–25%	56.9	(40.9–66.6)	41.7	(18.1–51.3)	0.0409
	Middle	25%–75%	84.7	(69.6–102.8)	60.0	(42.3–62.2)	0.0007
	Posterior	75%–100%	41.2	(31.5–48.5)	24.2	(20.3–32.35)	0.0012

PCA, palatal cleft area; TCA, true cleft area; IQR, interquartile range.

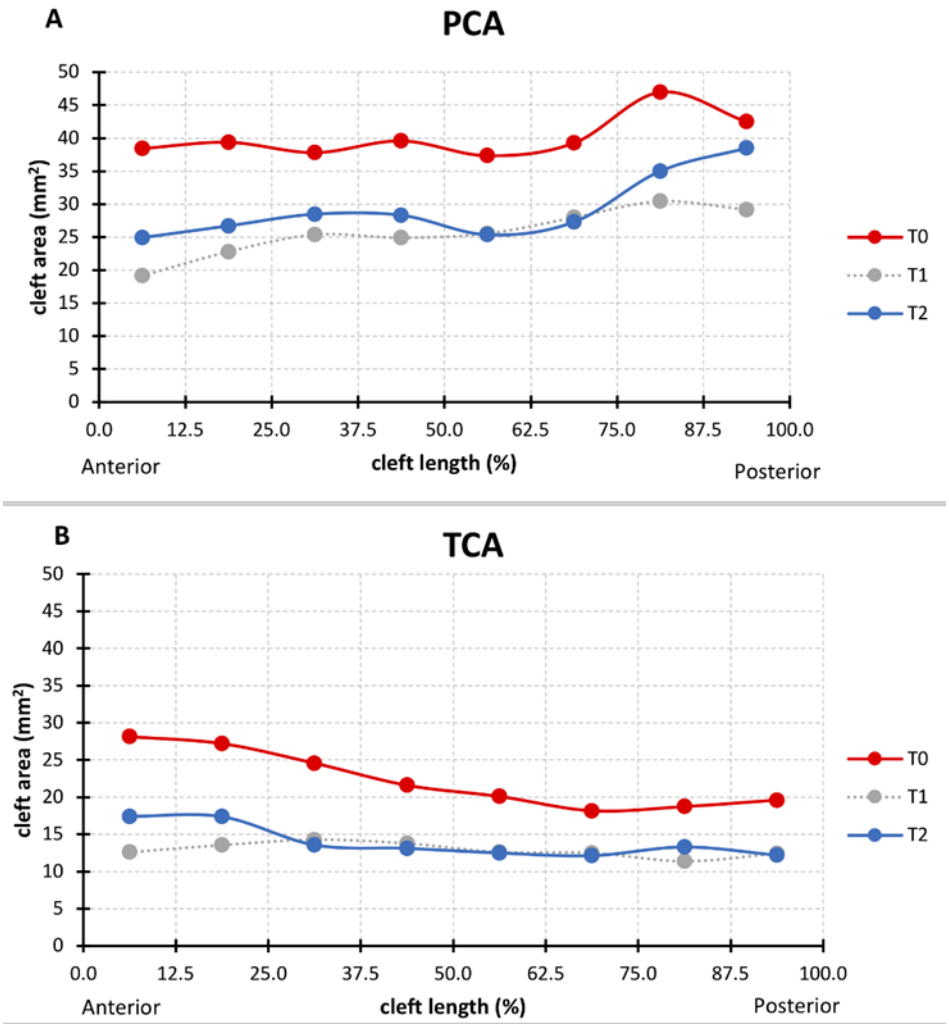

Figure 5. Median (**A**) palatal cleft area (PCA) and (**B**) true cleft area (TCA) at T0, T1, and T2 in eight equidistant quadrangles (0%–12.5%, 12.5%–25%, 25%–37.5%, and so forth) from anterior to posterior.

3.3. Changes in the Height of the Palatal Surface

The height of the palatal surface was measured to the horizontal plane (Q–T/T') along the longitudinal course of the cleft along three different paths: the greater palatal ridge (g), the lesser palatal ridge (l), and the vomer edge (v) (Figure 2C, D). At birth, the greater and lesser palatal shelf ridges followed a horizontal course at a height of around 8 mm, becoming skewed towards the posterior end. Both shelf ridges run at the same level, while the vomer edge paralleled their course at about 2 mm higher (Figure 6). The heights of the greater and lesser palatal shelf

ridges changed from T1 to T2 into a parabolic shape, being highest in the midpalatal section. At (T2), the shelf ridge of the lesser segment still ran parallel to that of the greater segment, but now at 2–3 mm higher. This meant that the shelf ridge of the lesser segment became closer to the course of the vomer edge (Figure 6). The change in the cross-section shape through the midpalatal region (cut through GM and LM perpendicular to the horizontal plane) highlights the change in the height of the palate to the horizontal plane and is displayed in Figure 7.

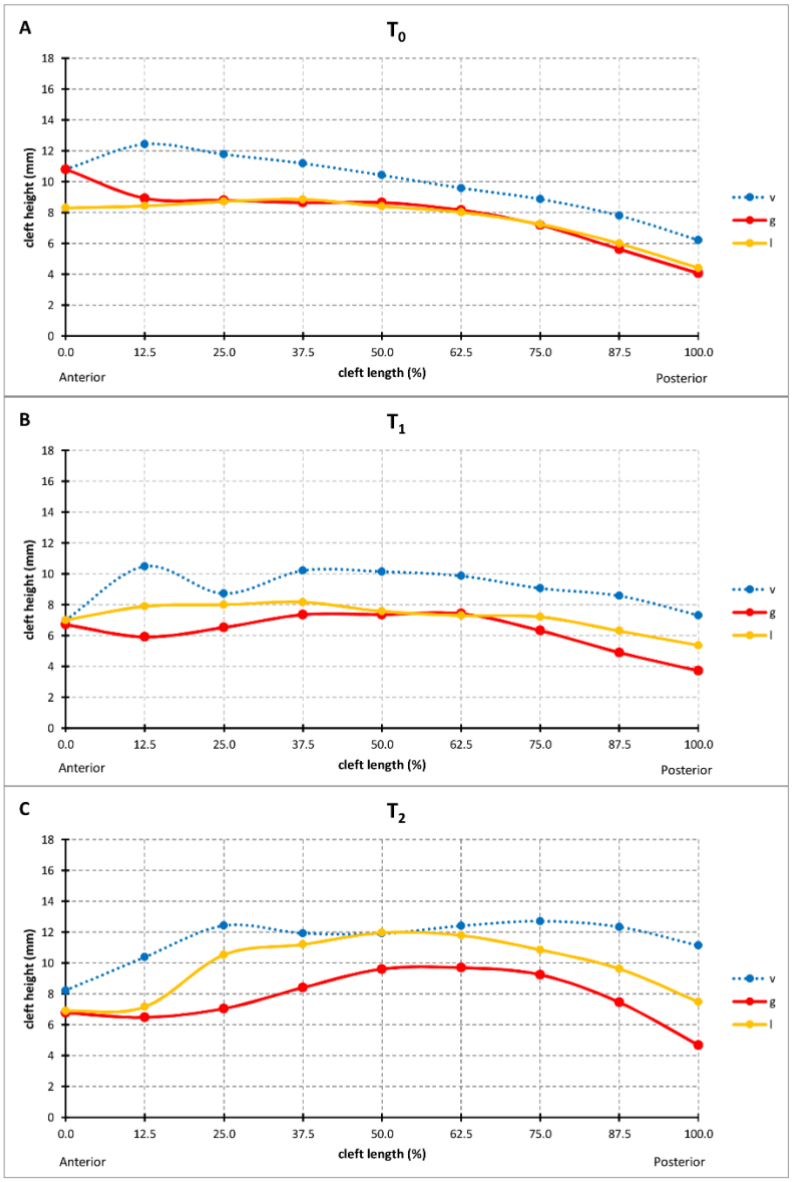

Figure 6. The median vertical height of vomer edge (v height), the junction between the palatal shelf of the greater segment and vomer (g height), and the palatal shelf ridge of the lesser segment (l height) at T0 (**A**), T1 (**B**), and T2 (**C**).

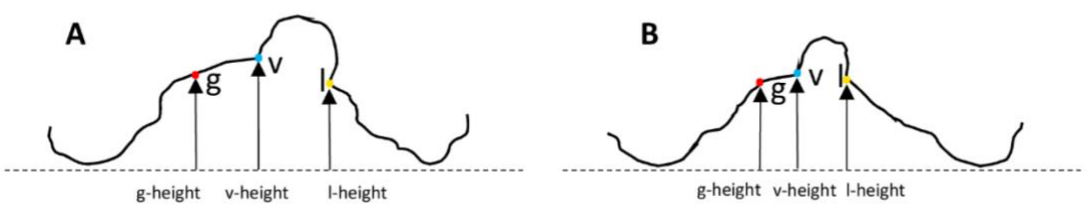

s

Figure 7. Cross-section through GM and LM perpendicular to the horizontal plane, displaying the height of g, v, and l above the horizontal plane at T0 (**A**) and T2 (**B**).

4. Discussion

4.1. Three-Dimensional Analysis

The dimensions and shape of the cleft alveolus and palate play an important role in the outcome of any primary surgery [18]. Different methods are used to measure the cleft dimensions, with some investigators only measuring the separation between two segments anteriorly, whereas others measure the cleft width at several palatal levels or measure the cleft area in relation to the total palatal area [2–7,10–13,18–20]. Aberrant anatomical structures on dental casts pose a major challenge to the clinician attempting to identify and determine the correct anatomical landmarks [20–22]. Vague landmarks are the most important factor contributing to inaccuracy of these measurement, and there is no standard protocol for identifying the points since demarcating these landmarks is extremely difficult [8,12,20,21].

4.2. Cleft Width

The palatal cleft width and true cleft width decreased in all cases, which is consistent with previous reports [3,9,18] (Figure 4). The true and palatal cleft width decreased evenly along its longitudinal course, but slightly less in the posterior region, whereas the main effect was already observed at T1 (Figure 4).

A presurgical reduction in the width of the cleft is considered a positive predictor of the surgical results, because this reduces the undermining mobilization of the tissues [5,23]. We reason this is achieved simply by blocking out the depressions on the plaster cast prior to plate fabrication to keep the palatal shelves and vomer surfaces free and not applying any pressure from the tongue. No gradual trimming of the plate was performed, which contrasts with other techniques such as nasoalveolar moulding (NAM) [5] and the Hotz-type plate [24].

4.3. Changes in the Palatal and True Cleft Areas

Measuring the cleft area indirectly quantifies the shortage of palatal tissue when performing surgical repairs, and this shortage seems to be related to the amount of subsequent maxillary growth disturbances later in life [5]. Assuming that no tissue is freely transplanted into the cleft area in a primary repair, greater tissue shortage during cleft repair leads inevitably to (a) an increased area of secondary wound healing over soft tissue or bone or (b) an increased volume of dead space between tissues. Both effects are typically present but to variable extents depending on the precise surgical technique used, whether it is tissue turnover, tissue shift in the horizontal or vertical direction, and single- or double-layer tissue closure. However, these two effects are considered to equally increase the invasiveness of surgical repair due to more scarring and a greater risk of wound healing disturbances with, for example fistula formation.

It has been proposed that a given ratio between the cleft area and the entire palatal vault surface within the alveolar ridges can help to define the time point when surgical repair leads to minimal side effects on growth [13]. When considering the effect of surgery on future growth, it is therefore important not only to discriminate between the surgical time point and technique, but also whether the surgical repair addresses the closure of the palatal or (in contrast) the true cleft region only—which constitutes only about half the surface area (Table 3)—and thus markedly reduces the degree of tissue shift.

However, in addition to the total amount of tissue shift differing between PCA and TCA, there are also differences in geometry. This becomes clear when the cleft area is divided into eight sections from anterior to posterior (Figure 5). The palatal cleft area was minimal in the central section while being largest in the posterior section (Figure 5A). Clinical translation of this finding means maximized need for tissue shift in the posterior section of the palate. However, in the posterior section the palatal artery might impede free tissue movement, thus resulting in increased tissue tension, which is also a negative factor for wound healing and thus a risk factor for a residual fistula. Indeed, a meta-analysis [25] identified a fistula as being most frequently located in the posterior hard palate section, at the junction with the soft palate.

In the true cleft region, the area of the posterior section was about the same as that in the central section (Figure 5B). If the surgical cleft closure was limited to the true cleft region, it would have to be investigated whether this

could lead to a more homogeneous tissue displacement and tissue tension due to the more even distribution of the area in all sections.

4.4. Changes in the Height of the Palatal Surface

3D changes of the palatal curved surface at different stages have been studied by taking the bilateral tuberosity points, incisal point or canine points, which lacks objectivity and reproducibility [26]. The measurement technique must instead be based on a larger number of data points along a curve denoting the actual height of the palatal segments. Our method offers objectivity, reproducibility, and reliability at different stages (Figure 2C,D). However, the changes measured in the present study cannot be compared to those in previous studies due to differences in the parameters measured and the protocols used when treating cleft lip and palate [27]. With respect to a potential palatal repair after 8 months of pure passive plate therapy, two important discrepancies between TCA and PCA were identified. First, the tissue borders in the true cleft region (the vomer edge and the lesser segment) are vertically closer together than the tissue borders in the palatal cleft region (the greater segment and the lesser segment), thus from a surgical point of view requiring less vertical tissue displacement to come into the same vertical plane for cleft repair, which also minimizes the contiguous amount of dead space (Figure 6C). Second, the tissue borders are higher in the true cleft region than in the palatal cleft region (Figure 7), with this difference being more pronounced in the anterior region (Figure 6C). Thus, a repair following the tissue levels in the true cleft region might allow more space for the tongue in the anterior palatal region to have an undisturbed posture and articulation.

4.5. Clinical Translation of the Findings

The long history of presurgical orthopaedic treatment [28] has led to various technical variations depending on the effect aimed for. Some techniques [29] aim to guide the alveolar positions into an optimal position, not mainly for surgery but rather with the intent to optimize the long-term arch form. The plate is periodically trimmed every couple of weeks to guide the alveolar segments, and the orthopaedic therapy continues after lip surgery and soft palate surgery until when hard palate surgery is performed. However, a large randomized controlled trial failed to demonstrate—aside from the narrowing effect before lip surgery [30]—any persistent effect on arch form [31] or occlusion [32] from this specific type of presurgical orthopaedics (Hotz-type plate). Those authors concluded that lip surgery and subsequent palatal surgery overrode the forming effect of presurgical orthopaedics. We therefore refrained from using grinding to actively guide the alveolar segments, instead using a purely passive type of plate therapy similar to the passive appliance of Huddart [28] but without extraoral wires.

In line with the findings of the aforementioned randomized trial, two main ways of clinical reasoning were observed: either presurgical orthopaedics are abandoned and one relies on the palatal shape changes that take place after lip surgery, or the presurgical orthopaedics focus mainly on the narrowing of the anterior cleft region to facilitate the primary repair in the lip, alveolus, and nose region (in NAM), with the palatal shape changes not being taken into account in the primary surgery.

However, the present finding of narrowing of the true cleft region would also allow a third clinical reasoning—using the effect of presurgical orthopaedics in exchange for performing a separate lip repair before palatal closure. As with most one-stage cleft repair techniques, the effect of preoperative orthopaedics is used in exchange for performing a separate lip repair prior to palatal closure. If the results can be confirmed in further studies, the common belief that early isolated lip surgery is necessary to provide optimal conditions for later palatal repair could be questioned.

4.6. Strengths and Limitations

We used the vomer edge (also called "Poutriquet's ridge") [1, 16] and innominate sulcus [16] as new anatomically reproducible landmarks that can be easily used to measure the true cleft width, area, and curvature in all dimensions (Figure 2). To the best of our knowledge, no previous 3D study has differentiated between TCA and PCA. Our measurement errors were found to be well within the ranges found in previous similar studies [8]. The landmarks used in the present study have biological correlates or distinct morphologies that facilitate their identification with high precision and reproducibility [22], which probably explains why the errors in the interrater transverse measurements were less than 0.5 mm, which is lower than that in all previous studies [8,21]. Moreover,

no previous study has measured the height of the vomer edge to the horizontal plane. The errors of our interrater measurements were within the acceptable limit of 1.0 mm, making it a practical cleft landmark with a defined cleft anatomical correlate—it is the zenith of the palatal vault prior to surgery (Figure 2D).

The limitation of our study were the small sample size and the lack of a control group without passive plate therapy. We cannot draw any conclusion about whether the passive plate is also purely passive towards the intrinsic growth of each palatal half. Further, no data on a potential long-term effect of the plate therapy on the growth or shape of segments can be provided. This will be further complicated by the additional bias of the wide range of surgical techniques. Future studies involving larger numbers of patients and longer observation times are necessary, as well as 3D evaluations of a control group that does not receive passive plate therapy, in order to fully appreciate the effect of on the growth, remodelling and relocation of the palatal segments and vomer.

5. Conclusions

In conclusion, few studies have investigated the morphological changes of the cleft palate width by using 3D standardized, reproducible landmarks in unilateral cleft lip and palate patients. We have introduced the vomer edge for establishing a validated measuring method for the width, area, and height of the true cleft. To the best of our knowledge, this is the first 3D study to show the 3D morphological changes of a pure passive plate therapy over a long period of 8 months in the absence of previous lip surgery. In the investigated cohort without prior lip repair, passive plate therapy provided favourable anatomical conditions for subsequent surgical palatal repair.

Author Contributions: Conceptualization, A.A.M.; data curation, P.N.; formal analysis, B.K.B. and M.D.; funding acquisition, P.N., C.V., and A.A.M.; investigation, P.N. and B.K.B.; methodology, P.N., B.K.B., M.D., and A.A.M.; project administration, A.A.M.; resources, C.V. and A.A.M.; software, P.N. and M.D.; supervision, M.D., C.V., and A.A.M.; validation, P.N. and B.K.B.; visualization, P.N., M.D., and C.V.; writing—original draft, P.N. and B.K.B.; writing—review and editing, P.N., B.K.B., M.D., C.V., and A.A.M. All authors have read and agreed to the published version of the manuscript.

Funding: This research was partially funded from a research grant of the Freiwillige Akademische Gesellschaft (FAG), Basel, Switzerland.

Conflicts of Interest: The authors declare no conflict of interest. The funders had no role in the design of the study; the collection, analysis, or interpretation of data; in the writing of the manuscript; or the decision to publish the results.

References

1. Veau, V. *Division Palatine. Anatomie. Chirurgie. Phonétique. Avec la Collaboration de Mlle S. Borel.*; Impr. Darantière Masson et Cie éditeurs: Dijon/Paris, France, 1931.
2. Stöckli, P.W. Application of a quantitative method for arch form evaluation in complete unilateral cleft lip and palate. *Cleft Palate J.* **1971**, *8*, 322–341.
3. Grabowski, R.; Kopp, H.; Stahl, F.; Gundlach, K.K.H. Presurgical orthopaedic treatment of newborns with clefts - functional treatment with long-term effects. *J. Cranio-Maxillofacial Surg.* **2006**, *34*, 34–44.
4. Wada, T.; Miyazaki, T. Treatment principles for the changing arch form in children with complete unilateral cleft lips and palates. *Cleft Palate J* **1976**, *13*, 273–283.
5. Peltomäki, T.; Vendittelli, B.L.; Grayson, B.H.; Cutting, C.B.; Brecht, L.E. Associations between Severity of Clefting and Maxillary Growth in Patients with Unilateral Cleft Lip and Palate Treated with Infant Orthopedics. *Cleft Palate-Craniofacial J.* **2001**, *38*, 582–586.
6. Jorge, P.K.; Gnoinski, W.; Vaz Laskos, K.; Felício Carvalho Carrara, C.; Gamba Garib, D.; Okada Ozawa, T.; Andrade Moreira Machado, M.A.; Pinelli Valarelli, F.; Oliveira, T.M. Comparison of two treatment protocols in children with unilateral complete cleft lip and palate: Tridimensional evaluation of the maxillary dental arch. *J. Craniomaxillofac. Surg.* **2016**, *44*, 1117–1122.
7. Yamanishi, T.; Nishio, J.; Kohara, H.; Hirano, Y.; Sako, M.; Yamanishi, Y.; Adachi, T.; Miya, S.; Mukai, T. Effect on Maxillary Arch Development of Early 2-Stage Palatoplasty by Modified Furlow Technique and Conventional 1-Stage Palatoplasty in Children With Complete Unilateral Cleft Lip and Palate. *J. Oral Maxillofac. Surg.* **2009**, *67*, 2210–2216.
8. Seckel, N.G.; Van der Tweel, I.; Elema, G.A.; Specken, T.F.J.M.C. Landmark positioning on maxilla of cleft lip and palate infant - A reality? *Cleft Palate-Craniofacial J.* **1995**, *32*, 434–441.
9. Shetty, V.; Agrawal, R.K.; Sailer, H.F. Long-term effect of presurgical nasoalveolar molding on growth of maxillary arch in unilateral cleft lip and palate: Randomized controlled trial. *Int. J. Oral Maxillofac. Surg.* **2017**, *46*, 977–987.
10. Mazaheri, M.; Harding, R.L.; Cooper, J.A.; Meier, J.A.; Jones, T.S. Changes in arch form and dimensions of cleft patients.

Am. J. Orthod. **1971**, *60*, 19–32.
11. Schmidt-Flath, I.; Fränkel, R.; Grabowski, R.; Opitz, C.; Wiemann, C. Methoden zur Ausmessung des Säuglingskiefers, des Milch- und bleibenden Gebisses beim Spaltträger. *Fortschr. Kieferorthop.* **1972**, *33*, 457–476.
12. Berkowitz, S.; Pruzansky, S. Stereophotogrammerty of serial casts of cleft palate. *Angle Orthod.* **1968**, *38*, 136–149.
13. Berkowitz, S.; Duncan, R.; Evans, C.; Friede, H.; Kuijpers-Jagtman, A.M.; Prahl-Anderson, B.; Rosenstein, S. Timing of cleft palate closure should be based on the ratio of the area of the cleft to that of the palatal segments and not on age alone. *Plast. Reconstr. Surg.* **2005**, *115*, 1483–1499.
14. Leighton, B.C. Morphologische Variationender Alveolarbögen beim Neugeborenen. *Fortschr. Kieferorthop.* **1976**, *37*, 8–14.
15. Botticelli, S.; Pedersen, T.K.; Küseler, A.; Nørholt, S.E.; Cattaneo, P.M. Novel 3-D Analysis for the Assessment of Cleft Dimensions on Digital Models of Infants With Unilateral Cleft Lip and Palate. *Cleft Palate. Craniofac. J.* **2019**, *56*, 127–133.
16. Malek, R. *Cleft Lip and Palate: Lesions, Pathophysiology and Primary Treatment*, 1st ed.; Martin, D., Ed.; CRC Press: London, UK, 27 November 2000; ISBN 978-1853174919.
17. Dahlberg, G. Statistical Methods for Medical and Biological Students. *Br. Med. J.* **1940**, *2*, 358.
18. Robertson, N.R.; Fish, J. Early dimensional changes in the arches of cleft palate children. *Am. J. Orthod.* **1975**, *67*, 290–303.
19. Long, R.E.; Daskalogiannakis, J.; Mercado, A.M.; Hathaway, R.R.; Fessler, J.; Russell, K.A. The americleft project: Plaster dental casts versus digital images for GOSLON yardstick ratings when used in intercenter comparisons. *J. Craniofac. Surg.* **2017**, *28*, 1269–1273.
20. Ye, B.; Ruan, C.; Hu, J.; Yang, Y.; Ghosh, A.; Jana, S.; Zhang, G. A Comparative Study on Dental-arch Morphology in Adult Unoperated and Operated Cleft Palate Patients. *J. Craniofac. Surg.* **2010**, *21*, 811–815.
21. Brief, J.; Behle, J.H.; Stellzig-Eisenhauer, A.; Hassfeld, S. Precision of landmark positioning on digitized models from patients with cleft lip and palate. *Cleft Palate. Craniofac. J.* **2006**, *43*, 168–173.
22. Oxnard, C.E. The measurement of form: Beyond biometrics. Sausages and stars, dumbbells and doughnuts: Peculiar views of anatomical structures. *Cleft Palate J.* **1986**, *23*, 110–128.
23. Santiago, P.E.; Grayson, B.H.; Cutting, C.B.; Gianoutsos, M.P.; Brecht, L.E.; Kwon, S.M. Reduced Need for Alveolar Bone Grafting by Presurgical Orthopedics and Primary Gingivoperiosteoplasty. *Cleft Palate-Craniofacial J.* **1998**, *35*, 77–80.
24. Hotz, M.M.; Gnoinski, W.M.; Nussbaumer, H.; Kistler, E. Early maxillary orthopedics in CLP cases: Guidelines for surgery. *Cleft Palate J.* **1978**, *15*, 405–411.
25. Bykowski, M.R.; Naran, S.; Winger, D.G.; Losee, J.E. The rate of oronasal fistula following primary cleft palate surgery: A meta-analysis. *Cleft Palate-Craniofacial J.* **2015**, *52*, e81–e87.
26. Isogawa, N.; Ochiai, S.; Mito, T.; Kindaichi, J.; Ishibashi, N.; Takagi, Y.; Ishikawa, M. Three-Dimensional Comparison in Palatal Forms Between Modified Presurgical Nasoalveolar Molding Plate and Hotz's Plate Applied to the Infants with Unilateral Cleft Lip and Palate. *Singapore Dent. J.* **2010**, *31*, 36–42.
27. Mishima, K.; Sugahara, T.; Mori, Y.; Sakuda, M. Three-Dimensional Comparison between the Palatal Forms in Infants with Complete Unilateral Cleft Lip, Alveolus, and Palate (UCLP) with and without Hotz's Plate. *Cleft Palate-Craniofacial J.* **1996**, *33*, 245–251.
28. Huddart, AG. Presurgical changes in unilateral cleft palate subjects. *Cleft Palate J.* **1979**, *16*, 147–157.
29. Gnoinski, W. *Infant Orthopedics and Later Orthodontic Monitoring for Unilateral Cleft Lip and Palate Patients in Zurich*; Bardach, J., Morris, H., Eds.; WB Saunders Co: Philadelphia, PA, USA, 1990.
30. Prahl, C.; Kuijpers-Jagtman, A.M.; van't Hof, M.A.; Prahl-Andersen, B. A randomised prospective clinical trial into the effect of infant orthopaedics on maxillary arch dimensions in unilateral cleft lip and palate (Dutchcleft). *Eur. J. Oral Sci.* **2001**, *109*, 297–305.
31. Bongaarts, C.A.M.; van 't Hof, M.A.; Prahl-Andersen, B.; Dirks, I.V.; Kuijpers-Jagtman, A.M. Infant orthopedics has no effect on maxillary arch dimensions in the deciduous dentition of children with complete unilateral cleft lip and palate (Dutchcleft). *Cleft Palate. Craniofac. J.* **2006**, *43*, 665–672.
32. Noverraz, R.L.M.; Disse, M.A.; Ongkosuwito, E.M.; Kuijpers-Jagtman, A.M.; Prahl, C. Transverse dental arch relationship at 9 and 12 years in children with unilateral cleft lip and palate treated with infant orthopedics: A randomized clinical trial (DUTCHCLEFT). *Clin. Oral Investig.* **2015**, *19*, 2255–2265.

7. Second study:

The biomechanical evaluation of magnetic forces to drive osteogenesis in newborn's with cleft lip and palate

Study design: Dr. Prasad Nalabothu, Prof. Michel Dalstra

Financing: FAG (Voluntary Academic Association): CHF 13,406

Project leaders: Professor Dr. med. dent. Carlalberta Verna

Publication: First authorship, Journal of Materials Science: Materials in Medicine, Impact factor 2.46 (2020), Ranking 7876 (Q2) in "Biomedical Engineering" and "Bioengineering".

Journal of Materials Science: Materials in Medicine (2020) 31:79
https://doi.org/10.1007/s10856-020-06421-6

ENGINEERING AND NANO-ENGINEERING APPROACHES FOR MEDICAL DEVICES

Original Research

The biomechanical evaluation of magnetic forces to drive osteogenesis in newborn's with cleft lip and palate

Prasad Nalabothu [1,2] · Carlalberta Verna[1] · Markus Steineck[1] · Andreas Albert Mueller[2] · Michel Dalstra[1]

Received: 26 February 2020 / Accepted: 20 July 2020 / Published online: 20 August 2020

Abstract

This study examined the potential for dental magnets to act as a driving force for osteogenesis in the palate of newborns with a unilateral cleft lip and palate. In the first part of the study dental magnets were arranged in a set up mimicking a distraction device and the curves of the magnetic attraction force versus gap distance curves generated, with and without the presence of palatal rugae tissue in between both sides of the distraction device. The attraction forces ranged from 1 to 12 N depending on the gap distance and the presence of soft tissue in the gap. In the second part of the study these forces were used as input for a 3D finite element model of the palate of a newborn affected by unilateral cleft lip and palate. In the analysis of load transfer, it was found that the strains generated by a magnetically induced distraction exceed 1,500 μstrain suggesting that bone locally is submitted to mild overload leading to bone apposition.

Graphical Abstract

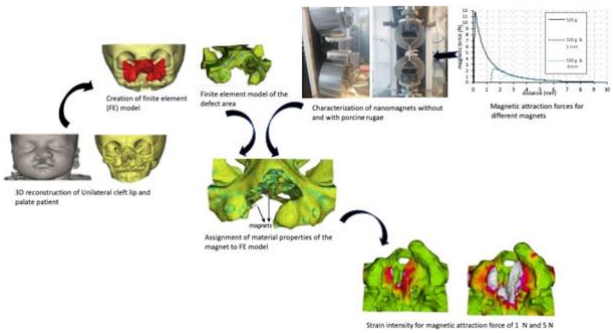

1 Introduction

Cleft lip and palate (CL/P) is the most common presenting congenital condition of the face and cranial bones [1]. It is the most frequent craniofacial malformation affecting 1:500 to 1:700 live births worldwide with tremendous variations across geographic areas, ethnic groups and socioeconomic status [2]. Cleft palate closure by surgery depends upon the adequacy of available palatal mucosal tissue. Insufficiency of such soft tissue is a cause for concern in the closure of severe wide clefts of the hard palate [3]. The tissue shortage makes it necessary to extensively mobilize the tissue adjacent to the cleft, leading to a wider tissue wound with consequent scarification due to the wound healing process. During wound repair, various

These authors contributed equally: Andreas Albert Mueller, Michel Dalstra

✉ Prasad Nalabothu
prasad.nalabothu@unibas.ch

[1] Department of Paediatric Oral Health and Orthodontics, University Center for Dental Medicine UZB, Basel, Switzerland

[2] Department of Oral and Craniomaxillofacial Surgery, University Hospital Basel, Basel, Switzerland

tissues are involved, including palatal skeletal muscle, skin and mucosa. Inadvertently, the CL/P surgery leaves scars, which may interfere with normal growth and development of the midface and dentition [4].The other complications include insufficient palatal muscle function, which hampers swallowing, sucking and speech [5].

Tissue expansion techniques, which have gained popularity in other areas of the body for reconstructive needs, have been proposed for cleft palate repair [6]. The tissue expansion techniques described for cleft palate repair are categorized into two broad categories: mucoperiosteal tissue expansion (MTE) and distraction osteogenesis (DO). The procedure of MTE intends to expand purely the soft tissue overlying the bone. It was initially employed for fistula closure and later extended for the repair of primary cleft palate [7]. The principle employed is that of an expander placed under the mucosa on either ends of the palatal defect in an effort to generate additional soft tissue that can be used to close the defect. However, on a contrary note seven out of eleven patients had fistulas and some of the patients were found to require premature removal of the tissue expanders due to cyanosis or pale tissue [7]. So far, the results seem to raise many doubts and dilemmas and its effectiveness is still questionable.

Distraction osteogenesis (DO) is a method of increasing bone volume by controlled daily separation of the bone ends on either side of a surgical bone cut. The increase in bone volume leads to expansion of its overlying soft tissue. Callus formation occurs after 5 to 7 days, followed by bony ingrowth. When the required bone length has been achieved, the distraction device remains in place to serve as a rigid skeletal fixation until maturation of the generated new bone is achieved in the consolidation period [8]. Till date, there is to our knowledge only one case report of distraction treating palatal fistula in adults [9] yet unfortunately it provides little evidence supporting the efficacy of DO in cleft palate repair.

The periosteal distraction osteogenesis (PDO) is a variation of DO, where the gradual tissue separation is made between the periosteum and the bony surface, allowing at the same time for new bone formation without corticotomy [10] and expansion of the overlying soft tissues, such as periosteum, muscle and skin.

Static magnetic fields have been used for bone formation in medical research under a weak magnetic force for a long period [11]. To understand the mechanism of the mucoperiosteal tissue expansion and tissue formation, the distribution of stresses and strains within the periosteal tissue is required.

Computational Finite Element (FE) modelling of the tissue provides a quantified estimate of the stresses and strains generated by a magnetic force through the mucoperiosteal tissue to the underlying bone. The irregular geometry of the periosteal tissue and microarchitecture of the underlying bone in the unilateral cleft models has been simplified in previous models, despite the fact that such differential anatomical features can significantly influence the spatial stress distribution in the palate [12]. To date there is no study investigating the mechanical loading during periosteal tissue expansion in cleft palate of newborns with unilateral clefts.

The objective of this study is to quantify the stresses and strains in the palate of a newborn with a unilateral cleft lip and palate (UCLP) simulating the periosteal loading through magnetic forces and to verify whether the loading could reach the threshold necessary for bone formation. The early formation of new bone would reduce the gap and therefore the strain induced by the surgical closure. As at this stage no *in-vivo* load transducers can be placed, patient- specific finite element modelling is the obvious approach to assess the magnetic load transfer across the neonatal palate.

2 Materials and methods

The study consisted of two parts. Firstly, the magnitude of dental magnets in various implant-like *in-vitro* setups were measured. Data from these experiments were subsequently used as input for a 3D FE-model of the cleft palate of newborn to assess the palatal load transfer.

2.1 Experimental characterization of the dental magnets

Two different types of magnets were used for testing (Dyna WR magnets, Dyna Dental Engineering B.V., Halsteren, Netherlands). The dental magnets were disc-shaped with dimensions: 1.7 mm (02MS1 Dyna WR magnet S3) and 2.7 mm height (02MS2 Dyna WR magnet S5), both with 4.5 mm diameter. The 1.7 mm magnet (S3) had a nominal attachment force of 300 g, whereas the 2.7 mm magnet (S5) had 500 g. The magnets are made of Neodymium/Boron/Iron alloy and belong to the group of rare earth or permanent magnets. The magnets were glued onto two plastic strips in five configurations (a single magnet, two in a row, etc. up to five in a row). Each strip was mounted into the opposing grips of a universal material testing machine (Instron® 3344 equipped with a 100 N load cell; Instron, Norwood, Massachusetts, USA) (Fig. 1a). The initial distance between the opposing strips with magnets was 10 mm and this gap was closed by the testing machine at a speed of 10 mm/min. A continuous readout of the attraction force values and gap distance was recorded, enabling the construction of force/distance plots. The experiments were repeated with a 2 mm and 4 mm thick slice of porcine palatal rugae tissue (obtained from a local butcher shop),

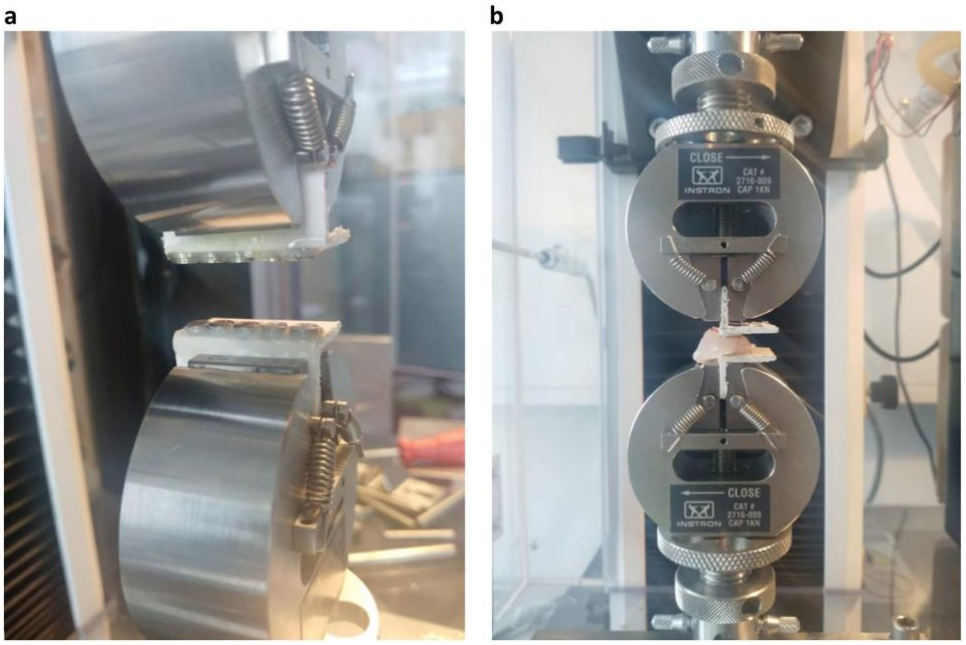

Fig. 1 a Magnets mounted in strips for testing on Universal material testing machine (Instron, Norwood, Massachusetts, USA). b Porcine rugae tissue with a thickness of 4 mm between the magnets

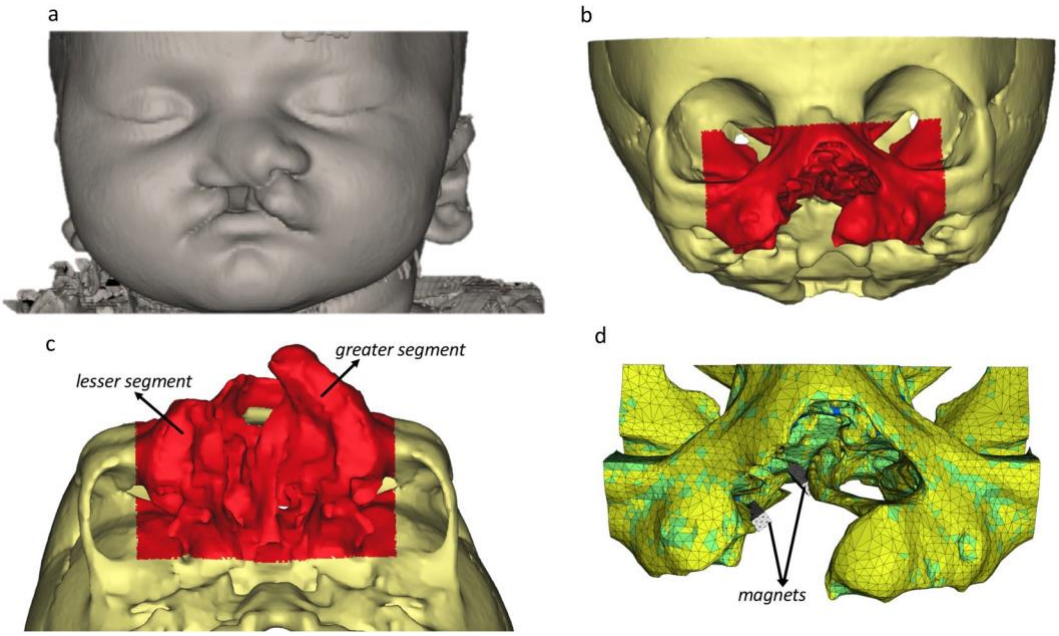

Fig. 2 From CT scan to FE-model. a The 3D reconstructions of the soft and hard tissues, b Frontal view of the region of interest for the FE model c Palatal view of the region of interest for the FE model d and the FE model of the dental magnet partially visible

placed between the magnets (Fig. 1b), simulating the fact that the magnets, once in use, would be implanted subcutaneously.

2.2 Creation of the FE-model

A computerized tomography (CT) scan of a 2-week old newborn with a unilateral cleft lip and palate from an anonymized database following the principles expressed in the Declaration of Helsinki was made available. The scans were imported into dedicated image analysis software (Mimics v.19, Materialise, Leuven, Belgium) and a 3D surface model was generated by thresholding and selecting only the hard tissues of the cranium and maxilla (Fig. 2a). The region of interest was further reduced by virtually cutting away everything except the mid-face (Fig. 2b, c). Two sides of a bone distraction/generation implant were constructed as two parallel bars ($5 \times 6 \times 23$ mm^3) and each was

Table 1 Mechanical properties of the materials used in the present study. For the different bone tissues (1 until 10) the percentage signifies the cumulative amount of bone elements belonging to this specific tissue

Material	Apparent Density (gr/cm^3)	Young's Modulus (MPa)	Poisson's Ratio (-)	Yield Strength	
				Compressive (MPa)	Tensile (MPa)
Bone 1 (0.1%)	0.04	5	0.4	−0.06	0.04
Bone 2 (0.5%)	0.10	51	0.4	−0.61	0.40
Bone 3 (30.9%)	0.18	157	0.4	−1.89	1.26
Bone 4 (89.6%)	0.26	351	0.4	−4.22	2.81
Bone 5 (97.8%)	0.36	677	0.4	−8.12	5.41
Bone 6 (98.8%)	0.50	1212	0.4	−14.54	9.70
Bone 7 (99.4%)	0.66	2115	0.4	−25.37	16.92
Bone 8 (99.8%)	0.83	3752	0.4	−45.02	30.02
Bone 9 (99.9%)	1.20	7226	0.4	−86.72	57.81
Bone 10 (100%)	1.90	18048	0.4	−216.58	144.38
Implant	–	100	0.4	–	–

placed at either side of the cleft (Fig. 2d). Using the program's FE module, the model, including the two implant bars, was transformed into a 3D FE-mesh consisting of 238,243 4-node tetrahedral elements with 43,822 nodes. The position of the centroid of each element was calculated and a grey value was associated to it, based on spatial interpolation of the grey values of the nearest voxels. Using arithmetic relationships between grey values, apparent densities and Young's moduli, relevant material properties were assigned to the elements [12–15] (Table 1). Subsequently, the Young's moduli were stratified into ten material property groups, ranging from 5.2 MPa, representing very low-density cancellous bone (ρ_{app} = 0.04 gr/cm^3) to 18,050 MPa, representing high density cortical bone (ρ_{app} = 1.90 gr/cm^3). The FE-model was then exported from the image analysis program in NASTRAN format and imported into an FE-analysis program (Strand7, Sydney, Australia). The material properties of the bone were assumed non-linear, as the stress-strain curves for the bone in the ten material property groups were adapted such that the bone would behave as a perfectly plastic material with a 150 per cent higher compressive strength than a tensile strength [16].

2.3 Preprocessing and FE-analysis

Prior to the analysis the boundary conditions were defined by restraining the degrees of freedom of the nodes on the cut border surfaces perpendicular to these surfaces of the model. The nodes were allowed to move in the plane of these border surfaces to simulate residual stiffness of the (non-modeled) rest of the skull.

External forces were assigned to the two facing sides of either bar implant. The force magnitude derived from the abovementioned experiments with the dental magnets, while the direction followed from the direction of mutual attraction. The FE-analysis was conducted with the above- mentioned material considerations, boundary conditions and external loading, using a non-linear solver with logarithmically increasing increments from 0.01 to 1 (100% load). The various components and invariants of the deformations, stresses and strains were calculated and used for subsequent post-processing.

3 Results

3.1 Experimental characterization of dental magnets

The experimental force/distance curves of each magnet with different combinations were obtained. The combination of two oppositely placed single 500 g magnets yielded a maximum attraction force of 2.8 N, right before the two magnets came in contact with each other and compressive forces started to develop. Adding up to 5 magnets on either side of the testing device increased the attraction force to 11.7 N (Fig. 3). The distance between the magnets, however, had a significant influence on the magnitude of the attraction force. When the separation between the magnets is 1 mm the attraction forces are merely 1.0 and 4.6 N for a set of one and five opposing magnets, respectively. Adding a layer of porcine palatal rugae tissue in itself did not influence the test curves, as long as the two sides were sufficiently apart. However, the presence of rugae tissue prevented the magnets to come closer together, which in turn prevented the attraction forces to reach levels seen for the curves without rugae tissue present (Fig. 4).

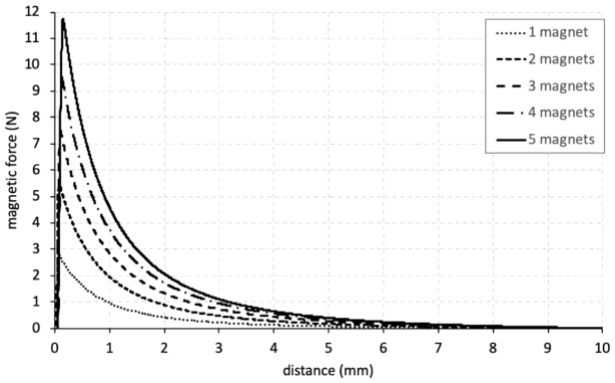

Fig. 3 The magnetic attraction forces as a function for the distance between the magnets for one until five magnets

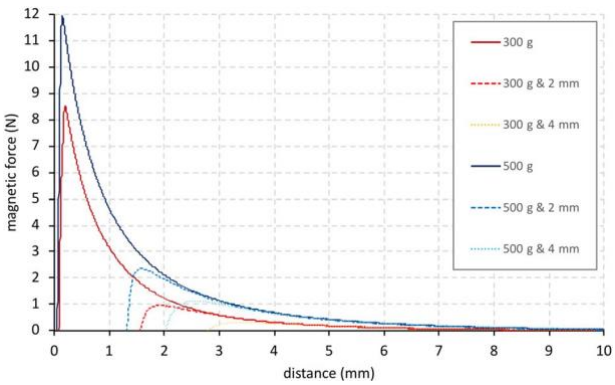

Fig. 4 The magnetic attraction forces for five 300 and 500 gram magnets with either no or 2 mm thick or 4 mm thick porcine rugae

3.2 Numerical assessment of palatal loading through dental magnets

The strain components in the X- (coronal), Y- (medial/lateral) and Z- (anterior/posterior) are different in each direction. The application of magnetic attraction forces of 1 N to the implant bars of the FE-model would represent the force level corresponding to the presence of rugae tissue at a separation of 3 to 4 mm between the two sides of the implant design, assuming the presence of five 500g-magnets. In the Y-direction, which approximates closely the direction of the magnetic forces, the strains are predominantly localized in the palatal shelf of the lesser segment and vomer edge (Fig. 5b). In the X- direction, the largest strains are concentrated in the posterior part of the vomerine edge of the cleft (Fig. 5a), while in the Z- direction the strains are mainly seen in the middle portion of greater segment's palatal shelf ridge (Fig. 5c). The distribution of the von Mises strains, a measure for the overall strain intensity, showed the largest values on both sides of the cleft and reached values between 750 and 1,500 µstrain (Fig. 5d).

The application of an attraction force of 5 N exceeded the experimental results with rugae tissue present and would thus represent an overestimation of the magnetic forces. In this case, the strain levels exceeded 1,500 µstrain. For the coronal (X-) direction the strains exceeding 1,500 µstrain are found in the vomerine ridge, in the palatal shelf of the lesser and in the greater segments of palatal shelf ridge (Fig. 6a). In the medial/lateral (Y-) direction the maximum strains are found on the palatal shelf of the lesser and greater segment and on the vomerine surface (Fig. 6b) and in the antero-posterior (Z-) aspect, the maximum strains are found on the greater segment of the palatal shelf ridge (Fig. 6c). The highest von Mises strains are found on both sides of the palatal cleft segment (Fig. 6d).

Visualizing in more detail at where in the model the strain levels are >1,500 µstrain, it can be seen that these occur predominantly in the direct vicinity of the cleft (Fig. 7). Although for the magnetic force of 1 N this limit has just been reached, the 5 N magnetic force caused a substantially larger area of periosteal tissue to be strained at >1,500 µstrain.

4 Discussion

The aim of this study was to assess whether dental mag- nets have the potential to act as a device to generate palatal bone tissue. Harold Frost hypothesized, in his Mechanostat theory, that the amount of tissue being formed (or resorbed) is dependent on the actual load level it is subjected to: a) Bone strained with less than 1,000 µstrain is in a state of disuse, which could lead to bone resorption and net bone loss [17–19]. b) Bone with 1,000–1,500 µstrain is in an adaptive state, whereby no bone is either lost or gained. c) Bone strained to more than 1,500 µstrain is in a state of mild overload and new bone will be formed. d) Finally, towards the upper limit of this window (15,000 µstrain) a case of severe overload might occur with the risk of fracture. Therefore, if a minimum strain level of 1,500 µstrain is to be achieved for bone apposition, a detailed insight in the palatal load transfer mechanism in newborns with cleft lip and palate is required.

To see whether dental magnets can generate sufficiently high forces, several set-ups were tested, including the absence or presence of rugae tissue between the magnets. For this, palatal rugae samples were excised from a pig's head, obtained at a local butchery, as porcine soft tissue is generally seen as to come close to the human equivalent. Depending on the number of magnets and the inter-magnet distance, attraction forces in the order of magnitude of 1 to 10 N were measured. It should be noted here, however, that the experimental set-up is not meant as the design for a

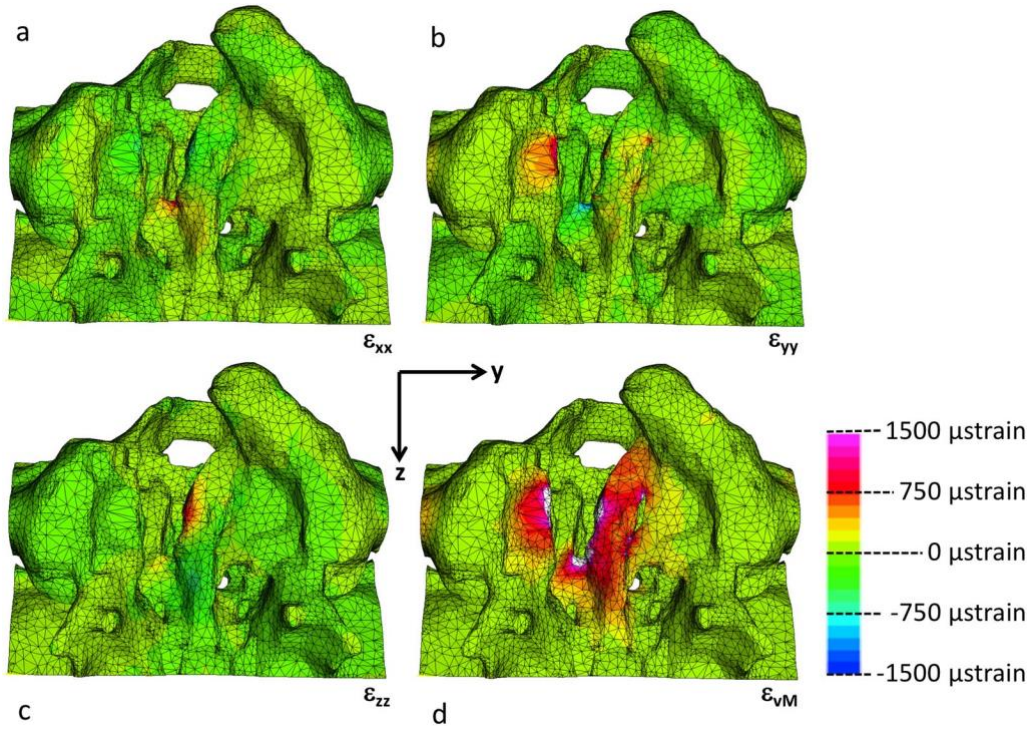

Fig. 5 The distribution of the three orthogonal strain components von Mises strains for magnetic attraction forces of 1 N a palatal view with the X-axis pointing coronally, b Y-axis pointing left, c Z-axis pointing posteriorly and d the strain intensity (von Mises strain)

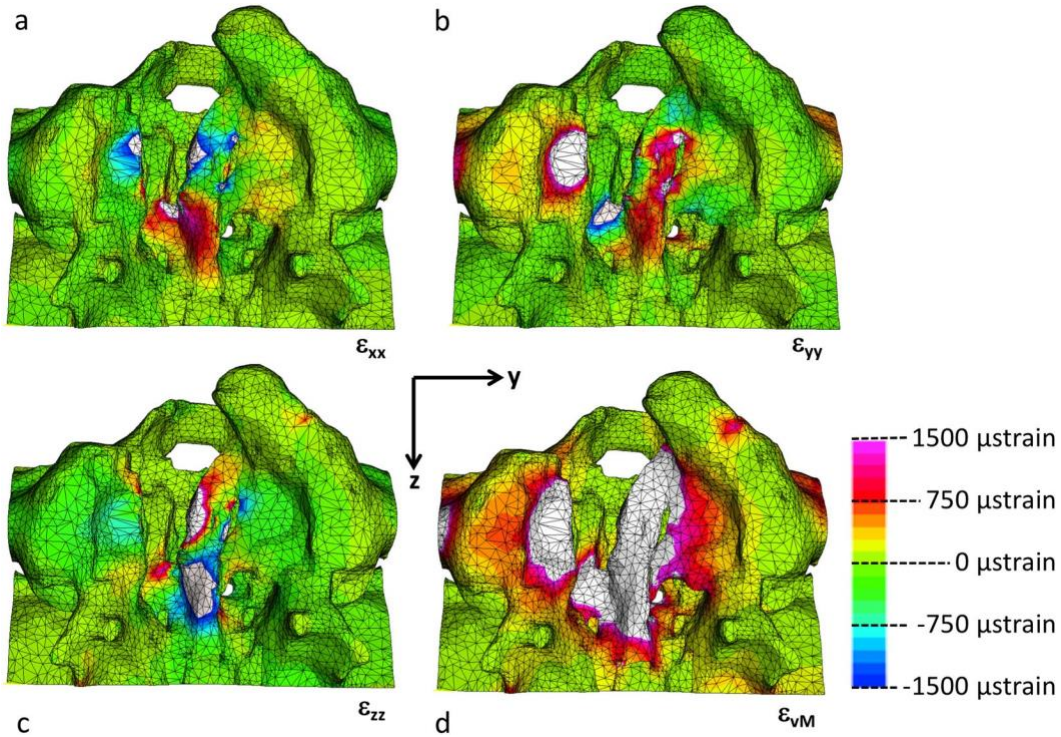

Fig. 6 The distribution of the three orthogonal strain components von Mises strains for magnetic attraction forces of 5 N a palatal view with the X-axis pointing coronally, b Y-axis pointing left, c Z-axis pointing posteriorly and d the strain intensity (von Mises strain)

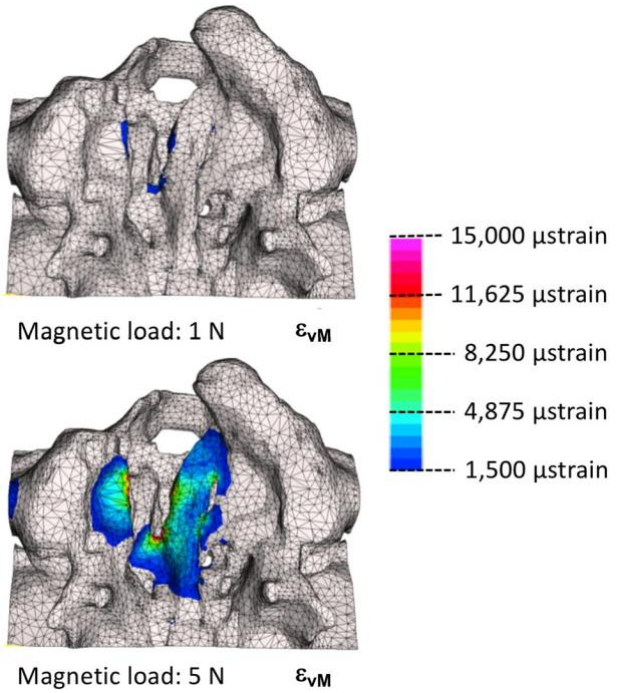

Fig. 7 The distribution of the von Mises strains for magnetic load of 1 N and 5 N in the range of 1,500 to 15,000 µstrain (palatal view with the X-axis pointing coronally, Y-axis pointing left and Z-axis pointing posteriorly). Note that the non-colored regions are not subject to adaptive remodeling

prototype of the palatal distraction device but only to establish the force/distance relationship.

Due to ethical reasons, strain-measuring devices or force transducers cannot be implanted in newborns with a cleft to assess the palatal load transfer at this stage. Therefore, an in-*silica* approach in the form of a detailed 3D FE-model was considered the only valid alternative for which a scan of an actual patient with unilateral cleft lip and palate was required. The scan, which was made available, had originally been taken for a medical condition (hydrocephaly) and it was justified and proven that this condition did not cause deformity in craniofacial growth and morphology [20], Provided an FE-model is well designed and constructed and its assumptions are well-founded, it can supply results which cannot be obtained through other means. Within orthopedics FE- modelling is a well-established and generally accepted method to analyze implant-to-bone load transfer and to support the design of new implants, often using patient- specific models [21]. In our study, 3D data from CT scans were used to create a geometrically accurate model of the palatal region of a newborn with a unilateral cleft lip/ palate. Furthermore, the spatial distribution of the grey values in the 3D data-set was used to provide the elements with material properties approximating the actual distribution of bone stiffness in the facial skeleton. Direct measurements of Young's modulus and other material properties of neonatal palatal bone are difficult to perform for both technical and ethical reasons. However, studies are available in which the relationships between grey values of CT data of bone, and its density and Young's modulus. In the present study, it was assumed that the highest grey values corresponded to the presence of a high-density cortical bone with a Young's modulus of 18 GPa. For the association of other grey values and bone stiffness, the relationships given by [13–15] were scaled to fit the 18 GPa upper limit.

As no information of the force levels for the facial musculature of newborns was available and tongue thrust and sucking forces are irregular, both in magnitude and frequency, it was decided only to incorporate the magnetic attraction forces of the virtual palatal implant in this study. It should thus be kept in mind that in reality the stresses and strains due to the magnetic distraction device would have to be added to those generated by the aforementioned physiological sources.

In the present study we found that magnetic forces of dental magnets range from 1–10 N in an implant- like set up. The strain levels in the palatal segments of the cleft for these load cases do reach the 1,500 µstrain limit for mild overuse, suggesting that periosteal tissue modelling will be induced. The amount of separation between the two sides of the implant will be important for the magnitude of the magnetic forces. Especially for a narrow gap between both sides of the implant generate large forces, yet a mere millimeter larger gap would see substantially lower attraction forces. As for a working distraction device both sides (greater and lesser segments of the cleft palate) of the implant would gradually come closer to each other due to a newly generated bone, the attraction would become larger and higher strain levels would be incurred. The presence of soft tissue due to the subcutaneous design of the implant, however, will prevent the full contact of the opposing magnets and generate their maximum attraction force potential.

The directional strain components were largest in the medio/lateral aspect, thereby following the magnetic forces on either side of the implant. The anterior portion of the lesser segment featured the largest tensile strains, followed by the strains in the greater segment. On the posterior part of the vomer mediolateral strains were compressive in nature and are caused by squeezing action during the distraction process. However, these will depend on individual anatomical variations and size of the cleft. Due to Poisson effect the strains in the coronal aspect are opposite in nature to the aforementioned strains in the mediolateral aspect. To a lesser degree it also occurs in the anteroposterior direction.

As mentioned above, it was not the aim of the current study to present a prototype of a magnetic palatal distraction

device for the use in newborns. It has merely confirmed the hypothesis that dental magnets do have the potential to generate levels of tissue strains, associated with mild overload, resulting in bone apposition. As the feasibility of dental magnets for the purpose of osteogenesis has now been demonstrated, the next step will be to produce a prototype design of the device, and test it in an ex-vivo and in- vivo animal model to validate the findings of the presented FE-analyses.

5 Conclusions

(1) Dental magnets can produce attraction forces large enough to be used for adaptive remodelling or guided bone formation on infant cranio-facial complexes.
(2) The strains in the periosteum and the underlying palatal bone generated by magnetic attraction forces are compatible with adaptive bone formation in the unilateral cleft palate model.
(3) With magnitudes exceeding 1,500 μstrains, the tensile strains in the lesser and greater segments will act as stimulus for guided bone formation in the medio-lateral aspect.

Acknowledgements The authors would like to thank Dyna Dental Engineering B.V., Halsteren, Netherlands for kindly supplying the magnets for this study. This study was partially supported from a grant of the Freiwillige Akademische Gesellschaft (FAG), Basel, Switzerland. Open access funding provided by University of Basel.

Compliance with ethical standards

Conflict of interest: The authors declare that they have no conflict of interest.

References

1. Mossey PA, Little J, Munger RG, Dixon MJ, Shaw WC. Cleft lip and palate. Lancet 2009; 374:1773–85.
2. Mossey P. Global strategies to reduce the healthcare burden of craniofacial anomalies. British Dental Journal. 2003; 195:613.
3. Latham RA, Smiley GR, Gregg JM. The problem of tissue deficiency in cleft palate: An experiment in mobilising the palatine bones of cleft dogs. Br J Plast Surg. 1973; 26:252–60.
4. Shetye PR, Evans CA. Midfacial morphology in adult unoperated complete unilateral cleft lip and palate patients. Angle Orthod 2006; 76:810–6.
5. Monroy PLC, Grefte S, Kuijpers-Jagtman AM, Wagener FADTG, Von Den Hoff JW. Strategies to improve regeneration of the soft palate muscles after cleft palate repair. Tissue Eng - Part B: Rev. 2012; 18:468–77.
6. Shash H, Al-Halabi B, Jozaghi Y, Aldekhayel S, Gilardino MS. A review of tissue expansion-assisted techniques of cleft palate repair. J Craniofac Surg. 2016; 27:760–6.
7. Kobus KF. Cleft palate repair with the use of osmotic expanders: a preliminary report. J Plast Reconstr Aesthetic Surg. 2007;60:414–21.
8. McCarthy JG, Schreiber J, Karp N, Thorne CH, Grayson BH. Lengthening the human mandible by gradual distraction. Plast Reconstr Surg. 1992; 89:1–8.
9. Alkan A, Baş B, Özer M, Bayram M. Closure of a large palatal fistula with maxillary segmental distraction osteogenesis in a cleft palate patient. Cleft Palate-Craniofacial J 2007; 44:112–5.
10. Schmidt BL, Kung L, Jones C, Casap N. Induced osteogenesis by periosteal distraction. J Oral Maxillofac Surg. 2002; 60:1170–5.
11. Yan QC, Tomita N, Ikada Y. Effects of static magnetic field on bone formation of rat femurs. Med Eng Phys. 1998; 20:397–402.
12. Wang D, Cheng L, Wang C, Qian Y, Pan X. Biomechanical analysis of rapid maxillary expansion in the UCLP patient. Med Eng Phys. 2009; 31:409–17.
13. McPherson GK, Kriewall TJ. The elastic modulus of fetal cranial bone: A first step towards an understanding of the biomechanics of fetal head molding. J Biomech 1980; 13:9–16.
14. Bauer FX, Heinrich V, Grill FD, Wölfle F, Hedderich DM, Rau A, et al. Establishment of a finite element model of a neonate's skull to evaluate the stress pattern distribution resulting during nasoalveolar molding therapy of cleft lip and palate patients. J Cranio- Maxillofac Surg. 2018; 46:660–7.
15. Pan X, Qian Y, Yu J, Wang D. Biomechanical Effects of Rapid Palatal Expansion on the Craniofacial Skeleton. Cleft Palate-Craniofacial J 2007; 44:149–54.
16. Carter DR, Schwab GH, Spengler DM. Tensile fracture of cancellous bone. Acta Orthop 1980; 51:733–41.
17. Frost HM. The Utah paradigm of skeletal physiology: An over- view of its insights for bone, cartilage and collagenous tissue

organs. J Bone Min Metab. 2000; 18:305–16.
18. Frost HM. A 2003 update of bone physiology and Wolff s law for clinicians. Angle Orthod 2004; 74:3–15.
19. Turner CH. Toward a mathematical description of bone biology: The principle of cellular accommodation. Calcif Tissue Int. 1999; 65:466–71.
20. Yusof A Craniofacial growth changes in Malaysian Malay children and young adults: a cross-sectional 3-dimensional CT study. [Internet]. University of Adelaide; 2007. Available from: https:// digital.library.adelaide.edu.au/dspace/handle/2440/39388.
21. Poelert S, Valstar E, Weinans H, Zadpoor AA. Patient-specific finite element modeling of bones. Proc Inst Mech Eng Part H J Eng Med. 2013; 227:464–78.

8. Third study:

Load transfer during magnetic mucoperiosteal distraction in newborns with complete unilateral and bilateral orofacial clefts: a three-dimensional finite element analysis

Study design: Dr. Prasad Nalabothu, Prof. Michel Dalstra and PD Dr. med. Dr. med. dent. Dr. phil. Andreas A. Mueller

Financing: FAG (Voluntary Academic Association): CHF 13,406

Project leaders: Professor Dr. med. dent. Carlalberta Verna

Publication: First authorship, Journal of applied Sciences, Impact factor 2.47 (2020), Ranking 85/299 (Q2) in ‘General engineering and 233/460 in ‘General Materials Science’.

applied sciences

MDPI

Article

Load Transfer during Magnetic Mucoperiosteal Distraction in Newborns with Complete Unilateral and Bilateral Orofacial Clefts: A Three-Dimensional Finite Element Analysis

Prasad Nalabothu [1,2,*], Carlalberta Verna [1], Benito K. Benitez [2], Michel Dalstra [1,†] and Andreas A. Mueller [2,†]

[1] Department of Paediatric Oral Health and Orthodontics, University Center for Dental Medicine UZB, 4058 Basel, Switzerland; carlalberta.verna@unibas.ch (C.V.); michel.dalstra@unibas.ch (M.D.)

[2] Department of Oral and Craniomaxillofacial Surgery, University Hospital Basel, 4031 Basel, Switzerland; benito.benitez@usb.ch (B.K.B.); andreas.mueller@usb.ch (A.A.M.)

* Correspondence: prasad.nalabothu@unibas.ch; Tel.: +41-61-328-60-95

† Joint last authors.

Received: 17 September 2020; Accepted: 23 October 2020; Published: 31 October 2020

Abstract: The primary correction of congenital complete unilateral cleft lip and palate (UCLP) and bilateral cleft lip and palate (BCLP) is challenging due to inherent lack of palatal tissue and small extent of the palatal shelves at birth. The tissue deficiency affects the nasal mucosa, maxillary bone and palatal mucosa. This condition has driven the evolution of several surgical and non-surgical techniques for mitigating the inherent problem of anatomical deficits. These techniques share the common principle of altering the neighboring tissues around the defect area in order to form a functional seal between the oral and nasal cavity. However, there is currently no option for rectifying the tissue deficiency itself. Investigations have repeatedly shown that despite the structural tissue deficiency of the cleft, craniofacial growth proceeds normal if the clefts remain untreated, but the cleft remains wide. Conversely, craniofacial growth is reduced after surgical repair and the related alteration of the tissues. Therefore, numerous attempts have been made to change the surgical technique and timing so as to reduce the effects of surgical repairs on craniofacial growth, but they have been only minimally effective so far. We have determined whether the intrinsic structural soft and hard tissue deficiency can be ameliorated before surgical repair using the principles of periosteal distraction by means of magnetic traction. Two three-dimensional maxillary finite element models, with cleft patterns of UCLP and BCLP, respectively, were created from computed tomography slice data using dedicated image analysis software. A virtual dental magnet was positioned on either side of the cleft at the mucoperiosteal borders, and an incremental magnetic attraction force of up to 5 N was applied to simulate periosteal distraction. The stresses and strains in the periosteal tissue induced by the magnet were calculated using finite element analysis. For a 1 N attraction force the maximum strains did not exceed 1500 µstrain suggesting that adaptive remodeling will not take place for attraction forces lower than 1 N. At 5 N the regions subject to remodeling differed between the UCLP and BCLP models. Stresses and strains at the periosteum of the palatal shelf ridges in the absence of compressive forces at the alveolar borders were greater in the UCLP model than the BCLP model. The findings suggest that in newborns with UCLP and BCLP, periosteal distraction by means of a magnetic 5 N attraction force can promote the generation of soft and hard tissues along the cleft edges and rectify the tissue deficiency associated with the malformation.

Keywords: cleft lip and palate; finite element model; periosteal bone remodeling; unilateral cleft palate; bilateral cleft palate; distraction

1. Introduction

Cleft lip and palate (CLP) is the most common craniofacial malformation, affecting one in every 500 to 700 live births, thus accounting for about 220000 new cases each year worldwide with disparity across geographic areas, racial groups, and socioeconomic status [1]. No effective preventive measures exist. The ongoing manifestation of CLP as well as its broad implications on psychological well-being, speech, orofacial development, and therapeutic burden underline the need to identify and targeting the intrinsic causes [2–4].

The etiology of CLP is complex, which could occur as a result of multiple genetic and environmental factors or a combination of both [5,6]. The clefting of the lip and/or palate may occur in a unilateral or bilateral fashion, and the embryological pattern of clefting results from a fusion failure during the development of maxilla and palate. The normal fusion of the medial frontonasal process with the maxillary process of the first pharyngeal arch takes place at 4–6 weeks of gestation forming a primary palate [7]. A complete fusion failure results in a cleft of the lip through the vermillion border that extends to the nasal sill and in a cleft of the alveolar process [7]. The cleft of the secondary palate occurs at 8–12 weeks of gestation due to fusion failure of the palatal shelves of the maxillary processes [8,9] that results in a cleft in the palatal roof and soft palate that extends to the uvula.

Affected children have a range of both functional and esthetic problems. They comprise feeding difficulties at birth due to incomplete oral seal, swallowing, nasal regurgitation, respiratory problems, hearing difficulties due to abnormalities in the palatal musculature, and speech impairments due to air escape and articulation problems [10]. Therefore, an ideal early and complete cleft treatment would allow the normalizing of food intake, speech development, growth and esthetics - while imposing minimal treatment burden to child and family.

Several different surgical protocols have been advocated for managing children with CLP. The amount of palatal mucosa present and timing of the surgery play important roles in healing success after surgery. Clefting of the palate at birth structurally results in 16% less palatal mucosa compared with a normal child [11] and anatomically smaller palatal shelves on the cleft and noncleft sides [12,13]. The intrinsic tissue deficiency in the palate has no spontaneous improvement trend. It persists until adulthood in both unilateral cleft lip and palate (UCLP) and bilateral cleft lip and palate (BCLP) [14].

A scientific basis was proposed in 2005 for determining the optimal conditions for palatal cleft closure in complete UCLP and BCLP [15]. This should be performed when the surface area of the cleft space does not exceed 10% of the surrounding palatal surface bounded by the alveolar ridges, because under these circumstances the facial growth is less affected, independent of the patient's age at surgery [15]. This recommendation may be applicable for clefts which are smaller in size, whereas in cases of wider clefts it is imperative for surgeons to mobilize the tissue adjoining the cleft more extensively which may lead to open wound areas that undergo secondary healing. This may lead to structural tissue deficiencies and pronounced interference with the normal growth and development of the midface [16].

The use of a palatal appliance for presurgical maxillary orthopedics is a widely accepted non-surgical therapeutic adjunct for addressing the problem of tissue deficiency in wider clefts. Such an appliance approximates the palatal shelves and thus reduces the alveolar and palatal cleft width prior to surgery [17]. The effect of those appliances on the growth is controversial. Some proponents of this technique have claimed that gradual adaptations of the appliance can stimulate palatal tissue growth [18,19]. Others have shown that this approach resulted in retarded growth of the palatal tissue [20]. Finally, a randomized controlled trial concluded that using a palatal appliance does not result in any permanent growth change or tissue gain [21].

Various surgical techniques have also been applied in an attempt to mitigate the problems of tissue deficiency. These techniques varied between surgeons, and there is still no consensus on which is the best protocol for treating CLP patients. Seventeen different surgical sequences for repairing unilateral complete clefts were identified in a survey of over 201 European cleft centers [22].

Three main surgical principles to mitigate the tissue deficiency in CLP have evolved [23]. The first principle limits the closure only to either the oral or the nasal mucosa layer by applying a so called single-layer closure [24–27]. This procedure involves turning over the mucosa from either the oral or the nasal cavity like a book page while leaving an open wound on the back side of the turned-over mucosa. The second principle involves detaching the oral tissue and shifting it over the cleft area while creating an open wound that heals outside the cleft area from where the tissue has been detached [28–30]. In the third principle, tissue from outside the palatal area is used to cover the open wound areas that result from the first or second technique [31–34]. While all of these surgical techniques are able to close the cleft gap using the available tissue, none of them result in the generation of new mucoperiosteal tissue.

Adjuvant therapies or strategies such as tissue expansion [35] and distraction osteogenesis (DO) [36] have been attempted to increase the volume of tissue in the areas of tissue deficiency in clefts. The principles of DO require a bone cut through the palatal shelf ridges. However, in infants this would damage the dental follicles that are embedded in the palatal shelf ridges. Most tissue engineering studies have focused on the application of biomaterials purely for bone generation [37]. However, the palatal cleft comprises bone and two mucosal layers, which makes it a difficult target for biomaterial or tissue-engineering techniques.

Animal experiments suggest that periosteal distraction osteogenesis (PDO) is an appealing option for utilizing the principles of DO [38–40] for combined bone and soft tissue generation without the need for a bone cut. PDO is performed by gradual lift-up on the mucoperiosteum from the underlying bone by applying mechanical loading. The physical tissue strain and biological tissue stimulus to bone and periosteum lead to new tissue formation. We therefore address PDO as a potential treatment strategy to target the tissue deficiency in orofacial clefts while using magnetic forces to exert the necessary tissue strain. Magnetic forces have been used in orthodontics to generate tooth movement and to promote tissue reactions [41].

Finite element (FE) analysis is a numerical tool to compute the stress and strain fields in the bone structure under external loading. It thereby reveals the distribution of the internal loads and deformations. Computational FE analysis has provided crucial basic data for understanding mechanical interactions between the magnets and mucoperiosteal tissue for tissue expansion [42]. The loading distribution depends on the shape and size of individual anatomical structures and malformation. Previously, this method has been used to assess the maxillary load transfer during conventional DO in patients with cleft lip and palate [43].

In our previous study we have examined the feasibility of dental magnets as distraction devices in newborns with UCLP [44]. Unilateral clefts form 76% of all CLP cases worldwide which still leaves the BCLP, accounting for one fourth (24%) of all CLP unaddressed [45]. As the anatomy of BCLP is different from UCLP, it is the aim of this study to compare the load transfer of magnetic forces used for PDO in both UCLP and BCLP in silico models. It examines whether the forces reach the threshold necessary for regeneration of the hard and soft tissue volumes along the cleft edges in both UCLP and BCLP.

2. Materials and Methods

2.1. Ethical Statement and Patient Data

The reported investigations and procedures were conducted according to the principles expressed in the Declaration of Helsinki. Two computed tomography (CT) scans of anonymized 2- and 3-week-old newborns with complete UCLP and BCLP, respectively, were obtained from an existing database and analyzed. The DICOM data sets of 2 CT scans were obtained from a commercial CT scanner using a voxel size of 0.3 mm (Philips CT scanner, Eindhoven, The Netherlands).

2.2. Model Construction

The CT scans of the UCLP and BCLP newborns were imported into dedicated image analysis software (Mimics version 19, Materialise, Leuven, Belgium) and three-dimensional (3D) surface models were generated by thresholding and selecting only the hard tissues of the cranium and maxilla. The region of interest was further defined by virtually removing all structures except for the midface, including the maxilla and the adjoining bony segments of the face (first, second and third rows in Figure 1).

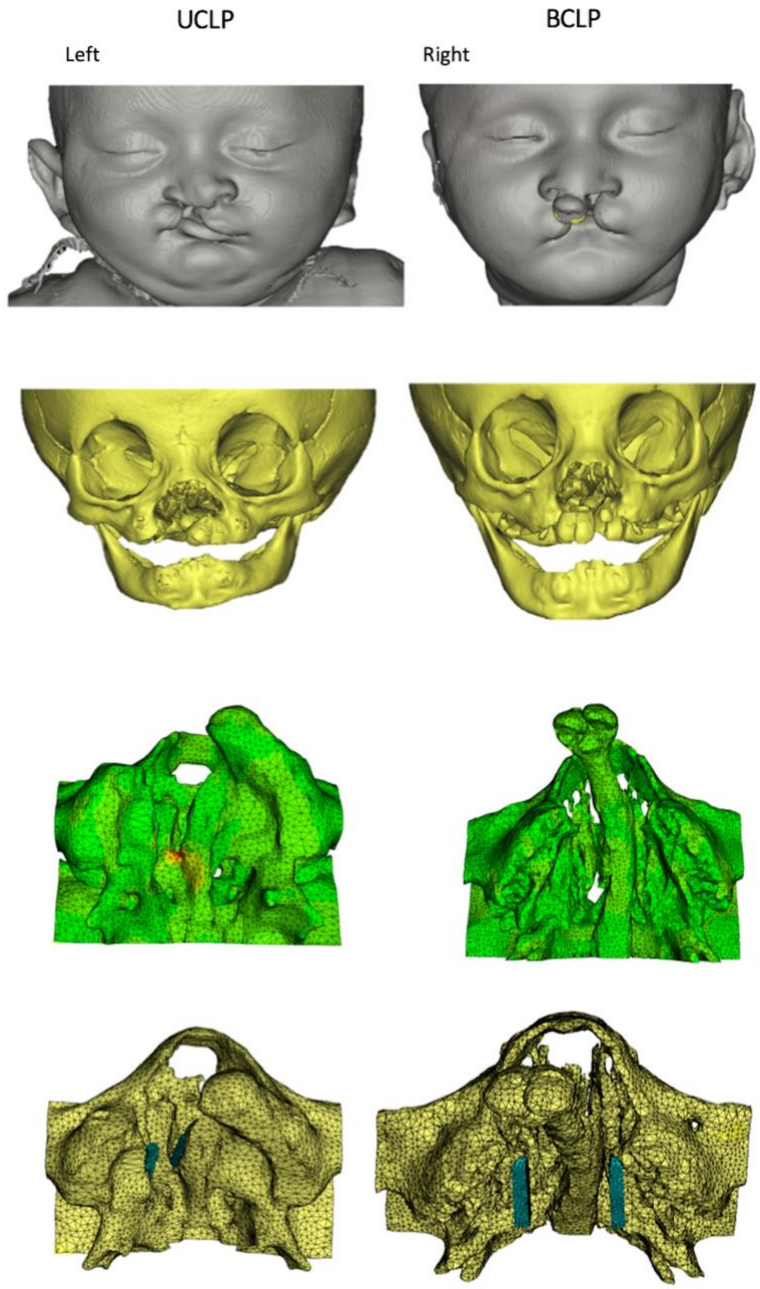

Figure 1. From computed tomography scans to finite element (FE) models with magnets in the unilateral cleft lip and palate (UCLP, left column) and bilateral cleft lip and palate (BCLP, right column). Frontal views of three-dimensional reconstructions of the soft tissue (first row) and hard tissue (second row). Regions of interest of the FE models (third row) and the models with magnetic strips which are blue in color (fourth row).

2.3. Magnet Implantation

The rare-earth permanent magnets used for in vitro testing were constructed from a neodymium-boron-iron alloy (Dyna WR magnets, Dyna Dental Engineering, Halsteren, The Netherlands). The magnets were disc shaped with a height of 1.7 mm and a diameter of 4.5 mm (02MS1 Dyna WR magnet S3). The mucoperiosteum borders on the cleft and non-cleft sides were covered with two 23 mm long parallel bars of five magnets each placed in a row in the UCLP and BCLP models (Figure 1, fourth row). In the following analyses, each row of the magnets was assumed to exert attracting forces relative to the oppositely placed row of magnets. Experimental force-distance curves for these magnets were measured [44] with the results used to define incremental forces with a magnitude of up to 5 N to either side of the cleft in the UCLP and BCLP models.

2.4. FE Model Design

The FE mesh was constructed based on the CT scans of the 3D UCLP and BCLP models. The UCLP FE mesh consisted of 238243 4-node tetrahedral elements with 43822 nodes, whereas the BCLP FE mesh consisted of 409027 4-node tetrahedral elements with 74551 nodes. The position of the centroid of each element was calculated and a gray scale was associated with it based on spatial interpolation of the gray scale values of the nearest voxels. The gray scale values from the CT scans were correlated with the material density and the material stiffness. Relevant material properties were assigned for the elements representing bone, arithmetic relationships between gray scale values, apparent densities and Young's moduli [46–49]. Depending on its apparent density and the associated gray scale values, the bone tissue was stratified into ten different material property groups, ranging from very low-density cancellous bone (bone 1) to dense cortical bone (bone 10). The material properties of these ten types of bone (apparent density, Young's modulus, Poisson's ratio and yield strength) were same as used by Nalabothu et al. [44].To highlight the compositional difference between the UCLP and BCLP model each type of bone density (bone 1 to bone 10) has been cumulatively compared between both models (Figure 2).

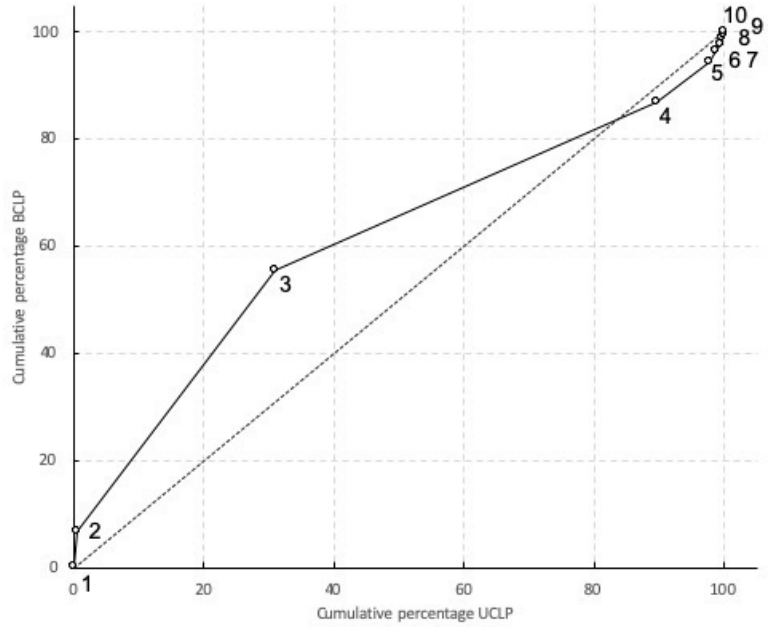

Figure 2. The cumulative percentage of the ten material property groups for the unilateral cleft lip and palate (UCLP) and bilateral cleft lip and palate (BCLP) models, respectively. The material properties of the ten different bone types are retrieved from Nalabothu et al. [44].

2.5. FE Analysis

The UCLP and BCLP FE models were exported from the image analysis program in NASTRAN format and imported into an FE analysis program (Strand7, Sydney, Australia). The material properties of the bone were assumed to be non-linear, with its stress-strain curves in the ten groups adapted so that the bone would behave as a perfectly plastic material whose compressive strength was 150% higher than its tensile strength [50]. The FE analyses were conducted using a nonlinear solver with logarithmically increasing increments from 0.01 to 1 (100% load). The calculated stresses and the associated strains were used for post-processing.

3. Results

The application of a 1 N attraction force did not produce strain levels in the 1500 μstrain range in both the UCLP and BCLP model. As this was considered a minimum requirement for adaptive remodeling, in the following only the results for a 5 N attraction force are presented.

3.1. Overall Deformation of the Maxilla

The maximum deformation in the UCLP and BCLP models occurred around the sites adjacent to the magnetic strips at the vomer edge of the greater and lesser segments of the palatal shelf ridge. The overall deformation was greater in the UCLP model (left column of Figure 3) than in the BCLP model. In the BCLP model, the deformations occurred more in the posterior area of the palatal shelf ridges (right column of Figure 3) than in the anterior one.

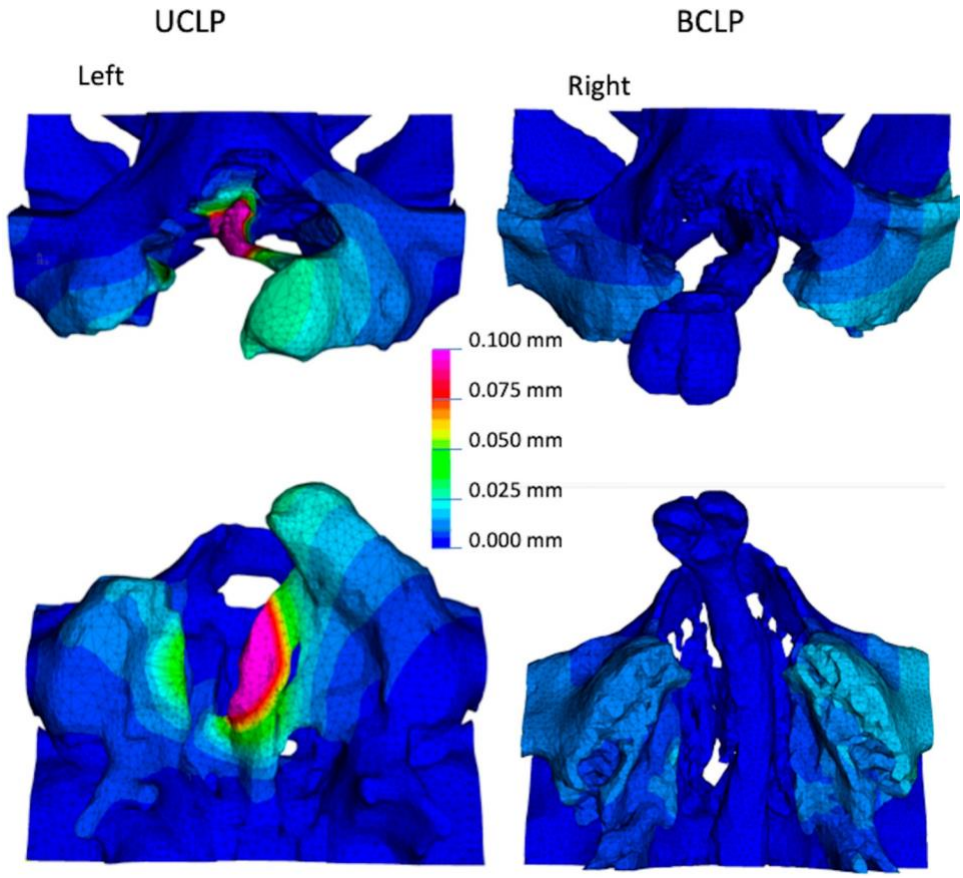

Figure 3. Distribution of the overall periosteal deformation in mm for 5 N loading in the UCLP (left column) and BCLP (right column) models. Frontal (top row) and palatal (bottom row) views are shown.

3.2. Stresses and Strains in the Maxilla

The obtained stress/strain components of the UCLP and BCLP FE models in the X-direction (coronal), Y-direction (medial/lateral) and Z-direction (anterior/posterior) were different in each aspect. In the BCLP model no strains higher than 1500 µstrain were seen for a magnetic load of 1 N (Figure 4). However, a load of 5 N regions with strains beyond 1500 µstrain were observed though less than the UCLP model [44].

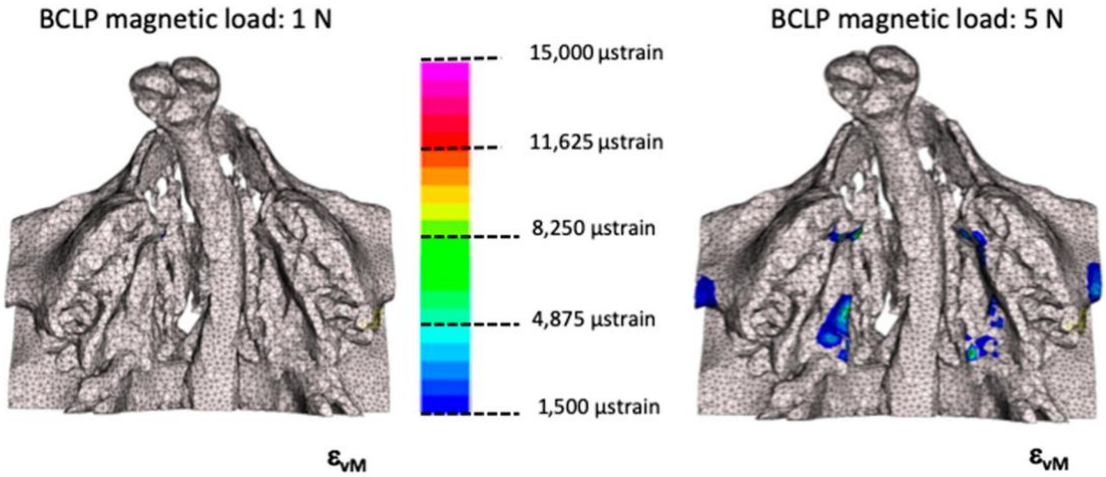

Figure 4. Areas showing the overall strain levels in BCLP model during loading of 1 N (left) and 5 N (right) from the palatal view.

The orthogonal stresses in the coronal (X) direction occurred in the UCLP model mainly at the anterior part of the ridge of the lesser segment and the posterior part of the vomer edge (Figure 5: left column, top row), while in the BCLP model it occurred bilaterally in the posterior border of palatal shelf ridge (Figure 5: right column, top row). The orthogonal stresses in the medial/lateral (Y)-direction occurred in the UCLP model mainly at the middle portion of the lesser segment's ridge and in some sparse areas at the middle portion of the vomer edge and the greater segment's ridge (Figure 5: left column, second row), while in the BCLP model it occurred bilaterally on the palatal shelf ridges at the anterior tip and posterior border (Figure 5: right column, second row).

The orthogonal stresses in the antero/posterior (Z) direction occurred in the UCLP model mainly on the anterior portion of the lesser segment's ridge and on the middle portion of the vomer edge and on the anterior portion of the greater segment's ridge (Figure 5: left column, third row), while there were no stresses in this direction in the BCLP model (Figure 5: right column, third row).

The von Mises stresses (stress intensity) in the UCLP model were highest on the entire greater and lesser palatal shelf ridges and on the vomer edge (Figure 5: left column, bottom row), while in the BCLP model von Mises stresses were highest bilaterally on the anterior and posterior parts of the palatal shelf ridges. (Figure 5: right column, bottom row).

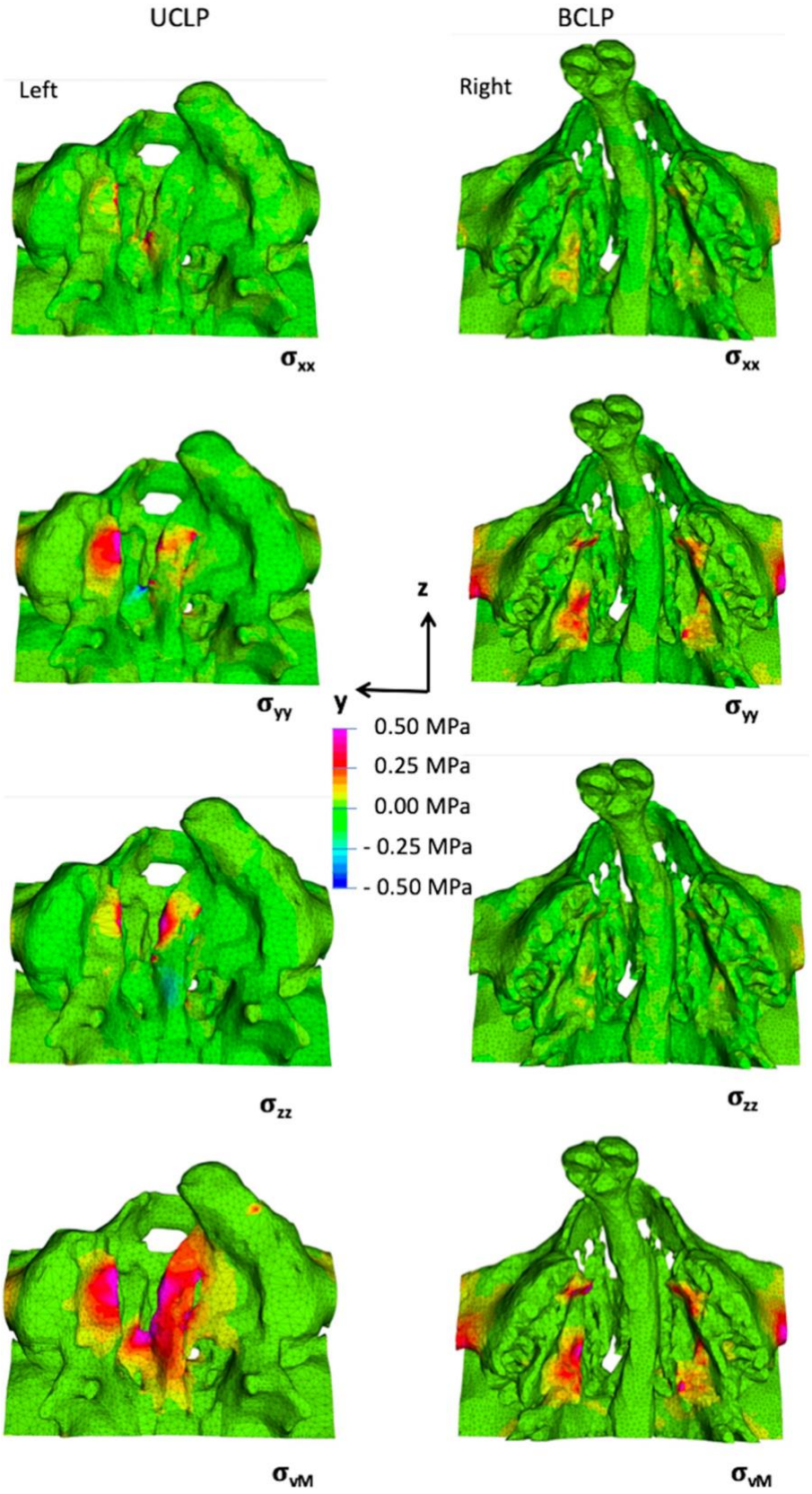

Figure 5. Distributions of the three orthogonal stress components and the von Mises stresses under a 5 N load from palatal view in the UCLP (left column) and BCLP (right column) models. The top second and third rows shows the orthogonal stresses in the X-, Y-, and Z-directions, respectively, and the bottom row shows the von Mises stresses (stress intensity).

4. Discussion

The success of surgical hard palate closure in UCLP and BCLP is dependent on the availability of tissue in relation to the cleft area that needs to be closed. In wider clefts it is imperative to mobilize the tissue adjacent to the cleft more extensively, which leads to a wider tissue wound and tissue reparation rather than regeneration [51]. This situation may interfere with the normal growth and development of the midface and dentition [12,52]. The growth in patients with clefts remains a challenge regardless of which surgical protocol is applied. Applying adjuvant therapies before surgery can alleviate the problems of tissue deficiency to some extent by approximation of the palatal shelves using active presurgical orthopedics [53] or passive plate therapy [17], which facilitate tissue closure across the cleft area. However, the stocks of bone and soft tissue still remain deficient since such therapies do not aid in the regeneration of local tissue.

Therefore, in this study we tested a contrasting strategy based on increasing the bone and soft tissue prior to cleft surgical repair by means of magnetic periosteal distraction. It aims for true generation of the deficient osteo-mucoperiosteal tissue—thus, tackling the inherent palatal tissue deficiency which is a basic feature of the cleft malformation that does not disappear over time. With this intention, we analyzed the in silico stress distribution induced by magnetic strips placed on the cleft palatal shelves in newborns with UCLP and BCLP. We tested the hypothesis that magnets can generate bone inducing strains in UCLP and BCLP newborns.

Analyses of load transfer, by studying the distribution of stresses and strains, are a prerequisite before in vivo testing since incorrect loading or overloading may lead to disorganized tissue structures, eventually leading to tissue necrosis. Determining these stresses and strains in vivo is not feasible in newborns for ethical reasons, and so 3D in silico models were deemed a valid alternative approach. Although our experiments were confined to tissue generation by means of stresses induced by magnetic periosteal distraction, there is increasing evidence that magnetic fields can further promote bone regeneration directly by attracting growth factors, hormones and polypeptides to the implantation site [54]. The length of the magnetic strips was defined as 23 mm since the average length of hard palate at birth is 25.6 mm ±1.6 mm [55]. Previous tests on the magnetic attraction forces across porcine palatal mucosa (rugae) tissue allowed the simulation of the thickness of mucosa in the newborns [44].

In the present study we found that applying 5 N attraction forces using magnetic strips induced stresses in the UCLP and BCLP models mainly at the vomer edge and the palatal shelf ridges of the greater and lesser segments (left and right columns, Figure 3). Areas of tissue generation were delineated by applying the principles of Frost's Mechanostat theory, which states that mechanical loading influences the bone structure by changing the mass (amount of bone) and architecture (arrangement of surrounding tissues) if the induced strain exceeds 1500 µstrain. This implies that periosteal tissue regeneration will be induced at sites where the strain in the underlying bone exceeds 1500 µstrain, as the periosteum is mechanically subservient to the bone [56] (Figure 4).

The area of periosteal tissue that was subjected to at least 1500 µstrain was larger in the UCLP model than the BCLP model, which could be due to differences in material properties of the bone and anatomical variations. In the two FE models there is more low-density bone type 3 present in BCLP than in the UCLP model (Figure 2). Moreover, the direction of the magnetic forces is also more horizontally oriented in BCLP model compared to the UCLP model. The stresses and strains, able to induce adaptive remodeling, as exhibited in both UCLP and BCLP models, were localized to the area of the intrinsic tissue deficit of the cleft malformation while at the same time not affecting the neighboring areas, thus providing evidence that no compressive forces were transmitted to the alveolar ridges by the magnets.

The abovementioned geometrical and structural differences between the bone anatomy of the UCLP and BCLP mean that each will require a different design of implant. The larger cleft width in case of BCLP would make a more powerful magnet necessary to generate equivalent forces as in case of UCLP. Alternatively, the use of spacers to partially bridge the distance, or the placement of an auxiliary implant at the vomer could be considered as an option. The present findings obtained in

the UCLP and BCLP FE models might not be generalizable to all clefts of similar distances between the affected and non-affected segments, since the 3D bone morphology might vary even when the morphology in the cleft area is identical. However, the results of this study give guidance about the distribution of palatal load transfer around the cleft segments by inducing PDO within the optimal biological limits [56]. Future studies could test this hypothesis of mucoperiosteal distraction in an in vivo cleft animal model [57] in order to validate the findings of the present FE analyses.

5. Conclusions

The following conclusions can be drawn from this study

1. The present FE models have shown that the use of magnets as approved for dental applications can exert attraction with the potential to induce PDO around the greater and lesser segments of the palatal shelf ridge in cases of UCLP and BCLP.
2. A magnetic attraction force of 5 N was found to be sufficient to reach strain values in excess of 1500 µstrain in the palatal bone in both UCLP and BCLP models, and thereby have the potential to initiate adaptive remodeling.
3. The effects of magnetic load transfer were localized to their area of application, and did not spread out to distant structures.
4. The anatomical variations both in external bone geometry and internal bone composition affect the load transfer across the palate.

Author Contributions: Conceptualization, A.A.M. and C.V.; data curation, P.N. and M.D.; formal analysis, P.N. and M.D.; funding acquisition, C.V., A.A.M. and H.F.Z.; investigation, P.N. and M.D.; methodology, P.N., M.D. and A.A.M.; supervision, M.D., C.V. and A.A.M.; validation, P.N., A.A.M. and M.D.; visualization, P.N., A.A.M., B.K.B., M.D. and C.V.; writing—original draft, P.N.; writing—review and editing, P.N., M.D., B.K.B., C.V. and A.A.M. All authors have read and agreed with submitting this version of the manuscript.

Funding: This study was partially funded by a research grant from the Freiwillige Akademische Gesellschaft (FAG), Basel, Switzerland.

Acknowledgments: The authors thank Dyna Dental Engineering B.V., Halsteren, Netherlands for kindly supplying the magnets used in this study. Ravi Kant Singh (chief consultant at Peace Pant Hospital, Varanasi, India) for providing the CT scans, Markus Steineck (University Center for Dental Medicine UZB, Basel, Switzerland) for supporting the magnet-based experiments and Hans Florian Zeilhofer for funding acquisition and support of the project.

Conflicts of Interest: The authors declare that they have no conflict of interest. The funders had no role in the design of the study; the collection, analysis, or interpretation of data; the writing of the manuscript; or the decision to publish the results.

References

1. Mossey, P. Global strategies to reduce the healthcare burden of craniofacial anomalies. *Br. Dent. J.* **2003**, *195*, 613. [CrossRef] [PubMed]
2. Mossey, P.A.; Little, J.; Munger, R.G.; Dixon, M.J.; Shaw, W.C. Cleft lip and palate. *Lancet* **2009**, *374*, 1773–1785. [CrossRef]
3. Schutte, B.C.; Murray, J.C. The many faces and factors of orofacial clefts. *Hum. Mol. Genet.* **1999**, *8*, 1853–1859. [CrossRef] [PubMed]
4. Mossey, P.A. Epidemiology of oral clefts: An international perspective. In *Cleft Lip and Palate: From Origin to Treatment*; Oxford University Press: Oxford, UK, 2002; ISBN 0195139062.
5. Mossey, P. Epidemiology underpinning research in the aetiology of orofacial clefts. *Orthod. Craniofac. Res.* **2007**, *10*, 114–120. [CrossRef]
6. Wong, F.K.; Hägg, U. An update on the aetiology of orofacial clefts. *Hong Kong Med. J.* **2004**, *10*, 331–336. [PubMed]
7. Nanci, A.; Ten, C.A.R. *Ten Cate's Oral Histology Development, Structure, and Function*; Elsevier: Amsterdam, The Netherlands, 2017.

8. Bush, J.O.; Jiang, R. Palatogenesis: Morphogenetic and molecular mechanisms of secondary palate development. *Development* **2012**, *139*, 231–243. [CrossRef]
9. Tarr, J.T.; Lambi, A.G.; Bradley, J.P.; Barbe, M.F.; Popoff, S.N. Development of normal and Cleft Palate: A central role for connective tissue growth factor (CTGF)/CCN2. *J. Dev. Biol.* **2018**, *6*, 18. [CrossRef]
10. Bührer, C.; Zimmermann, A. Cleft palate. In *Neonatal Emergencies: A Practical Guide for Resuscitation, Transport and Critical Care of Newborn Infants*; Cambridge University Press: Cambridge, UK, 2009; Volume 1, pp. 460–463. [CrossRef]
11. Huddart, A.G. Arch Alignment and Presurgical Treatment—The West Midlands Approach. In *Early Treatment of Cleft Lip and Palate*; Hans Huber: Berne, Switzerland, 1986; ISBN 3-456-81406-2.
12. Latief, B.S.; Lekkas, K.C.; Schols, J.G.J.H.; Fudalej, P.S.; Kuijpers, M.A.R. Width and elevation of the palatal shelves in unoperated unilateral and bilateral cleft lip and palate patients in the permanent dentition. *J. Anat.* **2012**, *220*, 263–270. [CrossRef]
13. Atherton, J.D. A Descriptive Anatomy of the Face in Human Fetuses with Unilateral Cleft Lip and Palate. *Cleft Palate J.* **1967**, *4*, 104–114. [CrossRef]
14. Diah, E.; Lo, L.J.; Huang, C.S.; Sudjatmiko, G.; Susanto, I.; Chen, Y.R. Maxillary growth of adult patients with unoperated cleft: Answers to the debates. *J. Plast. Reconstr. Aesthetic Surg.* **2007**, *60*, 407–413. [CrossRef]
15. Berkowitz, S.; Duncan, R.; Evans, C.; Friede, H.; Kuijpers-Jagtman, A.M.; Prahl-Anderson, B.; Rosenstein, S. Timing of Cleft Palate Closure Should Be Based on the Ratio of the Area of the Cleft to That of the Palatal Segments and Not on Age Alone. *Plast. Reconstr. Surg.* **2005**, *115*, 1483–1499. [CrossRef] [PubMed]
16. Kuijpers-Jagtman, A.M.; Long, R.E., Jr. The influence of surgery and orthopedic treatment on maxillofacial growth and maxillary arch development in patients treated for orofacial clefts. *Cleft Palate-Craniofac. J.* **2000**, *37*, 527. [CrossRef]
17. Nalabothu, P.; Benitez, B.K.; Dalstra, M.; Verna, C.; Mueller, A.A. Three-Dimensional Morphological Changes of the True Cleft under Passive Presurgical Orthopaedics in Unilateral Cleft Lip and Palate: A Retrospective Cohort Study. *J. Clin. Med.* **2020**, *9*, 962. [CrossRef] [PubMed]
18. McNeil, C.K. *Oral and Facial Deformity*; Pitman: London, UK, 1954.
19. Fish, J. Growth of the palatal shelves of post-alveolar cleft palate infants. Effects of stimulation appliances. *Br. Dent. J.* **1972**, *132*, 492–501. [CrossRef] [PubMed]
20. Huddart, A.G. Presurgical changes in unilateral cleft palate subjects. *Cleft Palate J.* **1979**, *16*, 147–157.
21. Prahl, C.; Kuijpers-Jagtmann, A.M.; Van't Hof, M.A.; Prahl-Andersen, B. A randomised prospective clinical trial into the effect of infant orthopaedics on maxillary arch dimensions in unilateral cleft lip and palate (Dutchcleft). *Eur. J. Oral Sci.* **2001**, *109*, 297–305. [CrossRef]
22. Shaw, W.C.; Semb, G.; Nelson, P.; Brattström, V.; Mølsted, K.; Prahl-Andersen, B.; Gundlach, K.K.H. The Eurocleft project 1996-2000: Overview. *J. Cranio-Maxillofac. Surg.* **2001**, *29*, 131–140. [CrossRef]
23. Dorrance, G.M.; Shirazy, E. *The Operative Story of Cleft Palate*; W.B. Saunders Company: Philadelphia, PA, USA, 1933.
24. Campbell, B.Y.A. The closure of congenital clefts of the hard palate. *Br. J. Surg.* **1926**, *13*, 715–719. [CrossRef]
25. Pichler, H. Zur Operation der doppelten Lippen-Gaumenspalten. *Dtsch. Z. Cir.* **1926**, *195*, 104–107. [CrossRef]
26. Bütow, K.W. Caudally-based single-layer septum-vomer flap for cleft palate closure. *J. Cranio-Maxillofac. Surg.* **1987**, *15*, 10–13. [CrossRef]
27. Abyholm, F.E. Primary Closure of Cleft Lip and Palate. In *Facial Clefts and Craniosynostosis: Principles and Management*; Turvey, T.A., Vig, K.W.L., Fonseca, R.J., Eds.; W.B. Saunders Company: Philadelphia, PA, USA, 1996.
28. Langenbeck, B. Die Uranoplastik mittelst Ablösung des mucös-periostalen Gaumenüberzuges. Uranoplasty by means of raising mucoperiosteal flaps. Hirschwald: Berlin, 1861. *Plast. Reconstr. Surg.* **1972**, *49*, 326–330. [CrossRef]
29. Veau, V.; Borel, S. *Division palatine: Anatomie, Chirurgie Phonétique/Victor Veau, Avec la Collaboration de S. Borel*; Masson: Paris, France, 1931.
30. Bardach, J. Two-Flap palatoplasty: Bardach's technique. *Oper. Tech. Plast. Reconstr. Surg.* **1995**, *2*, 211–214. [CrossRef]
31. Millard, D.R., Jr. The island flap in cleft palate surgery. *Surg. Gynecol. Obstet.* **1963**, *116*, 297–300. [CrossRef]
32. Mukherji, M.M. Cheek flap for short palates. *Cleft Palate J.* **1969**, *6*, 415–420. [PubMed]

33. Stricker, M.; Chancholle, A.R.; Flot, F.; Malka, G.; Montoya, A. La greffe periostee dans la reparation de la fente totale du palais primaire [Periosteal graft in the repair of complete primary cleft palate]. *Ann. Chir. Plast.* **1977**, *22*, 117–125.
34. Neiva, C.; Dakpe, S.; Gbaguidi, C.; Testelin, S.; Devauchelle, B. Calvarial periosteal graft for second-stage cleft palate surgery: A preliminary report. *J. Cranio-Maxillofac. Surg.* **2014**, *42*, e117–e124. [CrossRef]
35. Shash, H.; Al-Halabi, B.; Jozaghi, Y.; Aldekhayel, S.; Gilardino, M.S. A review of tissue expansion-assisted techniques of cleft palate repair. *J. Craniofac. Surg.* **2016**, *27*, 760–766. [CrossRef] [PubMed]
36. Alkan, A.; Baş, B.; Özer, M.; Bayram, M. Closure of a large palatal fistula with maxillary segmental distraction osteogenesis in a cleft palate patient. *Cleft Palate-Craniofac. J.* **2007**, *44*, 112–115. [CrossRef]
37. Martín-Del-Campo, M.; Rosales-Ibañez, R.; Rojo, L. Biomaterials for cleft lip and palate regeneration. *Int. J. Mol. Sci.* **2019**, *20*, 2176. [CrossRef]
38. Schmidt, B.L.; Kung, L.; Jones, C.; Casap, N. Induced osteogenesis by periosteal distraction. *J. Oral Maxillofac. Surg.* **2002**, *60*, 1170–1175. [CrossRef]
39. Sencimen, M.; Aydintug, Y.S.; Ortakoglu, K.; Karslioglu, Y.; Gunhan, O.; Gunaydin, Y. Histomorphometrical analysis of new bone obtained by distraction osteogenesis and osteogenesis by periosteal distraction in rabbits. *Int. J. Oral Maxillofac. Surg.* **2007**, *36*, 235–242. [CrossRef] [PubMed]
40. Sato, K.; Haruyama, N.; Shimizu, Y.; Hara, J.; Kawamura, H. Osteogenesis by gradually expanding the interface between bone surface and periosteum enhanced by bone marrow stem cell administration in rabbits. *Oral Surg. Oral Med. Oral Pathol. Oral Radiol. Endodontology* **2010**, *110*, 32–40. [CrossRef] [PubMed]
41. Darendeliler, M.A.; Darendeliler, A.; Mandurino, M. Clinical application of magnets in orthodontics and biological implications: A review. *Eur. J. Orthod.* **1997**, *19*, 431–442. [CrossRef]
42. Brand, R.A.; Stanford, C.M.; Swan, C.C. How do tissues respond and adapt to stresses around a prosthesis? A primer on finite element stress analysis for orthopaedic surgeons. *Iowa Orthop. J.* **2003**, *23*, 13–22.
43. Ghasemianpour, M.; Ehsani, S.; Tahmasbi, S.; Bayat, M.; Ghorbanpour, M.; Safavi, S.M.; Mirhashemi, F.S. Distraction osteogenesis for cleft palate closure: A finite element analysis. *Dent. Res. J.* **2014**, *11*, 92–99.
44. Nalabothu, P.; Verna, C.; Steineck, M.; Mueller, A.A.; Dalstra, M. The biomechanical evaluation of magnetic forces to drive osteogenesis in newborn's with cleft lip and palate. *J. Mater. Sci. Mater. Med.* **2020**, *31*, 1–8. [CrossRef]
45. Gundlach, K.K.H.; Maus, C. Epidemiological studies on the frequency of clefts in Europe and world-wide. *J. Cranio-Maxillofac. Surg.* **2006**, *34*, 1–2. [CrossRef]
46. Wang, D.; Cheng, L.; Wang, C.; Qian, Y.; Pan, X. Biomechanical analysis of rapid maxillary expansion in the UCLP patient. *Med. Eng. Phys.* **2009**, *31*, 409–417. [CrossRef]
47. McPherson, G.K.; Kriewall, T.J. The elastic modulus of fetal cranial bone: A first step towards an understanding of the biomechanics of fetal head molding. *J. Biomech.* **1980**, *13*, 9–16. [CrossRef]
48. Bauer, F.X.; Heinrich, V.; Grill, F.D.; Wölfle, F.; Hedderich, D.M.; Rau, A.; Wolff, K.D.; Ritschl, L.M.; Loeffelbein, D.J. Establishment of a finite element model of a neonate's skull to evaluate the stress pattern distribution resulting during nasoalveolar molding therapy of cleft lip and palate patients. *J. Cranio-Maxillofac. Surg.* **2018**, *46*, 660–667. [CrossRef]
49. Pan, X.; Qian, Y.; Yu, J.; Wang, D. Biomechanical Effects of Rapid Palatal Expansion on the Craniofacial Skeleton with cleft palate: A three-dimensional finite element analysis. *Cleft Palate-Craniofac. J.* **2007**, *44*, 149–154. [CrossRef] [PubMed]
50. Carter, D.R.; Schwab, G.H.; Spengler, D.M. Tensile fracture of cancellous bone. *Acta Orthop.* **1980**, *51*, 733–741. [CrossRef] [PubMed]
51. Kim, T.; Ishikawa, H.; Chu, S.; Handa, A.; Iida, J.; Yoshida, S. Constriction of the maxillary dental arch by mucoperiosteal denudation of the palate. *Cleft Palate-Craniofac. J.* **2002**, *39*, 425–431. [CrossRef] [PubMed]
52. Shetye, P.R.; Evans, C.A. Midfacial morphology in adult unoperated complete unilateral cleft lip and palate patients. *Angle Orthod.* **2006**, *76*, 810–816. [CrossRef]
53. Grayson, B.H.; Cutting, C.B. Presurgical nasoalveolar orthopedic molding in primary correction of the nose, lip, and alveolus of infants born with unilateral and bilateral clefts. *Cleft Palate-Craniofac. J.* **2001**, *38*, 193–198. [CrossRef]
54. Cutting, C.B.; Ortolani, A.; Bianchi, M.; Mosca, M.; Caravelli, S.; Fuiano, M.; Marcacci, M.; Russo, A. The prospective opportunities offered by magnetic scaffolds for bone tissue engineering: A review. *Joints* **2017**, *4*, 228–235. [CrossRef]

55. Ashley-Montagu, M.F. The form and dimensions of the palate in the newborn. *Int. J. Orthod. Dent. Child.* **1934**, *20*, 810–827. [CrossRef]
56. Frost, H.M. The Utah paradigm of skeletal physiology: An overview of its insights for bone, cartilage and collagenous tissue organs. *J. Bone Miner. Metab.* **2000**, *18*, 305–316. [CrossRef]
57. Stern, M.; Dodson, T.B.; Longaker, M.T.; Lorenz, H.P.; Harrison, M.R.; Kaban, L.B. Fetal cleft lip repair in lambs: Histologic characteristics of the healing wound. *Int. J. Oral Maxillofac. Surg.* **1993**, *22*, 371–374. [CrossRef]

9. Discussion

The primary correction of congenital clefts of the lip and palate in unilateral clefts (UCLP) and bilateral clefts (BCLP) is challenging due to inherent lack of palatal mucosa and petite extent of the palatal shelves at birth. The two main major factors, which influence a good surgical outcome and its assessment, are the interpretation of cleft size and generation of new tissue to close the defect.

Several different surgical and non-surgical techniques evolved to mitigate the inherent problem of anatomical deficits to an extent by altering the neighbouring tissues around the defect to form a functional seal between the oral and nasal cavity leaving but without option to rectify tissue deficiency itself. The vast majority of clinicians faced a challenge to measure the cleft size due to wide diversity in methodologies employed which resulted in not finding proper correlation in estimating the amount of deficient tissue. This produced contradictory result's in measuring the outcomes, such as occlusion or midface skeletal development [98][99][100].

The outcome measurement and assessments of the cleft width and dimensions of the maxillary dental arches is key to a successful treatment outcome of any primary cleft surgery [101][102][103]. However, the aberrant anatomical structures on the dental casts pose the biggest challenge to clinicians for identification and determination of correct landmarks [104]. Our study overcame this challenge with the use of high resolution scanners which have the advantage of rotating and manipulating the produced 3D images and were also able to give more details to an extent that positioning the landmarks is possible with accuracy and precision [105]. The vast majority of hard palate surgeries aim for tissue to cover the palatal and true cleft [33] in order to produce a functional seal between the nasal and oral cavities. Despite the

clinical importance of the true cleft region in all palate surgeries, this region has not been investigated in three dimensions. Our first study focussed on developing a new 3D standardized landmark analysis by identifying the true cleft width and observe the morphological changes of true cleft width passive plate therapy [58].

In our first study we used the vomers edge (also called “Poutriquet’s ridge) [33][106] and innominate sulcus [106] as new anatomically reproducible landmarks that can be easily used to measure the true cleft ,width, area and curvature in all dimensions [58]. Our measurement errors were found to be well within the ranges found in previous similar studies [99].The landmarks used in our first study have biological correlates or distinct morphologies that facilitate their identification with high precision and reproducibility [107], which probably explains why the errors in the interrater transverse measurements were less than 0.5mm, which is lower than in all previous studies [99][108]. Ours was the first study using vomer edge to compare the effects of passive plate therapy in three dimensions.

Presurgical orthopaedics has been widely used as a non-surgical method to approximate the segments to mitigate the problem of tissue deficiency [65], but it led to various technical variations depending on the effect. Adjuvant therapies are used for approximation of the palatal shelves prior to surgery by active [64] or passive plate therapy [58]. However, the stocks of bone and soft tissue remain deficient since such therapies do not aid in the regeneration of local tissue.

Various surgical techniques have also been attempted to mitigate the problem of tissue deficiency. There is still no consensus about the best protocol for treating CLP patients. Seventeen different surgical sequences for repairing unilateral complete clefts were identified in a survey of over 201 European cleft centres [54]. While all of the surgical techniques were able to close the cleft gap using the available tissue,

none of them result in the generation of new mucoperiosteal tissue [33] [44][45][46][47] [49][50][51][52][53][57]. The use of adjuvant therapies like tissue expansion [109] and distraction osteogenesis [70] have been attempted to increase the volume of tissue , but the principles of distraction osteogenesis requires cut which would damage the dental follicles that are embedded in the palatal shelf ridges. However the animal experiments suggested that periosteal distraction osteogenesis [78][79][80] is an appealing option that can be performed without cutting the bone by gradual lift-up on the mucoperiosteum from the underlying bone by applying mechanical loading. The physical tissue strain and biological tissue stimulus to bone and periosteum lead to new tissue formation. We therefore adopted the concept of PDO as a potential treatment strategy to target the tissue deficiency in orofacial clefts while using magnetic forces to exert the necessary strain.

In our second study we have assessed whether the dental magnets have the potential to act as a device to generate mucoperiosteal tissue in UCLP. The magnets have been widely used in the field of orthodontics for variety of tooth movement for a long period of time [92][110][111][112]. A clinical study on maxillary expansion with repulsive magnets reported that magnetic force can produce dental and skeletal movements in a light force expansion concept [113]. The magnets have been used for lengthening the long bones [114] but there is no evidence in the literature on the use of magnets to generate mucoperiosteal tissue in cleft palate defects. Hence, in our study we have tested the set-ups to see whether the magnets can generate sufficiently high forces by the absence or presence of rugae tissue between magnets. The porcine rugae obtained from the a local butcher shop was used for mimicking the normal palatal mucoperiosteum and thickness of 2-4mm was used based on the thickness levels in the literature [115]. This testing was done to establish the force/distance relationship

[116]. Since strain measuring devices or force transducers cannot be implanted in new born with a cleft to assess the palatal load transfer, we have used an *in silico* approach in the form of a detailed 3D FE-model. We found that the strain levels in the palatal segments of the cleft for these load cases do reach 1500 µstrain limit for mild overuse which was in accordance with the hypothesis of Harold Frost in his Mechanostat theory [117].

Unilateral clefts form 76% of all CLP cases worldwide which still leaves the BCLP accounting for one fourth (24%) of all CLP unaddressed [11].The third study examined whether forces reach the threshold necessary for regeneration of the hard and soft tissue volumes along the cleft edges in both UCLP and BCLP. Although our third study was confined to tissue generation by means of stresses induced by magnetic periosteal distraction, there is increasing evidence that magnetic fields can further promote bone regeneration directly by attracting growth factors, hormones and polypeptides to the implantation site [77]. The length of the magnetic strips was defined as 23mm since the average length of hard palate at birth is 25.6 mm ± 1.6mm [118]. The stresses and strains induced by the magnet were calculated using finite element analysis, for a 1 N attraction force the maximum strains did not exceed 1500 µstrain suggesting that adaptive remodelling will not take place for attraction forces lower than 1 N. At 5 N the regions subject to remodelling differed between the UCLP and BCLP models [119]. Stresses and strains at the periosteum of the palatal shelf ridges in the absence of compressive forces at the alveolar borders were greater in the UCLP model than the BCLP model. Thus, the findings suggest that in new-borns with UCLP and BCLP, periosteal distraction by means of a magnetic 5N attraction force can promote the generation of soft and hard tissues along the cleft edges. The results of this study give guidance about the distribution of palatal load transfer around

the cleft segments by inducing PDO within the optimal biological limits [120]. Future studies could test this hypothesis of mucoperiosteal distraction in an *in vivo* cleft animal model [121] in order to validate the findings of the present FE analyses.

10. Conclusion and future perspective

The conclusions from study I-III were as follows

Study I

The proposed three-dimensional (3D) analysis using vomer edge to define cleft size at palatal cleft and true cleft were validated with optimal intra-examiner and inter-examiner reliability scores. The results were further validated by quantifying the morphological changes of palatal cleft and true cleft width, area and height after passive plate therapy over a long period of 8 months in the absence of previous lip surgery.

Study II

The potential for dental magnets to act as a driving force for tissue expansion in the palate of new-borns was achievable in the computational finite element modelling. The strains produced on application of magnetic attraction forces are compatible with adaptive bone formation in the unilateral cleft palate model.

Study III

The magnets used for dental applications have shown the potential to induce PDO around the greater and lesser segments of palatal shelf ridge in cases of UCLP and BCLP. The potential to initiate adaptive remodelling by magnetic attraction force of 5 N was found to be sufficient to reach strain values in excess of 1500 μstrain in the palatal bone in both UCLP and BCLP models.

The area that surrounds the entrance from the oral into nasal cavity in cleft lip and palate which was described by Victor Veau as "fente vraie" [33] which when translated refers to as “true cleft”. The curved vomer together with the true cleft is referred to as “palatal cleft” and have until now received little attention despite the clinical importance to know the extent of tissue deficiency of the region in all cleft palate surgery techniques. This might be due to defining the landmarks and measuring the cleft palate are commonly performed in two dimensions [94][95][96][97] which represents a simplification of the three-dimensional (3D) complexity of the cleft palate. The vast majority of the measurement’s in cleft lip and palate studies are 3D in nature and are valid when evaluated in three dimensions [55]. The landmarks used in our study have biological correlates or distinct morphologies that facilitate their identification with high precision and reproducibility [108]. We have investigated our new landmark analysis on measuring the outcome of palatal cleft and true cleft areas with passive plate therapy. The limitations of our study were the small sample size and lack of control group without passive plate therapy. Moreover, most of the measurements were localized to the regions of the palatal cleft and true cleft without taking into consideration to the adjacent structures like alveolar ridges for total surface area evaluation. We intend to continue our research by extending our measurements to determine the optimal conditions for complete cleft closure in complete UCLP and BCLP based on the vomer edge landmark. A scientific basis was proposed in 2005 that the surface area of the cleft space should not exceed 10% of the surrounding palatal surface bounded by alveolar ridges, because under these conditions the facial growth is less affected [55]. This holds true when the measurements are made using anatomically reproducible vomer edge landmark. Hence, we continue our future research in measuring the total surface area of the palate in the control and UCLP

patients who received the passive plate to appreciate the effect of the growth, remodelling and relocation of the palatal segments and vomer.

Study II examined the potential for dental magnets to act as a driving force for tissue expansion in the palate of new-borns was achievable in the computational finite element modelling. It was found that the quantified stresses and strains in the palate of newborns with UCLP by simulating the periosteal loading through magnetic forces are compatible with adaptive bone formation. The limitations of our study are strain measuring devices or force transducers cannot be implanted to measure the palatal load transfer as this was computational study. The other limitation was the force levels for the facial musculature, tongue thrust and sucking forces could not be considered due to the *in vitro* model. We intend to continue these investigations in an in vivo animal model to validate the findings of the presented FE analysis.

Study III found that the load transfer of magnetic forces used for periosteal distraction around the greater and lesser segments of the palatal shelf ridge in UCLP and BCLP could promote generation of soft and hard tissues along the cleft edges to rectify the tissue deficiency. The results also gave the guidance for palatal load transfer around the cleft segments within the optimal biological limits [120].The limitations of this study are that the obtained findings [121] are from an *in silico* model. These can only be validated further in an in vivo transgenic mouse models where knockout in gene expression for Msx1 [122] [123] or Tgfb3 [124][125] in results in 100% cleft palate. The obtained results from the animal experiments will be extrapolated for clinical usage. The choice of materials and strategies are all variables in preclinical studies for future preclinical work. On a whole estimating the cleft size and decreasing the tissue deficit by implantation of the magnets with the potential to induce PDO around the greater

and lesser segments might have great potential to achieve functional and aesthetic treatment outcomes.

11. References

1. Mossey PA, L.J. Epidemiology of oral clefts: an international perspective. In Wyszynski DF (ed): *Cleft lip and palate, from origin to treatment. Oxford: Oxford University press*, 2002: ISBN 0195139062.

2. Losee, Joseph E., Richard E.Kirschner. *Comprehensive Cleft Care*; Volume 2, The McGraw Hill Company: New York, 2009: ISBN:9783132067516

3. Strong EB, Buckmiller LM. Management of the Cleft palate. *Facial plast Surg Clin North Am.* 2001, *9*, 15–25, vii. PMID:11465002

4. Mossey, P.A.; Little, J.; Munger, R.G.; Dixon, M.J.; Shaw, W.C. Seminar, Cleft lip and palate. *Lancet* 2009, *374*, 1773–1785.doi:1016/S01406736(09)60695-4

5. Vanderas, A.P. Incidence of cleft Lip, Cleft Palate, and Cleft Lip and Palate Among Races: A Review. *Cleft Palate J* 1987, *24*, 216–225.

6. Butali, A.; Mossey, P. Epidemiology of Orofacial clefts in Africa: Methodological challenges in ascertainment. *Pan Afr. Med. J.* 2010, *2*, 1–9, doi:10.4314/pamj.v2i1.51705.

7. Menegotto, B.G.; Salzano, F.M. Epidemiology of Oral Clefts in a Large South American Sample. *Cleft Palate-Craniofacial J.* 1991, *28*, 373–377.

8. Mitchell, L.E.; Christensen, K. Analysis of the recurrence patterns for nonsyndromic cleft lip with or without cleft palate in the families of 3,073 Danish probands. *Am. J. Med. Genet.* 1996, *61*, 371–376, doi:10.1002/(SICI)1096-8628(19960202)61:4<371::AID-AJMG12>3.0.CO;2-P.

9. Kapitanova, M.; Knebel, J.F.; El Ezzi, O.; Artaz, M.; de Buys Roessingh, A.S.; Richard, C. Influence of infancy care strategy on hearing in children and

adolescents: A longitudinal study of children with unilateral lip and /or cleft palate. *Int. J. Pediatr. Otorhinolaryngol.* 2018, *114*, 80–86, doi:10.1016/j.ijporl.2018.08.031.

10. Mossey, P. Epidemiology underpinning research in the aetiology of orofacial clefts. *Orthod. Craniofacial Res.* 2007, *10*, 114–120.

11. Gundlach, K.K.H.; Maus, C. Epidemiological studies on the frequency of clefts in Europe and world-wide. *J. Cranio-Maxillofacial Surg.* 2006, *34*, 1–2, doi:10.1016/S1010-5182(06)60001-2.

12. Stanier, P.; Moore, G.E. Genetics of cleft lip and palate: Syndromic genes contribute to the incidence of non-syndromic clefts. *Hum. Mol. Genet.* 2004, *13*, 73–81, doi:10.1093/hmg/ddh052.

13. Jugessur Astanand, Min Shi , Håkon Kristian Gjessing , Rolv Terje Lie, A.J.; Wilcox , Clarice Ring Weinberg , Kaare Christensen , Abee Lowman Boyles, S.; Daack-Hirsch , Truc Trung Nguyen , Lene Christiansen , Andrew Carl Lidral, and J.; Murray, C. Fetal genetic risk of isolated cleft lip only versus isolated cleft lip and palate: a subphenotype analysis using two population-based studies of orofacial clefts in Scandinavia. *Birth Defects Res A Clin Mol Teratol* 2011, *91*, 85–92, doi:10.1002/bdra.20747.

14. Poul, Fogh-Andersen. *Inheritance of Harelip and Cleft Palate*; Copenhagen: Munksgaard, 1942;

15. Elizabeth J. Curtis; F. Clarke Fraser; Dorothy Warburton. Risk Figures for Counseling. *Am J Dis Child.* 1961, *102*, 853–857, doi:10.1001/archpedi.1961.02080010855007.

16. Ardinger, H.H.; Buetow, K.H.; Bell, G.I.; Bardach, J.; VanDemark, D.R.; Murray, J.C. Association of genetic variation of the transforming growth factor-alpha gene with cleft lip and palate. *Am. J. Hum. Genet.* 1989, *45*, 348–353.

17. Beaty, T.H.; Ruczinski, I.; Murray, J.C.; Marazita, M.L.; Munger, R.G.; Hetmanski, J.B.; Murray, T.; Redett, R.J.; Fallin, M.D.; Yee, K. Evidence for gene-environment interaction in a genome wide study of isolated, non-

syndromic cleft palate. *Genet. Epidemiol.* 2011, *35*, 469–478, doi:10.1002/gepi.20595.Evidence.

18. Ludwig, K.U.; Mangold, E.; Herms, S.; Nowak, S.; Paul, A.; Becker, J.; Herberz, R.; Alchawa, T.; Böhmer, A.C.; Mattheisen, M.; et al. Genome-wide meta-analyses of nonsyndromic cleft lip with or without cleft palate identify six new risk loci. *Nat Genet.* 2012, *44*, 968–971, doi:10.1038/ng.2360.Genome-wide.

19. Elizabeth J. Leslie, Jenna C. Carlson, John R. Shaffer, Azeez Butali, Carmen J. Bux, Eduardo E. Castilla, Kaare Christensen, Fred W.-B. Deleyiannis, L. Leigh Field, Jacqueline T. Hecht, Lina Moreno, Ieda M. Orioli, Carmencita Padilla, Alexandre R. Vieira, and M.L.M. Genome-wide meta-analyses of nonsyndromic orofacial clefts identify novel associations between FOXE1 and all orofacial clefts, and TP63 and cleft lip with or without cleft palate. *Hum Genet.* 2017, *136*, 275–286, doi:0.1007/s00439-016-1754-7.

20. Theresa M. Zucchero, Margaret E. Cooper, Brion S. Maher, Sandra Daack-Hirsch, Buena Nepomuceno, Lucilene Ribeiro, Diana Caprau, Kaare Christensen, Yasushi Suzuki, Junichiro Machida, Nagato Natsume, Koh-Ichiro Yoshiura, Alexandre R. Vieira, Ieda M. Orioli, Eduardo E. Castilla, Lina Moreno, Mauricio Arcos-Burgos, Andrew C. Lidral, L. Leigh Field, You-e Liu, Ajit Ray, Toby H. Goldstein, Rebecca E. Schultz, Min Shi, Marla K. Johnson, Shinji Kondo, Brian C. Schutte, Mary L. Marazita and Jeffrey C. Murray. Interferon Regulatory Factor 6 (IRF6) Gene Variants and the Risk of Isolated Cleft Lip or Palate. *N Engl J Med* 2004, *351*, 769–780, doi:10.1056/NEJMoa032909.

21. Kondo, S.; Schutte, B.C.; Richardson, R.J.; Bjork, B.C.; Knight, A.S.; Watanabe, Y.; Howard, E.; de Lima, R.L.L.F.; Daack-Hirsch, S.; Sander, A.; et al. Mutations in IRF6 cause Van der Woude and popliteal pterygium syndromes. *Nat. Genet.* 2002, *32*, 285–289, doi:10.1038/ng985.

22. Rizos, M.; Spyropoulos, M.N. Van der Woude syndrome: A review. Cardinal signs, epidemiology, associated features, differential diagnosis, expressivity, genetic counselling and treatment. *Eur. J. Orthod.* 2004, *26*, 17–24, doi:10.1093/ejo/26.1.17.

23. Marie-José H. van den Boogaard, Marinus Dorland, F.A.B.& H.K.P. van A. MSX1 mutation is associated with orofacial clefting and tooth agenesis in humans. *Nat. Genet.* 2000, *24*, 342–343, doi:https://doi.org/10.1038/74155.

24. Abbott, B.D. The etiology of cleft palate: A 50-year search for mechanistic and molecular understanding. *Birth Defects Res. Part B - Dev. Reprod. Toxicol.* 2010, *89*, 266–274, doi:10.1002/bdrb.20252.

25. Shaw, G.M.; Wasserman, C.R.; Lammer, E.J.; O'Malley, C.D.; Murray, J.C.; Basart, A.M.; Tolarova, M.M. Orofacial clefts, parental cigarette smoking, and transforming growth factor-alpha gene variants. *Am. J. Hum. Genet.* 1996, *58*, 551–561.

26. Kelly, D.; O'Dowd, T.; Reulbach, U. Use of folic acid supplements and risk of cleft lip and palate in infants: A population-based cohort study. *Br. J. Gen. Pract.* 2012, *62*, 466–472, doi:10.3399/bjgp12X652328.

27. Winter RM, B.M. *London dysmorpholgy Database, London neurogenetics database and Dysmorphology photo library on CD-ROM (version 3) Oxford*; Oxford university Press: Oxford, 2001;

28. Calzolari, E.; Pierini, A.; Astolfi, G.; Bianchi, F.; Neville, A.J.; And, F.R.; Group, E.W. Associated Anomalies in Multi-MalformedInfants With Cleft Lip and Palate:An Epidemiologic Study of Nearly 6 MillionBirths in 23 EUROCAT Registries. *Am. J. Med Genet.* 2007, *143A*, 528–537, doi:10.1002/ajmg.a.

29. Alper, C.M.; Losee, J.E.; Seroky, J.T.; Mandel, E.M.; Richert, B.C.; Doyle, W.J. Resolution of otitis media with effusion in children with cleft palate followed through five years of age. *Cleft Palate-Craniofacial J.* 2016, *53*, 607–613, doi:10.1597/15-130.

30. Giselle Firmino Torres de Sousa, Angelo Giuseppe Roncalli. Orofacial clefts in Brazil and surgical rehabilitation under the Brazilian National Health System. Braz. oral. res. 2017,31:e23. https://doi.org/10.1590/1807-3107bor-2017.vol.31.0023

31. Sommerlad, B. Anatomy and Function. In *Management of cleft lip and palate*;

Watson, A.C.H., Sell, D., Grunwell, P., Eds.; Whurr Publishers: London, 2001; pp. 25–43.

32. Janusz Bardach; Morris, H.L. *Multidisciplinary management of cleft lip and palate*; W.B. Saunders Ltd: Philadelphia,Pennsylvania, 1990;

33. Veau, V.; Borel, S. *Division palatine: anatomie,chirurgie phonétique/Victor Veau, avec la collaboration de S. Borel.*; 1931st ed.; Paris: Masson: Dijon, Paris, 1931;

34. Kernahan, D.A.; Stark, R.B. A New Classification for cleft lip and cleft palate. *Plast. Reconstr. Surg.* 1958, *22*, 435–441.

35. Allori, A.C.; Mulliken, J.B.; Meara, J.G.; Shusterman, S.; Marcus, J.R. Classification of cleft lip/palate: Then and now. *Cleft Palate-Craniofacial J.* 2017, *54*, 175–188, doi:10.1597/14-080.

36. P, Tessier. Anatomical classification facial, cranio-facial and latero-facial clefts. *J Maxillofac Surg.* 1976, *4*, 69–92, doi:10.1016/s0301-0503(76)80013-6.

37. Otto Kriens What is a cleft lip and palate? In Proceedings of the A multidisciplinary update : proceedings of an advanced workshop, Bremen 1987; Thieme: Stuttgart, 1989.

38. Shkoukani, Mahdi A.Lawrence A Lauren,Liebertz J Daniel, S.F.P. Cleft palate: a clinical review. *Birth Defects Res C Embryo Today* 2014, *102*, 333–42, doi:10.1002/bdrc.21083.

39. WHO International Statistical Classification of Diseases and Related Health Problems 10th Revision (ICD-10)-2015-WHO Version for ;2015 Available online: https://icd.who.int/browse10/2015/en#/XVII (accessed on Aug 6, 2020).

40. Shetye, P.R.; Evans, C.A. Midfacial morphology in adult unoperated complete unilateral cleft lip and palate patients. *Angle Orthod.* 2006, *76*, 810–816, doi:10.1043/0003-3219(2006)076[0810:MMIAUC]2.0.CO;2.

41. Liao, Y.F.; Prasad, N.K.K.; Chiu, Y.T.; Yun, C.; Chen, P.K.T. Cleft size at the time of palate repair in complete unilateral cleft lip and palate as an indicator of

maxillary growth. *Int. J. Oral Maxillofac. Surg.* 2010, *39*, 956–961, doi:10.1016/j.ijom.2010.01.024.

42. Ross, R. Treatment Variables Affecting Facial Growth in complete Unilateral Cleft lip and Palate. Part 7: An overview of treatment and facial growth. *Cleft Palate-Craniofacial J.* 1987, *24*, 5–77.

43. Mølsted, K. Treatment outcome in cleft lip and palate: Issues and perspectives. *Crit. Rev. Oral Biol. Med.* 1999, *10*, 225–239, doi:10.1177/10454411990100020801.

44. Campbell, B.Y.A. The closure of congenital clefts of the hard palate. *Br. J. Surg.* 1926, *13*, 715–719.

45. Pichler,H. Zur operation der doppelten lippen-gaumenspalten. *Dtsch Z Cir* 1926, *195*, 104.

46. Bütow, K.W. Caudally-based single-layer septum-vomer flap for cleft palate closure. *J. Cranio-Maxillofacial Surg.* 1987, *15*, 10–13, doi:10.1016/S1010-5182(87)80006-9.

47. Abyholm,F.E., *Primary closure of cleft lip and palate*; Turvey TA, Vig KWL, F.R., Ed.; WB Saunders Co: Philadelphia, 1996;

48. Langenbeck B. Die Uranoplastik mittelst Ablösung des Mucös-periostalen Gaumenüberzuges.Uranoplasty by means of raising mucoperiosteal flaps.Hirschwald: Berlin,1861 *Plast. Reconstr. Surg.* 1972, *49*, 326–330, doi:10.1097/00006534-197203000-00016.

49. Bardach, J. Two-Flap palatoplasty: Bardach's technique. *Oper. Tech. Plast. Reconstr. Surg.* 1995, *2*, 211–214, doi:10.1016/S1071-0949(06)80034-X.

50. Millard, D.R. The island flap in cleft palate surgery. *Surg Gynecol Obs.* 1963, *116*, 297–300.

51. Mukherji, M.M. Cheek flap for short palates. *Cleft Palate J.* 1969, *6*, 415–420.

52. Stricker M, Chancholle AR, Flot F, Malka G, Montoya A.; La greffe periostee

dans la reparation de la fente totale du palais primaire [The periosteal graft in the repair of primary cleft palate]. *Ann.Chir.Plast.* 1976, *22*, 117-125.

53. Neiva, C.; Dakpe, S.; Gbaguidi, C.; Testelin, S.; Devauchelle, B. Calvarial periosteal graft for second-stage cleft palate surgery: A preliminary report. *J. Cranio-Maxillofacial Surg.* 2014, *42*, e117–e124, doi:10.1016/j.jcms.2013.07.007.

54. Shaw, W.C.; Semb, G.; Nelson, P.; Brattström, V.; Mølsted, K.; Prahl-Andersen, B.; Gundlach, K.K.H. The Eurocleft project 1996-2000: Overview. *J. Cranio-Maxillofacial Surg.* 2001, doi:10.1054/jcms.2001.0217.

55. Berkowitz, S.; Duncan, R.; Evans, C.; Friede, H.; Kuijpers-Jagtman, A.M.; Prahl-Anderson, B.; Rosenstein, S. Timing of Cleft Palate Closure Should Be Based on the Ratio of the Area of the Cleft to That of the Palatal Segments and Not on Age Alone. *Plast. Reconstr. Surg.* 2005, *115*, 1483–1499, doi:10.1097/01.PRS.0000161673.31770.23.

56. Kuijpers-Jagtman, A.M.; Long, J. The influence of surgery and orthopedic treatment on maxillofacial growth and maxillary arch development in patients treated for orofacial clefts. *Cleft Palate-Craniofacial J.* 2000, *37*, 527, doi:10.1597/1545-1569(2000)037<0527:TIOSAO>2.0.CO;2.

57. Dorrance,G.M.; *The operative story of cleft palate*; W.B.Saunders Company: Philadelphia,PA,USA 1933.

58. Nalabothu, P.; Benitez, B.K.; Dalstra, M.; Verna, C.; Mueller, A.A. Three-Dimensional Morphological Changes of the True Cleft under Passive Presurgical Orthopaedics in Unilateral Cleft Lip and Palate: A Retrospective Cohort Study. *J. Clin. Med.* 2020, *9*, 962, doi:10.3390/jcm9040962.

59. McNeil CK *Oral and Facial Deformity*; Pitman: London,UK, 1954;

60. Fish, J. Growth of the palatal shelves of post-alveolar cleft palate infants. Effects of stimulation appliances. *Br. Dent. J.* 1972, *132*, 492–501, doi:10.1038/sj.bdj.4802863.

61. Gnoinski, W.M.; Nussbaumer, H.; Speech-pathologist, C.; Kistler, E.; Speech-pathologist, C. Early Maxillary Orthopedics in CLP Cases: Guidelines for Surgery. *Cleft Palate J.* 1978, *15*, 405–411.

62. Latham, R.A.; Kusy, R.P.; Georgiade, N.G. An extraorally activated expansion appliance for cleft palate infants. *Cleft Palate J.* 1976, *13*, 253–261.

63. Millard, D.R.; Latham, R.A. Improved primary surgical and dental treatment of clefts. *Plast. Reconstr. Surg.* 1990, *86*, 856–871, doi:10.1097/00006534-199011000-00006.

64. Grayson, B.H.; Cutting, C.B. Presurgical nasoalveolar orthopedic molding in primary correction of the nose, lip, and alveolus of infants born with unilateral and bilateral clefts. *Cleft Palate-Craniofacial J.* 2001, *38*, 193–198, doi:10.1597/1545-1569(2001)038<0193:PNOMIP>2.0.CO;2.

65. Huddart, A.G. Presurgical changes in unilateral cleft palate subjects. *Cleft Palate J.* 1979, *16*, 147–157.

66. Prahl, C., Kuilpers-Jagtman,A.M.,, Van't Hof M.A., Prahl -Andersen, B. A randomised prospective clinical trial into the effect of infant orthopaedics on maxillary arch dimensions in unilateral cleft lip and palate (Dutchcleft). *Eur. J. Oral Sci.* 2001, *109*, 297–305.

67. McCarthy, J.G.; Schreiber, J.; Karp, N.; Thorne, C.H.; Grayson, B.H. Lengthening the human mandible by gradual distraction. *Plast. Reconstr. Surg.* 1992, *89*, 1–8, doi:10.1097/00006534-199289010-00001.

68. Figueroa, A.; Polley, J.; Ko, E. Maxillary distraction for the management of cleft maxillary hypoplasia with a rigid external distraction system. *Semin. Orthod.* 1999, *5*, 46–51, doi:10.1016/s1073-8746(99)80042-5.

69. Liou, E.; Chen, P.; C, H.; Y, C. Interdental distraction osteogenesis and rapid orthodontic tooth movement: a novel approach to approximate a wide alveolar cleft or bony defect. *Plast. Reconstr. Surg.* 2000, *105*, 1262–1272, doi:10.1097/00006534-200004040-00002.

70. Alkan, A.; Baş, B.; Özer, M.; Bayram, M. Closure of a large palatal fistula with maxillary segmental distraction osteogenesis in a cleft palate patient. *Cleft Palate-Craniofacial J.* 2007, *44*, 112–115, doi:10.1597/05-195.

71. Zhao, D.; Wang, Y.; Han, D. Periosteal Distraction Osteogenesis: An Effective Method for Bone Regeneration. *Biomed Res. Int.* 2016, *2016*, doi:10.1155/2016/2075317.

72. Kessler Peter, Bumiller Lars, Schlegel Andreas, Birkholz Torsten, N.W.F. Dynamic periosteal elevation. *Br. J. Oral Maxillofac. Surg.* 2006, *45*, 284–287, doi:https://doi.org/10.1016/j.bjoms.2006.09.010.

73. Casap, N.; Venezia, N.B.; Wilensky, A.; Samuni, Y. Induction of osteogenesis by periosteal distraction in rabbits. *Int. J. Oral Maxillofac. Surg.* 2007, *36*, 1005, doi:10.1016/j.ijom.2007.08.163.

74. Abrahamsson, P.; Isaksson, S.; Gordh, M.; Andersson, G. Periosteal expansion of rabbit mandible with an osmotic self-inflatable expander. *Scand. J. Plast. Reconstr. Surg. Hand Surg.* 2009, *43*, 121–125, doi:10.1080/02844310902771798.

75. Oda, T.; Kinoshita, K.; Ueda, M. Effects of Cortical Bone Perforation on Periosteal Distraction: An Experimental Study in the Rabbit Mandible. *J. Oral Maxillofac. Surg.* 2009, *67*, 1478–1485, doi:10.1016/j.joms.2008.06.085.

76. Lethaus B, Tudor C, Bumiller L, Birkholz T, Wiltfang J, K.P. Guided bone regeneration: dynamic procedures versus static shielding in an animal model. *J Biomed Mater Res B Appl Biomater.* 2010, *95*, 126–130, doi:doi:10.1002/jbm.b.31691.

77. Bianchi, M.; Mosca, M.; Caravelli, S.; Fuiano, M.; Marcacci, M. The prospective opportunities offered by magnetic scaffolds for bone tissue engineering: a review. 2016, *4*, 228–235.

78. Schmidt, B.L.; Kung, L.; Jones, C.; Casap, N. Induced osteogenesis by periosteal distraction. *J. Oral Maxillofac. Surg.* 2002, *60*, 1170–1175, doi:10.1053/joms.2002.34993.

79. Sencimen, M.; Aydintug, Y.S.; Ortakoglu, K.; Karslioglu, Y.; Gunhan, O.; Gunaydin, Y. Histomorphometrical analysis of new bone obtained by distraction osteogenesis and osteogenesis by periosteal distraction in rabbits. *Int. J. Oral Maxillofac. Surg.* 2007, *36*, 235–242, doi:10.1016/j.ijom.2006.08.016.

80. Sato, K.; Haruyama, N.; Shimizu, Y.; Hara, J.; Kawamura, H. Osteogenesis by gradually expanding the interface between bone surface and periosteum enhanced by bone marrow stem cell administration in rabbits. *Oral Surgery, Oral Med. Oral Pathol. Oral Radiol. Endodontology* 2010, *110*, 32–40, doi:10.1016/j.tripleo.2009.11.005.

81. De Mey, A.; Malevez, C.; Lejour, M. Treatment of palatal fistula by expansion. *Br. J. Plast. Surg.* 1990, *43*, 362–364, doi:10.1016/0007-1226(90)90090-M.

82. Abramo, A.; Viola, J.; Angelo, A. Intraoperative rapid expansion in cleft palate repair. *Plast. Reconstr. Surg.* 1993, *91*, 441–445, doi:10.1097/00006534-199303000-00008.

83. Peled, I.J.; Barak, A.; Taran, A.; Ullman, Y. Intraoperative Expansion of the Palate by the Tumescent Technique. *Plast. Reconstr. Surg.* 1997, *100*, 100–103.

84. Kobus, K.F. Cleft palate repair with the use of osmotic expanders: a preliminary report. *J. Plast. Reconstr. Aesthetic Surg.* 2007, *60*, 414–421, doi:10.1016/j.bjps.2006.01.053.

85. Sasaki, G.H. Intraoperative Sustained Limited Expansion (ISLE) as an Immediate Reconstructive Technique. *Clin. Plast. Surg.* 1987, *14*, 563–573, doi:https://doi.org/10.1016/S0094-1298(20)31526-1.

86. Machida, B.K.; Liu-Shindo, M.; Sasaki, G.H.; Rice, D.H.; Chandrasoma, P. Immediate versus chronic tissue expansion. *Ann. Plast. Surg.* 1991, *26*, 227—31; discussion 232, doi:10.1097/00000637-199103000-00004.

87. Facca, S.; Cortez, C.; Mendoza-Palomares, C.; Messadeq, N.; Dierich, A.; Johnston, A.P.R.; Mainard, D.; Voegel, J.C.; Caruso, F.; Benkirane-Jessel, N. Active multilayered capsules for in vivo bone formation. *Proc. Natl. Acad. Sci.*

U. S. A. 2010, *107*, 3406–3411, doi:10.1073/pnas.0908531107.

88. Mendoza-Palomares, C.; Ferrand, A.; Facca, S.; Fioretti, F.; Ladam, G.; Kuchler-Bopp, S.; Regnier, T.; Mainard, D.; Benkirane-Jessel, N. Smart hybrid materials equipped by nanoreservoirs of therapeutics. *ACS Nano* 2012, *6*, 483–490, doi:10.1021/nn203817t.

89. Schiavi, J.; Keller, L.; Morand, D.-N.; Isla, N. De; Huck, O.; Lutz, J.C.; Mainard, D.; Schwinté, P.; Benkirane-Jessel, N. Active implant combining human stem cell microtissues and growth factors for bone-regenerative nanomedicine. *Nanomedicine* 2015, *10*, 753–763, doi:10.2217/nnm.14.228.

90. Martín-Del-Campo, M.; Rosales-Ibañez, R.; Rojo, L. Biomaterials for cleft lip and palate regeneration. *Int. J. Mol. Sci.* 2019, *20*, doi:10.3390/ijms20092176.

91. Yan, Q.C.; Tomita, N.; Ikada, Y. Effects of static magnetic field on bone formation of rat femurs. *Med. Eng. Phys.* 1998, *20*, 397–402, doi:10.1016/S1350-4533(98)00051-4.

92. Ali Darendeliler, M.; Darendeliler, A.; Mandurino, M. Clinical application of magnets in orthodontics and biological implications: A review. *Eur. J. Orthod.* 1997, *19*, 431–442, doi:10.1093/ejo/19.4.431.

93. Brand, R.A.; Stanford, C.M.; Swan, C.C. How do tissues respond and adapt to stresses around a prosthesis? A primer on finite element stress analysis for orthopaedic surgeons. *Iowa Orthop. J.* 2003, *23*, 13–22.

94. Stöckli, P.W. Application of a quantitative method for arch form evaluation in complete unilateral cleft lip and palate. *Cleft Palate J* 1971, *8*, 322–341.

95. Grabowski. R. ; Kopp H.; Stahl, F.; Gundlacj, K.K.H. Presurgical orthopaedic treatment of newborns with clefts - functional treatment with long-term effects. *J. Cranio-Maxillofacial Surg.* 2006, *34*, 34–44, doi:10.1016/S1010-5182(06)60009-7.

96. Wada, T.; Miyazaki, T. Treatment principles for the changing arch form in children with complete unilateral cleft lips and palates. *Cleft Palate J* 1975, *13*,

273–283.

97. Grayson, B.H.; Cutting, C.B.; Brecht, L.E.; Peltomäki, T.; Vendittelli, B.L. Associations between Severity of Clefting and Maxillary Growth in Patients with Unilateral Cleft Lip and Palate Treated with Infant Orthopedics. *Cleft Palate-Craniofacial J.* 2001, *38*, 582–586, doi:10.1597/1545-1569_2001_038_0582_absoca_2.0.co_2.

98. Yamanishi, T.; Nishio, J.; Kohara, H.; Hirano, Y.; Sako, M.; Yamanishi, Y.; Adachi, T.; Miya, S.; Mukai, T. Effect on Maxillary Arch Development of Early 2-Stage Palatoplasty by Modified Furlow Technique and Conventional 1-Stage Palatoplasty in Children With Complete Unilateral Cleft Lip and Palate. *J. Oral Maxillofac. Surg.* 2009, *67*, 2210–2216, doi:10.1016/j.joms.2009.04.038.

99. Seckel, N.G.; Van der Tweel, I.; Elema, G.A.; Specken, T.F.J.M.C. Landmark positioning on maxilla of cleft lip and palate infant - A reality? *Cleft Palate-Craniofacial J.* 1995, doi:10.1597/1545-1569(1995)032<0434:LPOMOC>2.3.CO;2.

100. Shetty, V.; Agrawal, R.K.; Sailer, H.F. Long-term effect of presurgical nasoalveolar molding on growth of maxillary arch in unilateral cleft lip and palate: randomized controlled trial. *Int. J. Oral Maxillofac. Surg.* 2017, *46*, 977–987, doi:10.1016/j.ijom.2017.03.006.

101. Robertson, N.R.E.; Fish, J. Early dimensional changes in the arches of cleft palate children. *Am. J. Orthod.* 1975, *67*, 290–303, doi:10.1016/0002-9416(75)90051-2.

102. Botticelli, S.; Pedersen, T.K.; Küseler, A.; Nørholt, S.E.; Cattaneo, P.M. Novel 3-D Analysis for the Assessment of Cleft Dimensions on Digital Models of Infants With Unilateral Cleft Lip and Palate. *Cleft Palate. Craniofac. J.* 2019, *56*, 127–133, doi:10.1177/1055665618770795.

103. Botticelli, S.; Küseler, A.; Marcusson, A.; Mølsted, K.; Nørholt, S.E.; Cattaneo, P.M.; Pedersen, T.K. Do Infant Cleft Dimensions Have an Influence on Occlusal Relations? A Subgroup Analysis Within an RCT of Primary Surgery in Patients

With Unilateral Cleft Lip and Palate. *Cleft Palate-Craniofacial J.* 2020, *57*, 378–388, doi:10.1177/1055665619875320.

104. Botticelli, S.; Küseler, A.; Mølsted, K.; Ovsenik, M.; Nørholt, S.E.; Dalstra, M.; Cattaneo, P.M.; Pedersen, T.K. Palatal morphology in unilateral cleft lip and palate patients: Association with infant cleft dimensions and timing of hard palate repair. *Orthod. Craniofacial Res.* 2019, *22*, 270–280, doi:10.1111/ocr.12318.

105. Long, R.E.; Daskalogiannakis, J.; Mercado, A.M.; Hathaway, R.R.; Fessler, J.; Russell, K.A. The americleft project: Plaster dental casts versus digital images for GOSLON yardstick ratings when used in intercenter comparisons. *J. Craniofac. Surg.* 2017, *28*, 1269–1273, doi:10.1097/SCS.0000000000003728.

106. Malek, R. *Cleft Lip and Palate: Lesions, Pathophysiology and Primary Treatment*; 1ST ed.:Martin, D., ED.; CRC Press: London,UK., 27November 2000: ISBN 978-1853174919.

107. Oxnard, C.E. The measurement of form: beyond biometrics. Sausages and stars, dumbbells and doughnuts: peculiar views of anatomical structures. *Cleft Palate-Craniofacial J.* 1986, *23 Suppl 1*, 110–128.

108. Jakob Brief., Jan H Behle, Angelika Stellzig-Eisenhauer, Stefan Hassfeld. Precision of landmark positioning on digitized models from patients with cleft lip and palate. *Cleft Palate-Craniofacial J.* 2006, *43*, 168–173, doi:10.1597/04-106.1.

109. Shash, H.; Al-Halabi, B.; Jozaghi, Y.; Aldekhayel, S.; Gilardino, M.S. A review of tissue expansion-assisted techniques of cleft palate repair. *J. Craniofac. Surg.* 2016, *27*, 760–766, doi:10.1097/SCS.0000000000002468.

110. Muller, M. The use of magnets in orthodontics: An alternative means to produce tooth movement. *Eur. J. Orthod.* 1984, *6*, 247–253, doi:10.1093/ejo/6.1.247.

111. Gianelly, A.A.; Vaitaa, A.S.; Thomas, W.M. The use of magnets to move molars distally. *Am. J. Orthod. Dentofac. Orthop.* 1989, *96*, 161–167, doi:10.1016/0889-5406(89)90257-6.

112. Darendeliler, M.A.; Joho, J.P. Magnetic activator device II (MAD II) for correction of Class II, division 1 malocclusions. *Am. J. Orthod. Dentofac. Orthop.* 1993, *103*, 223–239, doi:10.1016/0889-5406(93)70003-7.

113. Darendeliler, M.A.; Strahm, C.; Joho, J.P. Light maxillary expansion forces with the magnetic expansion device. A preliminary investigation. *Eur. J. Orthod.* 1994, *16*, 479–490, doi:10.1093/ejo/16.6.479.

114. Cheung, J.P.Y.; Cahill, P.; Yaszay, B.; Akbarnia, B.A.; Cheung, K.M.C. Special article: Update on the magnetically controlled growing rod: Tips and pitfalls. *J. Orthop. Surg.* 2015, *23*, 383–390, doi:10.1177/230949901502300327.

115. Lee, S.M.; Park, J.H.; Bayome, M.; Kim, H.S.; Mo, S.S.; Kook, Y.A. Palatal Soft Tissue Thickness at Different Ages Using an Ultrasonic Device. *J. Clin. Pediatr. Dent.* 2012, *36*, 405–409, doi:10.17796/jcpd.36.4.58tm38928v522283.

116. Nalabothu, P.; Verna, C.; Steineck, M.; Mueller, A.A.; Dalstra, M. The biomechanical evaluation of magnetic forces to drive osteogenesis in newborn's with cleft lip and palate. *J. Mater. Sci. Mater. Med.* 2020, *31*, 1–8, doi:10.1007/s10856-020-06421-6.

117. Frost, H.M. A 2003 update of bone physiology and Wolff s law for clinicians. *Angle Orthod.* 2004, *74*, 3–15, doi:10.1043/0003-3219(2004)074<0003:AUOBPA>2.0.CO;2.

118. Ashley-Montagu M.F. The form and dimensions of the palate in the newborn. *Int J orthod Dent Child* 1934, *20*, 694–704. https://doi.org/10.1016/S0097-0522(34)90177-5.

119. Nalabothu, P.; Verna, C.; Benitez, B.K.; Dalstra, M.; Mueller, A.A. Load transfer during magnetic mucoperiosteal distraction in newborns with complete unilateral and bilateral orofacial clefts: A three-dimensional finite element analysis. *Appl. Sci.* 2020, *10*, 1–13, doi:10.3390/app10217728.

120. Frost, H.M. The Utah paradigm of skeletal physiology: An overview of its insights for bone, cartilage and collagenous tissue organs. *J. Bone Miner. Metab.* 2000, *18*, 305–316, doi:10.1007/s007740070001.

121. Stern M, Dodson TB, Longaker MT, Lorenz HP, Harrison MR, K.L. Fetal cleft lip repair in lambs: histologic characteristics of the healing wound. *Int J Oral Maxillofac Surg.* 1993, *22*, 371–374, doi:10.1016/s0901-5027(05)80672-1.

122. Satokata, I.; Maas, R. Msx1 deficient mice exhibit cleft palate and abnormalities of craniofacial and tooth development. *Nat. Genet.* 1994, *6*, 348–356, doi:https://doi.org/10.1038/ng0494-348.

123. Houzelstein, D.; Cohen, A.; Buckingham, M.E.; Robert, B. Insertional mutation of the mouse Msx1 homeobox gene by an nlacZ reporter gene. *Mech. Dev.* 1997, *65*, 123–133, doi:10.1016/S0925-4773(97)00065-8.

124. Proetzel, G.; Pawlowski, S.A.; Wiles, M. V; Yin, M.; Gregory, P.; Howles, P.N.; Ding, J.; Ferguson, M.W.J.; Doetschman, T. Transforming growth factor-β3 is required for secondary palate fusion. *Nat. Genet.* 1995, *11*, 409–414, doi:10.1038/ng1295-409.Transforming.

125. Kaartinen, V.; Voncken, J.W.; Shuler, C.; Warburton, D.; Bu, D.; Heisterkamp, N.; Groffen, J. Abnormal lung development and cleft palate in mice lacking TGF–β3 indicates defects of epithelial–mesenchymal interaction. *Nat. Genet.* 1995, *11*, 415–421, doi:https://doi.org/10.1038/ng1295-415.

12. List of publications on PhD topic

Journal publications

Nalabothu P, Benitez BK, Dalstra M, Verna C, Mueller AA.
Three-Dimensional Morphological Changes of the True Cleft under Passive Presurgical Orthopaedics in Unilateral Cleft Lip and Palate: A Retrospective Cohort Study. J Clin Med. 2020 Mar 31;9(4):962. doi: 10.3390/jcm9040962. PMID: 32244361; PMCID: PMC7230798.

Nalabothu P, Verna C, Steineck M, Mueller AA, Dalstra M.
The biomechanical evaluation of magnetic forces to drive osteogenesis in newborn's with cleft lip and palate. J Mater Sci Mater Med. 2020 Aug 20;31(9):79. doi: 10.1007/s10856-020-06421-6. PMID: 32816120; PMCID: PMC7441089.

Nalabothu, P.; Verna, C.; Benitez, B.K.; Dalstra, M.; Mueller, A.A.
Load Transfer during Magnetic Mucoperiosteal Distraction in Newborns with Complete Unilateral and Bilateral Orofacial Clefts: A Three-Dimensional Finite Element Analysis. *Appl. Sci.* 2020, *10*, 7728.

Proceedings

Prasad Nalabothu, Michel Dalstra, Hans-Florian Zeilhofer, Andreas Mueller, Carlalberta Verna. Periosteal distraction by magnets for cleft palate defects – a finite element study. available online page 148, abstract no.350 Abstracts of Lectures and Scientific Posters, *European Journal of Orthodontics*, Volume 40, Issue 5, October 2018, Pages e1–e223, https://doi.org/10.1093/ejo/cjy060

Prasad Nalabothu, Michel Dalstra, Hans-Florian Zeilhofer, Andreas Mueller, Carlalberta Verna. Biomechanical analysis of mucoperiosteal tissue strains during

treatment of cleft palate defects. Available online page 130, abstract no.288 Abstracts of Lectures and Scientific Posters, *European Journal of Orthodontics*, Volume 41, Issue 5, October 2019, Pages e1–e189, https://doi.org/10.1093/ejo/cjz073

Prasad Nalabothu, Benito Benitez, Andreas Mueller, Carlalberta Verna, Michel Dalstra. Three dimensional morphological changes of true cleft width passive plate therapy in patients with a cleft lip and palate. Available online Page 29, abstract no.4320. Abstracts of short oral and scientific poster presentations, *European Journal of Orthodontics*, Volume42, Issue5, October 2020, Pages e1–e44, https://doi.org/10.1093/ejo/cjaa059

Oral presentations

10/10/ 2020	Comprehensive cleft care workshop. Anterior Maxillary distraction in growing children. (Virtual mode)
14/06/2019	European cleft palate craniofacial anomalies (ECPCA), Utrecht, Netherlands. Periosteal distraction by magnets for cleft palate defects,
30/11/2018	SGLKG Swiss society for clefts and Craniofacial anomalies. Inselspital, Bern, Switzerland. Periosteal distraction by magnets for cleft palate defects
25/08/2017	VIDEC 10, Hanoi, Vietnam. Maxillary hypoplasia in growing and non-growing patients with cleft lip and palate.
28/07/2017	Faculty of medicine University of Indonesia. Distraction of severe maxillary hypoplasia in patients with cleft
28/06/2017	Summer school (Nanomedicine) Biomaterial science center, University of Basel, organized at Saas fe, Switzerland Smart implants for mucoperiosteal tissue expansion in cleft palate defects.
16/06/2017	13th International Bern Spiessl symposium, Basel, Switzerland. Stability of anterior maxillary advancement using tooth supported distraction osteogenesis.
10/02/2017	International Cleft congress, Chennai, India. Tooth supported anterior maxillary distraction in cleft lip and palate patients.